

Enhanced Condensate Recovery via Gas Dumpflood from Multiple High CO₂
Gas Reservoirs

Mr. Wisaroot Lerthaweedech



จุฬาลงกรณ์มหาวิทยาลัย

CHULALONGKORN UNIVERSITY

บทคัดย่อและแฟ้มข้อมูลฉบับนี้ของวิทยานิพนธ์ตั้งแต่ปี ๒๕๕๑-๒๕๕๔ ที่ทำขึ้นและนำขึ้นสู่คลังข้อมูลจุฬาฯ (CUIR)

เพื่อเป็น Degree of Master of Engineering ที่ Program in Petroleum Engineering

The abstract and full text of theses from the academic year 2011 in Chulalongkorn University Intellectual Repository (CUIR)

are the thesis authors' files submitted through the University Graduate School.

Faculty of Engineering
Chulalongkorn University

Academic Year 2015

Copyright of Chulalongkorn University

การเพิ่มปริมาณการผลิตก๊าซธรรมชาติเหลวโดยใช้การแทนที่แบบถ่ายเทจากแหล่งกักเก็บก๊าซที่มี
ปริมาณก๊าซคาร์บอนไดออกไซด์สูงหลายชั้น

นายวิศรุต เลิศทวีเดช



วิทยานิพนธ์นี้เป็นส่วนหนึ่งของการศึกษาตามหลักสูตรปริญญาวิศวกรรมศาสตรมหาบัณฑิต

สาขาวิชาวิศวกรรมปิโตรเลียม ภาควิชาวิศวกรรมเหมืองแร่และปิโตรเลียม

คณะวิศวกรรมศาสตร์ จุฬาลงกรณ์มหาวิทยาลัย

ปีการศึกษา 2558

ลิขสิทธิ์ของจุฬาลงกรณ์มหาวิทยาลัย

Thesis Title	Enhanced Condensate Recovery via Gas Dumpflood from Multiple High CO ₂ Gas Reservoirs
By	Mr. Wisaroot Lertthaweedeck
Field of Study	Petroleum Engineering
Thesis Advisor	Assistant Professor Suwat Athichanagorn, Ph.D.

Accepted by the Faculty of Engineering, Chulalongkorn University in Partial
Fulfillment of the Requirements for the Master's Degree

.....Dean of the Faculty of Engineering
(Associate Professor Supot Teachavorasinskun, Ph.D.)

THESIS COMMITTEE

.....Chairman
(Assistant Professor Jirawat Chewaroungroj, Ph.D.)

.....Thesis Advisor
(Assistant Professor Suwat Athichanagorn, Ph.D.)

.....External Examiner
(Pichit Vardcharragosad, Ph.D.)

5771218221 : MAJOR PETROLEUM ENGINEERING

KEYWORDS: ENHANCED CONDENSATE RECOVERY / DUMPFLOOD / MULTI-LAYER GAS RESERVOIRS

WISAROOT LERTTHAWEEDECH: Enhanced Condensate Recovery via Gas Dumpflood from Multiple High CO₂ Gas Reservoirs. ADVISOR: ASST. PROF. SUWAT ATHICHANAGORN, Ph.D., 137 pp.

In the Gulf of Thailand, many gas fields are multi-stack gas condensate and dry gas reservoirs. Some of these dry gas reservoirs are not economically produced because of high CO₂ content. However, these reservoirs can be used to perform gas dumpflood into a gas-condensate reservoir instead of gas injection to enhance condensate recovery due to much lower cost. In this study, a hypothetical reservoir model consisting of a gas-condensate reservoir with four thin-layered high CO₂ gas reservoirs having typical properties found in the Gulf of Thailand was created using compositional reservoir simulation software in order to investigate the performance of the proposed method.

This simulation study found that gas dumpflood can increase condensate recovery up to 17.5% over natural depletion scenario depending on several parameters. Although its recovery is lower than that of conventional gas injection, gas dumpflood is an attractive alternative due to lower cost. The important parameter is the fluid composition in the gas condensate reservoir. The rich gas condensate yielding higher condensate to gas ratio is more favorable for gas dumpflood from high CO₂ source gas reservoir. On the contrary, for lean condensate, excessive amount of dumped source gas results in a large reduction of condensate recovery. The amount of CO₂ should be limited in this case. Regarding perforation of the high CO₂ source gas reservoirs, different sequences result in similar gas and condensate recovery as long as the same amount of total original gas in place is present in those perforated layers.

Department: Mining and Petroleum Student's Signature

Engineering Advisor's Signature

Field of Study: Petroleum Engineering

Academic Year: 2015

ACKNOWLEDGEMENTS

First of all, I would like to express my sincere gratitude to Assistant Professor Suwat Athichanagorn, my thesis advisor, for all his invaluable support and guidance. This thesis would not have been successfully achieved without his counselling and assistance.

I am grateful to all faculty members in Department of Mining and Petroleum Engineering for knowledge, suggestions, and all their help. I also would like to give big thanks to the thesis committee members for their comments and recommendations on my thesis.

I would like to thank Schlumberger for providing ECLIPSE simulator software to Department of Mining and Petroleum Engineering, Chulalongkorn University. Moreover, I am so grateful to Mr. Nattaphon Temkiatvises, reservoir engineer from Schlumberger, for his valuable advice and discussion to find the solution for problems encountered with ECLIPSE reservoir simulation software. I would like to give the special thanks to Chevron Thailand Exploration and Production, Ltd. for financial support for this study.

I appreciate all of my friends from this department including my classmates and senior students for their help, support and good friendship given to me during my study.

Finally, I most gratefully acknowledge my family and my friends for all their encouragement and support which are the big motivation toward my successful achievement of the study.

CONTENTS

	Page
THAI ABSTRACT.....	iv
ENGLISH ABSTRACT.....	v
ACKNOWLEDGEMENTS	vi
CONTENTS.....	vii
LIST OF TABLES	xi
LIST OF FIGURES.....	xv
LIST OF ABBREVIATIONS	xxiv
NOMENCLATURES	xxviii
Latin Alphabet	xxviii
Greek Symbol.....	xxx
CHAPTER 1 INTRODUCTION	1
1.1 Background	1
1.2 Objectives.....	2
1.3 Outline of Methodology	2
1.4 Outline of Thesis	3
CHAPTER 2 LITERATURE REVIEW.....	4
2.1 Study of Gas Dumpflood.....	4
2.2 Study of Conventional Carbon Dioxide Injection	5
CHAPTER 3 THEORY AND CONCEPT.....	8
3.1 Gas Condensate Reservoir.....	8
3.1.1 Phase Behavior of Gas-Condensate	8
3.1.2 Flow Behavior of Gas Condensate	10

	Page
3.1.3 Fluid Composition Change by Condensation Process.....	12
3.2 CO ₂ Flooding in Gas Condensate Reservoir	13
3.2.1 Flooding Patterns.....	14
3.2.2 Overall Sweep Efficiency	16
3.2.3 Fluid Composition Change by Flooding Process.....	17
3.2.4 Fracture Pressure	18
3.3 Recovery Calculation.....	18
3.4 Two Phase Vertical Flow Regimes.....	19
CHAPTER 4 RESERVOIR SIMULATION MODEL.....	21
4.1 Case Definition	21
4.2 Grid.....	22
4.2.1 Target Gas-Condensate Reservoir	22
4.2.2 Source Gas Reservoirs.....	23
4.2 Fluid Properties.....	24
4.3.1 Water Properties	24
4.3.2 Gas and Condensate Properties.....	26
4.4 Special Core Analysis.....	29
4.5 Production Schedule	31
4.5 Details of Methodology	34
CHAPTER 5 SIMULATION RESULTS AND DISSUSION.....	40
5.1 Natural Depletion.....	41
5.2 Conventional Gas Injection	49
5.2.1 Composition Yielding High CGR of Original Reservoir Fluid.....	51

	Page
5.2.2 Composition Yielding Low CGR of Original Reservoir Fluid.....	65
5.3 Gas Dumpflood from Multiple-Gas Reservoirs.....	72
5.3.1 Composition Yielding High CGR of Original Reservoir Fluid.....	75
5.3.1.1 25-ft Thickness of Source Gas Reservoirs.....	75
5.3.1.2 50-ft Thickness of Source Gas Reservoirs.....	86
5.3.1.3 Comparison between 25-ft and 50-ft Thickness of Source Gas Reservoirs.....	91
5.3.2 Composition Yielding Low CGR of Original Reservoir Fluid.....	95
5.3.2.1 25-ft Thickness of Source Gas Reservoirs.....	95
5.3.2.2 50-ft Thickness of Source Gas Reservoirs.....	105
5.3.2.3 Comparison between 25-ft and 50-ft Thickness of Source Gas Reservoirs.....	109
5.4 Comparison among Different Production Scenarios.....	113
5.4.1 Composition Yielding High CGR of Original Reservoir Fluid.....	113
5.4.2 Composition Yielding Low CGR of Original Reservoir Fluid.....	117
CHAPTER 6 CONCLUSIONS AND RECOMMENDATIONS.....	121
6.1 Conclusions.....	121
6.2 Recommendations.....	123
REFERENCES.....	124
APPENDIX A PRODUCTION SCHEDULE.....	127
A.1 Well Specification (keyword: WELSPECS).....	127
A.2 Well Completion Specification Data (keyword: COMPDAT).....	127
A.3 Segmented Well Definition (keyword: WELSEGS).....	129
A.4 Segmented Well Completion (keyword: COMPSEGS).....	129

	Page
A.5 Segmented Vertical Flow Performance Table (keyword: WSEGTABL).....	130
A.6 Production Well Control (keyword: WCONPROD).....	131
A.7 Vertical Flow Performance (keyword: VFPPROD).....	132
APPENDIX B ECONOMIC LIMIT	135
B.1 Field Abandonment Condition.....	135
B.2 Conventional Gas Injection Limit.....	135
VITA	137



LIST OF TABLES

	Page
Table 3.1: Physical characteristics of different types of gas condensate [12]	10
Table 3.2: Areal sweep efficiencies for various flooding patterns [14]	15
Table 3.3: The higher heating values of each gas composition [18]	19
Table 4.1: Geometries and properties of the target gas-condensate reservoir	22
Table 4.2: Geometries and properties of the source gas reservoirs	23
Table 4.3: Input parameters used to calculate the properties of water	25
Table 4.4: Water properties resulting from using correlations provided in ECLIPSE 300	26
Table 4.5: The initial composition of the target-reservoir fluid [10]	27
Table 4.6: The initial composition of gas in the source reservoirs and the injected fluids	27
Table 4.7: Physical properties of each component [18]	28
Table 4.8: Binary interaction coefficient between components	29
Table 4.9: Parameters used in Corey correlation	30
Table 4.10: Production control data for all production wells	32
Table 4.11: Operational constraints of the production well	32
Table 4.12: Operational constraints of the middle well or the dumping well for dumpflood scenario and the injector for conventional gas injection scenario	33
Table 5.1: Summarized results for different composition cases of natural depletion scenario	47
Table 5.2: Economic condensate rate for different gas injection rates	50

Table 5.3: Summarized results of different gas injection rates of conventional gas injection scenario with high CGR composition of original reservoir fluid ..62	62
Table 5.4: Summarized results of different gas injection rates of conventional gas injection scenario with low CGR composition of original reservoir fluid ...70	70
Table 5.5: Descriptions of all cases with varying operating and reservoir parameters.....74	74
Table 5.6: Summarized results of different perforation sequences of gas dumpflood scenarios starting at the beginning with high CGR composition of original reservoir fluid and 25-ft thickness of the source gas reservoirs79	79
Table 5.7: Summarized results of different starting times of dumpflood operation having simultaneous perforation all of source reservoirs with high CGR composition of original reservoir fluid and 25-ft thickness of the source gas reservoirs84	84
Table 5.8: Summarized results of different perforation sequences of gas dumpflood scenarios starting at the beginning with high CGR composition of original reservoir fluid and 50-ft thickness of the source gas reservoirs89	89
Table 5.9: Descriptions of all cases in Section 5.3.1.3.....91	91
Table 5.10: Summarized results of different thickness of gas source reservoirs and numbers of perforated source reservoirs with high CGR composition of original reservoir fluid.....94	94
Table 5.11: Summarized results of different perforation sequences of gas dumpflood scenarios starting at the beginning with low CGR composition of original reservoir fluid and 25-ft thickness of the source gas reservoirs98	98

Table 5.12: Summarized results of different starting times of dumpflood operation for simultaneous perforation of all four source reservoirs with low CGR composition of original reservoir fluid and 25-ft thickness of the source gas reservoirs	100
Table 5.13: Summarized results of different starting time of dumpflood operation for simultaneous perforation of the two upper source reservoirs with low CGR composition of original reservoir fluid and 25-ft thickness of the source gas reservoirs.....	102
Table 5.14: Summarized results of different perforation sequences of gas dumpflood scenarios starting at the beginning with low CGR composition of original reservoir fluid and 50-ft thickness of the source gas reservoirs	107
Table 5.15: Descriptions of all cases in Section 5.3.2.3.....	109
Table 5.16: Summarized results of different thickness of gas source reservoirs and numbers of perforated source reservoirs with low CGR composition of original reservoir fluid.....	112
Table 5.17: Summarized results of the optimal cases for each production scenario in high CGR.....	116
Table 5.18: Summarized results of the optimal cases for each production scenario in low CGR.....	120
Table A.1: Data for well specification (keyword: WELSPECS)	127
Table A.2: Data for well completion specification of production well (keyword: COMPDAT).....	128
Table A.3: Data for well completion specification of dumping well (keyword: COMPDAT).....	128
Table A.4: Data for segmented well definition (keyword: WELSEGS).....	129

Table A.5: Data for segmented well completion (keyword: COMPSEGS).....	129
Table A.6: Data for segmented vertical flow performance table (keyword: WSEGTABL).....	130
Table A.7: Data for production well control of PROD1 and PROD3 (keyword: WCONPROD).....	131
Table A.8: Data for production well control of PROD2 and DUMP (keyword: WCONPROD).....	131
Table A.9: Data for VLP modeling by PROSPER software.....	132
Table A.10: Temperature gradient for VLP modeling by Prosper.....	133
Table A.11: Variables for VLP modeling by Prosper	134
Table B.1: The economic condensate rates for gas injection of different injection rates.....	136

LIST OF FIGURES

	Page
Figure 3.1: Phase diagram of a gas-condensate system [1].....	9
Figure 3.2: An example of phase diagram of rich (a), middle (b), and poor (c) gas condensate fluids [12].....	10
Figure 3.3: Pressure profile of a gas condensate reservoir illustrating flow region [1]	12
Figure 3.4: Oil saturation profile of a gas condensate reservoir illustrating flow region [13]	12
Figure 3.5: Shift of phase envelope with composition change [13].....	13
Figure 3.6: Flooding patterns [14].....	14
Figure 3.7: Drying effects of CO ₂ concentration in mole percent on two-phase envelope for a CO ₂ -Gas Condensate Mixture [15]	17
Figure 3.8: Two phase vertical flow regimes [19]	20
Figure 4.1: Three-dimensional view of the reservoir model.....	24
Figure 4.2: Two-phase relative permeabilities of gas/oil system.....	30
Figure 4.3: Two-phase relative permeabilities of water/oil system	31
Figure 4.4: Phase behaviors of initial gas condensate composition for two fluid compositions used in this study including (a) high CGR and (b) low CGR	35
Figure 4.5: Diagram of simulation cases for natural depletion scenario.....	37
Figure 4.6: Diagram of simulation cases for conventional gas injection scenario.....	38
Figure 4.7: Diagram of simulation cases for conventional gas dumpflood scenario...39	
Figure 5.1: Field gas production rate profiles of different composition cases of natural depletion scenarios	41

Figure 5.2: Field oil production rate profiles of different composition cases of natural depletion scenarios.....	42
Figure 5.3: Oil saturation distribution of natural depletion scenario with high CGR reservoir fluid when condensate production rate starts to decline (i.e. 31 days of production).....	43
Figure 5.4: Oil saturation distribution of natural depletion scenario with low CGR reservoir fluid when condensate production rate starts to decline (i.e. 90 days of production).....	43
Figure 5.5: Oil saturation distribution at layer $j = 8$ of natural depletion scenario with high CGR reservoir fluid when condensate production rate starts to decline (i.e. 90 days of production).....	44
Figure 5.6: Oil saturation distribution at layer $j = 8$ of natural depletion scenario with low CGR reservoir fluid when condensate production rate starts to decline (i.e. 90 days of production).....	44
Figure 5.7: Phase behaviors of gas condensate composition for high CGR case	45
Figure 5.8: Phase behaviors of gas condensate composition for low CGR case	45
Figure 5.9: Oil saturation distribution of natural depletion scenario with high CGR reservoir fluid at abandonment date (i.e. 670 days of production).....	48
Figure 5.10: Oil saturation distribution of natural depletion scenario with low CGR reservoir fluid at abandonment date (i.e. 731 days of production).....	48
Figure 5.11: Field gas production rate profiles for different gas injection rates of conventional gas injection scenario with high CGR composition of original reservoir fluid.....	51
Figure 5.12: Field condensate production rate profiles for different gas injection rates of conventional gas injection scenario with high CGR composition of original reservoir fluid.....	52

Figure 5.13: (a) Oil saturation distribution and (b) Carbon dioxide mole fraction distribution of case with injection rate of 1.0 MMSCFD of conventional gas injection scenario with high CGR composition of original reservoir fluid when condensate starts to dropout (i.e. 58 days of production)	54
Figure 5.14: (a) Oil saturation distribution and (b) Carbon dioxide mole fraction distribution of case with injection rate of 4.0 MMSCFD of conventional gas injection scenario with high CGR composition of original reservoir fluid when condensate starts to dropout (i.e. 58 days of production)	55
Figure 5.15: (a) Oil saturation distribution and (b) Carbon dioxide mole fraction distribution of case with injection rate of 8.0 MMSCFD of conventional gas injection scenario with high CGR composition of original reservoir fluid when condensate starts to dropout (i.e. 90 days of production)	56
Figure 5.16: (a) Oil saturation distribution and (b) Carbon dioxide mole fraction distribution of case with injection rate of 12.0 MMSCFD of conventional gas injection scenario with high CGR composition of original reservoir fluid when condensate starts to dropout (i.e. 140 days of production)...	57
Figure 5.17: (a) Oil saturation distribution and (b) Carbon dioxide mole fraction distribution of case with injection rate of 16.0 MMSCFD of conventional gas injection scenario with high CGR composition of original reservoir fluid when condensate starts to dropout (i.e. 272 days of production)...	58
Figure 5.18: (a) Oil saturation distribution and (b) Carbon dioxide mole fraction distribution of case with injection rate of 20.0 MMSCFD of conventional gas injection scenario with high CGR composition of original reservoir fluid when condensate starts to dropout (i.e. 546 days of production)...	59
Figure 5.19: Carbon dioxide content of produced gas for different gas injection rates of conventional gas injection scenario with high CGR composition of original reservoir fluid.....	60

Figure 5.20: Cumulative oil production versus time for different gas injection rates of conventional gas injection scenario with high CGR composition of original reservoir fluid.....	61
Figure 5.21: Condensate recovery factor for different starting times of gas injection with high CGR composition of original reservoir fluid	63
Figure 5.22: HC gas recovery factor for different starting times of gas injection with high CGR composition of original reservoir fluid.....	64
Figure 5.23: Field gas production rate profiles for different gas injection rates of conventional gas injection scenario with low CGR composition of original reservoir fluid.....	66
Figure 5.24: Field condensate production rate profiles for different gas injection rates of conventional gas injection scenario with low CGR composition of original reservoir fluid.....	66
Figure 5.25: Carbon dioxide content of produced gas for different gas injection rates of conventional gas injection scenario with low CGR composition of original reservoir fluid.....	68
Figure 5.26: Cumulative condensate production for different gas injection rates of conventional gas injection scenario with low CGR composition of original reservoir fluid.....	68
Figure 5.27: Condensate recovery factor for different starting times of gas injection with low CGR composition of original reservoir fluid	71
Figure 5.28: HC gas recovery factor for different starting times of gas injection with low CGR composition of original reservoir fluid	71
Figure 5.29: Cumulative gas production for different perforation sequences of gas dumpflood scenarios starting at the beginning with high CGR composition of original reservoir fluid and 25-ft thickness of the source gas reservoirs	76

Figure 5.30: Cumulative condensate production for different perforation sequences of gas dumpflood scenarios starting at the beginning with high CGR composition of original reservoir fluid and 25-ft thickness of the source gas reservoirs	76
Figure 5.31: Dumped gas rate profiles for different perforation sequences of gas dumpflood scenarios starting at the beginning with high CGR composition of original reservoir fluid and 25-ft thickness of the source gas reservoirs	77
Figure 5.32: Carbon dioxide mole fraction distribution of simultaneously perforated all four source reservoirs at the beginning with high CGR composition of original reservoir fluid and 25-ft thickness of the source gas reservoirs when abandonment (i.e. 2053 days of production).....	77
Figure 5.33: Carbon dioxide mole fraction distribution of simultaneously perforated two lower source reservoirs at the beginning with high CGR composition of original reservoir fluid and 25-ft thickness of the source gas reservoirs when abandonment (i.e. 1550 days of production).....	78
Figure 5.34: Gas production profiles for different starting times of dumpflood operation having simultaneous perforation all of source reservoirs with high CGR composition of original reservoir fluid and 25-ft thickness of the source gas reservoirs	81
Figure 5.35: Condensate production for different starting times of dumpflood operation having simultaneous perforation all of source reservoirs with high CGR composition of original reservoir fluid and 25-ft thickness of the source gas reservoirs	82
Figure 5.36: Cumulative gas production versus time for starting times of dumpflood operation having simultaneous perforation all of source reservoirs with high CGR composition of original reservoir fluid and 25-ft thickness of the source gas reservoirs	82

Figure 5.37: Cumulative oil production rates versus time for different starting times of dumpflood operation having simultaneous perforation all of source reservoirs with high CGR composition of original reservoir fluid and 25-ft thickness of the source gas reservoirs	83
Figure 5.38: Carbon dioxide content in produced gas for different starting times of dumpflood operation having simultaneous perforation all of source reservoirs with high CGR composition of original reservoir fluid and 25-ft thickness of the source gas reservoirs	83
Figure 5.39: Condensate, HC gas, and total BOE recoveries for all cases with high CGR composition of original reservoir fluid and 25-ft thickness of the source gas reservoirs.....	85
Figure 5.40: Cumulative gas production for different perforation sequences of gas dumpflood scenarios starting at the beginning with high CGR composition of original reservoir fluid and 50-ft thickness of the source gas reservoirs	87
Figure 5.41: Cumulative condensate production for different perforation sequences of gas dumpflood scenarios starting at the beginning with high CGR composition of original reservoir fluid and 50-ft thickness of the source gas reservoirs	87
Figure 5.42: Cumulative dumped gas for different perforation sequences of gas dumpflood scenarios starting at the beginning with high CGR composition of original reservoir fluid and 50-ft thickness of the source gas reservoirs	88
Figure 5.43: Condensate, HC gas, and total BOE recoveries for all cases with high CGR composition of original reservoir fluid and 50-ft thickness of the source gas reservoirs.....	90

Figure 5.44: Cumulative gas production versus time for different thickness of gas source reservoirs and numbers of perforated source reservoirs with high CGR composition of original reservoir fluid.....	92
Figure 5.45: Cumulative gas production versus time for different thickness of gas source reservoirs and numbers of perforated source reservoirs with high CGR composition of original reservoir fluid.....	93
Figure 5.46: Cumulative condensate production versus time for different thickness of gas source reservoirs and numbers of perforated source reservoirs with high CGR composition of original reservoir fluid	93
Figure 5.47: Condensate production profiles for different perforation sequences of gas dumpflood scenarios starting at the beginning with low CGR composition of original reservoir fluid and 25-ft thickness of the source gas reservoirs	96
Figure 5.48: Cumulative dumped gas for different perforation sequences of gas dumpflood scenarios starting at the beginning with low CGR composition of original reservoir fluid and 25-ft thickness of the source gas reservoirs	96
Figure 5.49: Cumulative condensate production for different perforation sequences of gas dumpflood scenarios starting at the beginning with low CGR composition of original reservoir fluid and 25-ft thickness of the source gas reservoirs	97
Figure 5.50: Gas production profiles for different perforation sequences of gas dumpflood scenarios starting at the beginning with low CGR composition of original reservoir fluid and 25-ft thickness of the source gas reservoirs	97

Figure 5.51: Cumulative condensate production for different starting times of dumpflood operation for simultaneous perforation of all source reservoirs with low CGR composition of original reservoir fluid and 25-ft thickness of the source gas reservoirs	99
Figure 5.52: Cumulative condensate production for different starting times of dumpflood operation for simultaneous perforation of the two upper source reservoirs with low CGR composition of original reservoir fluid and 25-ft thickness of the source gas reservoirs	101
Figure 5.53: Condensate production profiles for cases 1-3 and 4-3 with low CGR composition of original reservoir fluid and 25-ft thickness of the source gas reservoirs	101
Figure 5.54: Condensate, HC gas, and total BOE recoveries for all cases with low CGR composition of original reservoir fluid and 50-ft thickness of the source gas reservoirs.....	104
Figure 5.55: Cumulative gas production for different perforation sequences of gas dumpflood scenarios starting at the beginning with low CGR composition of original reservoir fluid and 25-ft thickness of the source gas reservoirs	106
Figure 5.56: Cumulative condensate production for different perforation sequences of gas dumpflood scenarios starting at the beginning with low CGR composition of original reservoir fluid and 25-ft thickness of the source gas reservoirs	106
Figure 5.57: Condensate, HC gas, and total BOE recoveries for all cases with low CGR composition of original reservoir fluid and 50-ft thickness of the source gas reservoirs.....	108

Figure 5.58: Cumulative gas production versus time for different thickness of gas source reservoirs and numbers of perforated source reservoirs with low CGR composition of original reservoir fluid.....	110
Figure 5.59: Cumulative gas production versus time for different thickness of gas source reservoirs and numbers of perforated source reservoirs with low CGR composition of original reservoir fluid.....	111
Figure 5.60: Cumulative condensate production versus time for different thickness of gas source reservoirs and numbers of perforated source reservoirs with low CGR composition of original reservoir fluid.....	111
Figure 5.61: Cumulative gas production profiles of the optimal cases for each production scenario.....	115
Figure 5.62: Cumulative condensate production profiles of the optimal cases for each production scenario.....	115
Figure 5.63: Cumulative oil-equivalent gas production profiles of the optimal cases for each production scenario.....	119
Figure 5.64: Cumulative condensate production profiles of the optimal cases for each production scenario.....	119

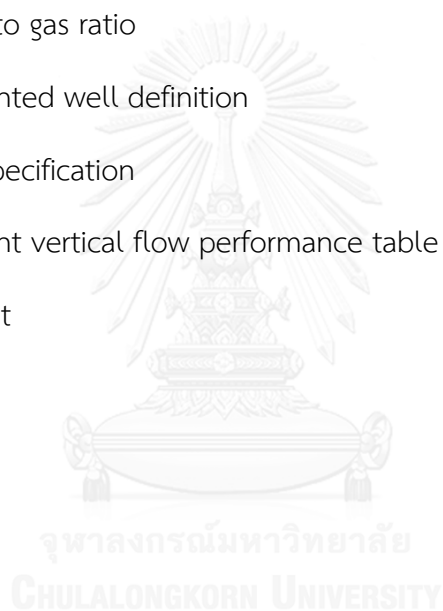
LIST OF ABBREVIATIONS

API	American Petroleum Institute
BCF	billion standard cubic feet
BHP	bottomhole pressure
BOE	barrel of oil equivalent
BTU	British thermal unit
°C	degree Celsius
C ₁	methane
C ₂	ethane
C ₃	propane
i-C ₄	isobutane
n-C ₄	normal butane
i-C ₅	isopentane
n-C ₅	normal pentane
C ₆	hexane
C ₇	heptane
C ₇₊	heptane and hydrocarbon compound that is heavier than heptane
CGR	condensate to gas ratio
cm	centimeter
CO ₂	carbon dioxide
COMPDAT	well completion specification data
COMPSEGS	segmented well completion
cP	centipoise

D	day
EGAT	Electricity Generating Authority of Thailand
EOR	enhanced oil recovery
EOS	equation of state
°F	degree Fahrenheit
FH	Friction and hydrostatic losses
FIX	Fixing the lookup value of the flow rate at the first flow point in the table
ft	feet
g	gram
GOR	gas to oil ratio
h	hour
HC	hydrocarbon
HP	horse power
ID	internal diameter
in.	inch
lb	pound mass
lbmole	pound mole
kW	kilowatt
kWh	kilowatt-hour
LEN	The interpolated pressure drop is scaled in proportion to the length of the segment relative to the table's datum length
m	meter
M	thousand

MBOE	thousand barrel of oil equivalent
mD	millidarcy
MM	million
MMBOE	million barrel of oil equivalent
MMP	minimum miscibility pressure
MMSCF	million standard cubic feet
MMSCFD	million standard cubic feet per day
MMSTB	million stock tank barrel
MSCF	thousand standard cubic feet
MSTB	thousand stock tank barrel
N ₂	nitrogen
ppm	parts per million
psi	pound force per square inch
psia	pound force per square inch absolute
psig	pound force per square inch gauge
PVT	pressure volume temperature
°R	degree Rankine
RB	reservoir barrel
SCAL	special core analysis
SCF	standard cubic feet
sec	second
STB	stock tank barrel
THP	tubing head pressure
TVD	true vertical depth

USD	United States dollars
USGS	United States Geological Survey
VFP	vertical flow performance
VFPPROD	vertical flow performance table for production wells
VLP	vertical lift performance
VRR	voidage replacement ratio
WCONPROD	production well control
WGR	water to gas ratio
WELSEGS	segmented well definition
WELSPECS	well specification
WSEGTABL	segment vertical flow performance table
%	percent



NOMENCLATURES

Latin Alphabet

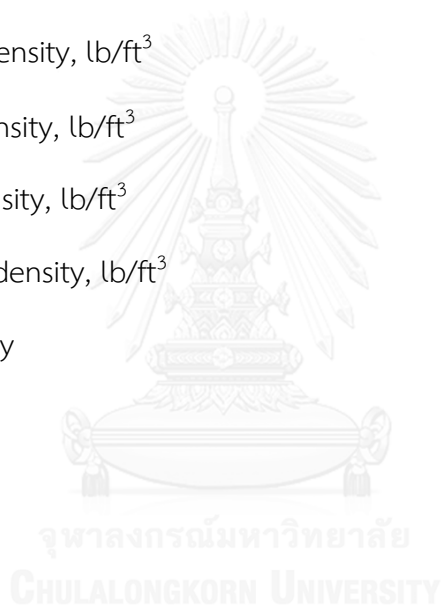
E	overall sweep efficiency
E_A	areal sweep efficiency
E_D	displacement efficiency
E_I	invasion or vertical sweep efficiency
E_V	volumetric sweep efficiency
k	absolute permeability, mD
k_r	relative permeability
k_{rg}	relative permeability to gas
$k_{rg}(s_{g\max})$	relative permeability to gas at maximum gas saturation
$k_{rg}(s_{org})$	relative permeability to gas at residual oil saturation in oil-gas system
k_{ro}	relative permeability to oil
$k_{ro}(s_{g\min})$	relative permeability to oil at minimum gas saturation
$k_{ro}(s_{w\min})$	relative permeability to oil at minimum water saturation
k_{rw}	relative permeability to water
$k_{rw}(s_{orw})$	relative permeability to water at residual oil saturation in water-oil system
$k_{rw}(s_{w\max})$	relative permeability to water at maximum water saturation
L_c	higher heating value of gas mixture, BTU/SCF
L_{cj}	higher heating value of component j, BTU/SCF
P	compression power, HP

p_1	compressor suction pressure, psia
p_2	compressor discharge pressure, psia
p_d	dewpoint pressure, psia
p_f	fracture pressure, psia
p_R	reservoir pressure, psia
$p_{R, Abandonment}$	reservoir pressure at abandonment, psia
$p_{R, Origin}$	reservoir pressure at origin, psia
p_{ref}	reference pressure, psia
$\left(\frac{dp}{dx}\right)_f$	fracture pressure gradient, psia/ft.
q_g	gas compression or injection rate, MSCF/D
S_g	gas saturation
S_{gcr}	critical gas saturation
S_{gi}	initial gas saturation
S_{gmin}	minimum gas saturation
S_o	oil saturation
S_{org}	residual oil saturation in the gas-oil system
S_{orw}	residual oil saturation in the oil-water system
S_w	water saturation
S_{wcr}	critical water saturation
S_{wi}	initial water saturation
S_{wmax}	maximum water saturation
S_{wmin}	minimum water saturation

T_R	reservoir temperature, °F
y_j	mole fraction in gas of component j

Greek Symbol

μ	fluid viscosity, cP
μ_g	gas viscosity, cP
μ_o	oil viscosity, cP
μ_w	water viscosity, cP
ρ	fluid density, lb/ft ³
ρ_g	gas density, lb/ft ³
ρ_o	oil density, lb/ft ³
ρ_w	water density, lb/ft ³
ϕ	porosity



CHAPTER 1

INTRODUCTION

1.1 Background

A gas-condensate reservoir contains a single-phase fluid in the form of gas at initial reservoir conditions. As the fluid is produced from producing wells, the reservoir pressure decreases with the largest pressure drop near the producing wells. Consequently, the less distance from the producing wells, the more pressure drop. At a certain region where the pressure is just below the dewpoint pressure, condensate liquid first drops out from the gas phase and it is immobile because of capillary forces acting on the fluids and not enough condensate saturation. Thus, there is still single-phase gas flow in this condensate buildup region. The valuable components of the gas-condensate fluids are unrecoverable and lost in the reservoir. In the region closer to the producing wells, the condensate saturation may be greater than the critical condensate saturation. As a result, both gas and liquid condensate would flow in this region. The gas relative permeability would reduce and eventually cause the additional pressure drop [1]. This phenomenon is called condensate blockage or condensate banking and resulting in significant reduction in the productivity of the well.

Gas injection can be used to increase the reservoir pressure in order to enhance condensate recovery. However, this technique can cause high capital and operating costs. A more economic method of gas dumpflood has been proposed to eliminate the cost of gas injection. Gas dumpflood is relatively low-cost and an attractive alternative than gas injection because it requires additional investment only on simple adjustment of downhole completion. Nevertheless, a source gas reservoir is required to perform this technique. Since, in the Gulf of Thailand, many gas reservoirs are multi-stack thin layers of small sizes [2] and some of these reservoirs are not economically produced because of high carbon-dioxide content, dumping gas from multiple gas source reservoirs into a gas-condensate reservoir should be considered.

To evaluate the performance of gas dumpflood from multiple source reservoirs into a condensate reservoir, ECLIPSE 300 reservoir simulator is used in this study to construct a hypothetical model. The simulation model consists of a gas-condensate reservoir with several underlying thin-layered high carbon-dioxide gas reservoirs. Several parameters and production scenarios are considered in this study such as condensate gas ratio, sizes of source reservoirs, perforation sequence of dumping well, and timing of the dumpflood process. The performance of each case is evaluated based on condensate recovery.

1.2 Objectives

1. To compare performance of natural depletion, conventional gas injection, and dumpflood from multiple high carbon-dioxide reservoirs in terms of hydrocarbon recovery.
2. To investigate effects of several parameters including condensate gas ratio, sizes of source reservoirs, perforation sequence of dumping well, and timing on gas dumpflood process from multiple sources into a condensate reservoir.

1.3 Outline of Methodology

1. Construct a base-case model and perform simulation of hydrocarbon production using three techniques:
 - 1.1 Natural depletion
 - 1.2 Conventional gas injection
 - 1.3 Gas dumpflood from multiple-gas reservoirs into a condensate reservoir
2. Perform three strategies for two different fluid compositions yielding different condensate to gas ratios.
3. Simulate conventional gas injection models with different gas injection rates in order to evaluate the optimal gas injection rate.
4. Simulate gas dumpflood model with different system parameters in order to determine the optimal condition for gas dumpflood scenario.

- 4.1 Size of multiple source reservoirs for dumping
- 4.2 Perforation sequence of dumping well
- 4.3 Starting time of dumpflood
5. Analyze the results from the simulations and discuss the results
6. Conclude the results of the research and express the recommendation of this study

1.4 Outline of Thesis

There are six chapters in this thesis consisting of:

Chapter 1 introduces the background and obstacle of gas condensate production by conventional techniques and the basic concept how this research can help solve the existing problem. The objectives and the outline of methodology are included in this chapter as well.

Chapter 2 presents several reviews of previously published literatures related to gas dumpflood and gas injection into a gas condensate reservoir.

Chapter 3 summarizes crucial theories and concepts involving gas dumpflood and gas injection into a gas condensate reservoir.

Chapter 4 illustrates the details of the reservoir model including case definition, grid, fluid properties, special core analysis, and production parameters used in the simulation.

Chapter 5 discusses the results of the reservoir simulations obtained from different production strategies and critical parameters.

Chapter 6 provides conclusions for this research and recommendations for further study.

CHAPTER 2

LITERATURE REVIEW

Previous studies related to carbon dioxide flooding into a condensate reservoir are reviewed and summarized in this chapter. These studies are categorized into two sections including 1) study of gas dumpflood both simulated models and actual field implementation and 2) study related to conventional carbon dioxide injection consisting of core flooding experiments, simulation models, and real field implementations. These literatures show the successful implementation of gas dumpflood and CO₂ injection in gas and condensate reservoirs. Some of finding and information from this literature are used as guideline to design the reservoir model and the production plan in this study.

2.1 Study of Gas Dumpflood

Rinadi et al. [3] studied the implementation of in-situ gas lift and gas dumpflood technologies to increase production and improve recovery from a partially depleted oil reservoir in North Arthit field that stopped producing due to a low gas oil ratio and insufficient lifting capacity. Although several methods had been performed to reactivate the well including several blow downs and additional perforation, the outcome was not successful. The simulation study illustrates that the well could be successfully reactivated by using in-situ gas lift. The gas oil ratio of the well was increased three fold from the previous 450 SCF/STB. The in-situ gas dumpflood would further increase the oil rate to the highest value of 3,000 barrel of oil per day at well head pressure of 50 barg.

Kridsanan [4] studied the mechanism of gas dumpflood in gas-condensate reservoir to enhance condensate recovery using a compositional reservoir model consisting of a gas-condensate reservoir and a source reservoir (high CO₂ content). Several production scenarios have been investigated such as natural depletion, conventional injection, and gas dumpflood. The results indicate that both conventional CO₂ injection and gas dumpflood can provide higher condensate

recovery than natural depletion. Although CO₂ injection has a bit higher cumulative condensate recovery and slightly longer production life time than gas dumpflood, this process needs investment on gas injection system which is the important disadvantage of CO₂ injection.

The author also evaluated several parameters that affect gas dumpflood process including starting time of the process, concentration of CO₂ in the source reservoir, and depth difference between the source and target reservoirs. As a result, starting dumpflood process before the pressure of the target reservoir falls below the dewpoint results in high condensate recovery. A higher concentration of CO₂ in the source gas results in a slightly higher condensate recovery but lower hydrocarbon gas recovery due to high CO₂ content. The larger depth difference or pressure difference between the source and target reservoirs slightly increases condensate recovery and effectively shortens the producing time.

2.2 Study of Conventional Carbon Dioxide Injection

Shi et al. [5] performed core flooding experiment with two component synthetic gas-condensate and compositional simulations of multicomponent gas-condensate fluid. The objectives of this study are to investigate the behavior of condensate composition variation, condensate saturation build-up and condensate recovery during a gas-condensate production process. From the simulation results, it can be concluded that high total gas production can be temporarily achieved by rapid ramping time or using low BHP. However, slower ramping time or higher BHP can minimize condensate banking blockage and hence result in enhancing the liquid and gas recovery. In other words, higher BHP may be a better strategy for a long-term production. In summary, they concluded that there is no standard way to optimize the production strategy and that the optimal approach of BHP is likely to be dependent on the original composition of fluids in the reservoirs.

Al-Hashami et al. [6] simulated a compositional model with options for diffusion and gas dissolution in water to investigate the process of injecting CO₂ into gas reservoir for enhanced gas recovery. Their study includes the effects of gas diffusion and

solubility, timing of the injection, and injection rate. The reservoir simulation model indicates that CO₂ injection can technically enhance gas recovery up to 8-11% increment in general. High gas diffusion can cause an early CO₂ breakthrough. However, effect of diffusion can be ignored if the gas diffusion is less than 10⁻⁶ m²/sec. The dissolubility in formation water is beneficial for delaying CO₂ breakthrough. Although high injection rate can be used to enhance gas recovery, an excessive rate can reduce gas recovery because of early CO₂ breakthrough and high CO₂ concentration in produced gas.

Jalil et al. [7] studied CO₂ injection and sequestration in a depleted gas condensate reservoir in Malaysia. A black oil model was generated and used as history matching mode. After that, it was converted into compositional model in order to simulate CO₂ injection and storage modeling. As a result, effective CO₂ storage capacity can be determined from numerical simulation model which accounts well injectivity potential and injection constraints such as BHP limit and geomechanical concerns. The storage estimation from volumetric and production data provides less accurate results. Although the reservoir has potential to accommodate CO₂ 40% bigger than GIIP from the simulation results, this requires high CO₂ injection rate with shorter injection plateau period, leading to impractical and uneconomical surface facility.

Kalra et al. [8] constructed a depleted gas reservoir model using compositional simulation in order to investigate CO₂ phase behavior in subsurface conditions. In this study, several parameters including reservoir depth, depletion pressure ratio which is pressure at starting of the injection to initial pressure ratio, aquifer activity, inclination angle, reservoir heterogeneity with various permeability arrangement, injection rate, and producer bottom hole pressure were studied.

The simulation results indicate that shallow reservoirs below depths of 4,000 ft. provides less storage capacity and can be ignored for carbon storage and enhanced gas recovery. The density and viscosity contrast between CO₂ and CH₄ is very high beyond 4,000 ft. making these reservoirs a suitable candidate for enhanced gas recovery and CO₂ storage. Although an additional 60% or more of gas in the depleted reservoir can be recovered, highly heterogeneous reservoir will lower natural gas

recovery and reduce the pore volume of CO₂ being sequestered because of bigger mixing zones in the formation. Strong aquifer can sustain high production rate. However, aquifer invasion also traps a large quantity of gas which cannot be produced. The lower depletion pressure ratios provided higher natural gas recovery and more CO₂ storage.

Clark et al. [9] presented a method developed for Boquerón field to compute voidage replacement ratio (VRR) using compositional full field model and an EOS program. VRR is cumulative volume of injection fluid at reservoir conditions to cumulative volume of production fluid at reservoir conditions ratio which is commonly used to measure the rate of change in reservoir energy and is often an important factor in planning EOR projects. The VRR will be balanced when it equals to 1 or, in another word, volume of production equals to volume of injection. A mechanism to control regional voidage can be provided by calculating VRR on a continuous basis. For example, if a particular region is more depleted than the others, supplementary gas can be additionally injected into that region.

Thitaram [10] investigated the effect of fluid composition in gas condensate reservoir on CO₂ injection in order to maximize condensate recovery. A hypothetical reservoir model was developed with ten different compositions of reservoir fluid yielding different condensate to gas ratios. This study found that the higher CO₂ concentration after mixing between injection and reservoir fluids, the lower dewpoint of the new mixture which results in better revaporization of the liquid dropout. The reservoir fluid which has higher dewpoint pressure requires earlier CO₂ injection or higher injection rate. If CO₂ injection is started too early or the injection rate is too high, CO₂ breakthrough time will be accelerated, resulting in shorter production life and lower condensate and gas recovery. In contrast, if CO₂ injection is started too late or the injection rate is too low, the liquid dropout will not be completely revaporized, resulting in lower recovery.

CHAPTER 3

THEORY AND CONCEPT

Crucial concepts and theories involving CO₂ dumpflood into a gas condensate reservoir are summarized in this chapter. The contents are divided into three main parts: 1) behavior of gas condensate reservoir including phase and flow behavior and also composition change during depletion, 2) CO₂ flooding in gas condensate reservoir consisting of several mechanism and basic theories of gas flooding, 3) recovery calculation concept applied in this study which is calculated in term of barrel of oil equivalent, and 4) two phase flow regimes inside the vertical tubing.

3.1 Gas Condensate Reservoir

There are five types of reservoir fluids which are black oil, volatile oil, retrograde gas, wet gas, and dry gas. These types of reservoir fluids have been defined because each has unique characteristics. Five indicators can be primarily used to identify the type of reservoir fluids which are initial producing gas-oil ratio, gravity of the stock-tank liquid, color of the stock-tank liquid, oil formation volume factor, and mole fraction of heptane plus. If all five indicators do not fit the ranges, the types of the reservoir fluid have to be confirmed by observation in the laboratory [11].

Gas-condensate reservoir is a reservoir that consists of single phase retrograde gas as a reservoir fluid at the initial reservoir condition. It is considered as the most complex reservoir among other types of petroleum reservoirs. As reservoir pressure declines and reaches the dewpoint, condensate starts to drop out of the gas and results in one unique phenomenon in near wellbore region of gas-condensate reservoir which is condensate blockage.

3.1.1 Phase Behavior of Gas-Condensate

Gas-condensate or retrograde gas has unique characteristics of phase diagram as illustrated in Figure 3.1. The saturated envelope in the phase diagram of a retrograde gas is smaller than that for oils, and the critical point is further down the left side of

the envelope. The phase diagram of a retrograde gas also has reservoir pressure greater than the critical temperature but less than the cricondentherm, the highest temperature on the saturated envelope.

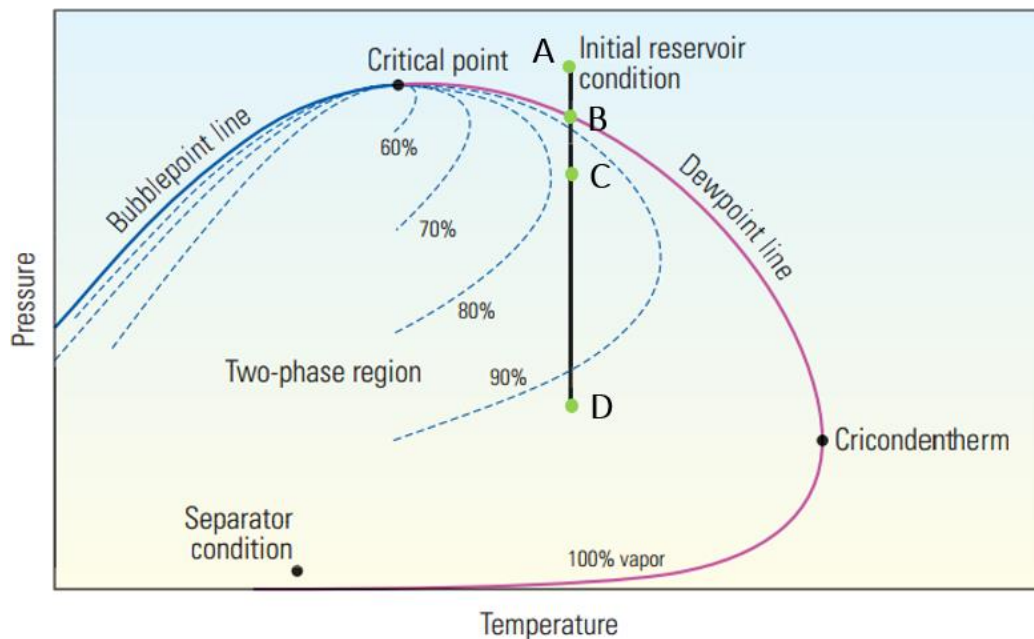


Figure 3.1: Phase diagram of a gas-condensate system [1]

The fluid in the gas-condensate reservoir is totally single phase gas at the original reservoir condition (point A). As the reservoir pressure decreases to a certain condition called dewpoint pressure, liquid that is a retrograde condensate starts to drop out from the gas phase (point B). The condensate dropout or blockage in the pore space will lead to a reduction in the gas production of the well. The condensate continually drops out more and more until the point of maximum liquid volume is reached (point C). Further reduction in the reservoir pressure will cause revaporization process (point C to point D). This process, however, typically happens after economic life of the field. Thus, this stage will not be reached in practice.

The quantity of condensate dropout does not only depend on the reservoir conditions including temperature and pressure but also depends on the composition of the reservoir fluid. Gas condensate fluid can be classified into three main types: poor, middle, and rich gas condensate [12]. The physical characteristics and the classifications are listed in Table 3.1.

Table 3.1: Physical characteristics of different types of gas condensate [12]

Fluid type	Heavier hydrocarbon content C_{7+}	Reservoir fluid density	Production GOR	Condensate content
	Percent mole	g/cm^3	m^3/m^3	g/m^3
Poor	0.5 – 2.0	0.20 – 0.25	18000 – 5000	< 150
Middle	2.0 – 4.0	0.25 – 0.35	5000 – 2000	150 – 350
Rich	4.0 – 9.0	0.30 – 0.45	2000 – 1000	250 – 600

A rich gas condensate shown in Figure 3.2 (a) forms higher percentage of liquid volume than a middle and a poor gas condensate shown in Figure 3.2 (b) and Figure 3.2 (c), respectively.

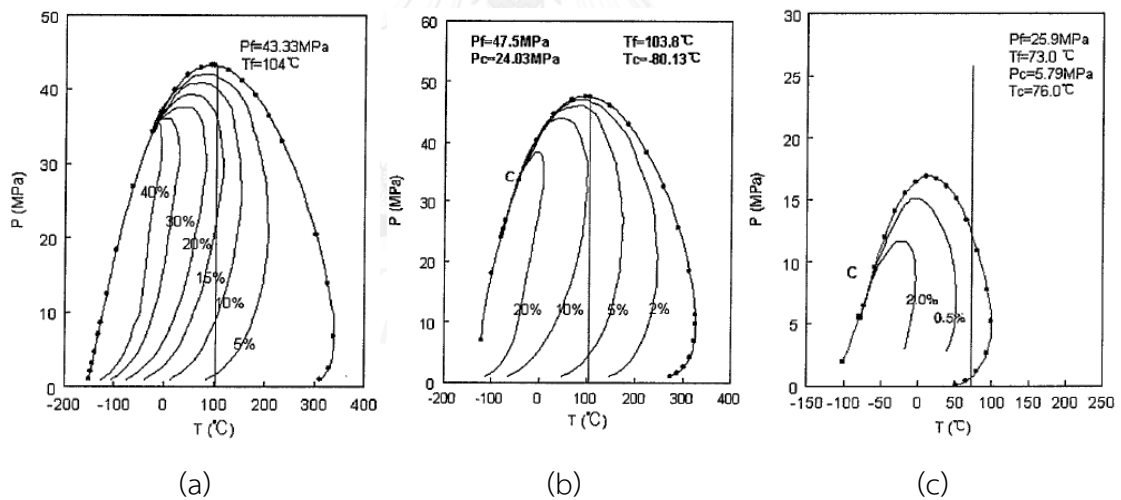


Figure 3.2: An example of phase diagram of rich (a), middle (b), and poor (c) gas condensate fluids [12]

3.1.2 Flow Behavior of Gas Condensate

Conceptually, fluid flow in gas condensate reservoirs during production period can be divided into three main flow regions as depicted in Figure 3.3 and Figure 3.4, even though not all three regions are present in some situations [1]. The first two

regions are closest to the producing well. They exist when the pressure is below the dewpoint pressure and the third region exists when its pressure is above the dewpoint pressure.

The first one is near-wellbore region, close to the producing well. Since condensate saturation here is greater than the critical point, both gas and condensate phase flow in this near-wellbore region with different velocities depending on relative permeability of each phase. The oil relative permeability increases with condensate saturation while gas relative permeability decreases, illustrating the blockage effect.

The second one is condensate-buildup region. The condensate starts to drop out of the gas but it is immobile because of capillary force acting on the liquid. In this condensate-buildup region, both liquid and gas phases are present, but only gas flows. As a consequence, the valuable condensate that forms in this region cannot be produced and the produced gas contains fewer valuable heavy ends of hydrocarbon. The interior boundary of this region is where the condensate saturation reaches the critical point for flowing as shown in Figure 3.4.

The third region is far away from the producing well and includes most of the reservoir. Since the pressure is higher than the dewpoint pressure, only gas phase is present and flowing in this region. The gas composition in this region is similar to the original reservoir gas, and the gas velocity is generally low because the cross sectional area is high. The boundary between third region and second region occurs where the pressure equals the dewpoint pressure of the original reservoir gas. This boundary moves outward from the well as the pressure declines because of the production as shown in Figure 3.3. Eventually, it disappears as the outer-boundary pressure drops below the dewpoint pressure.

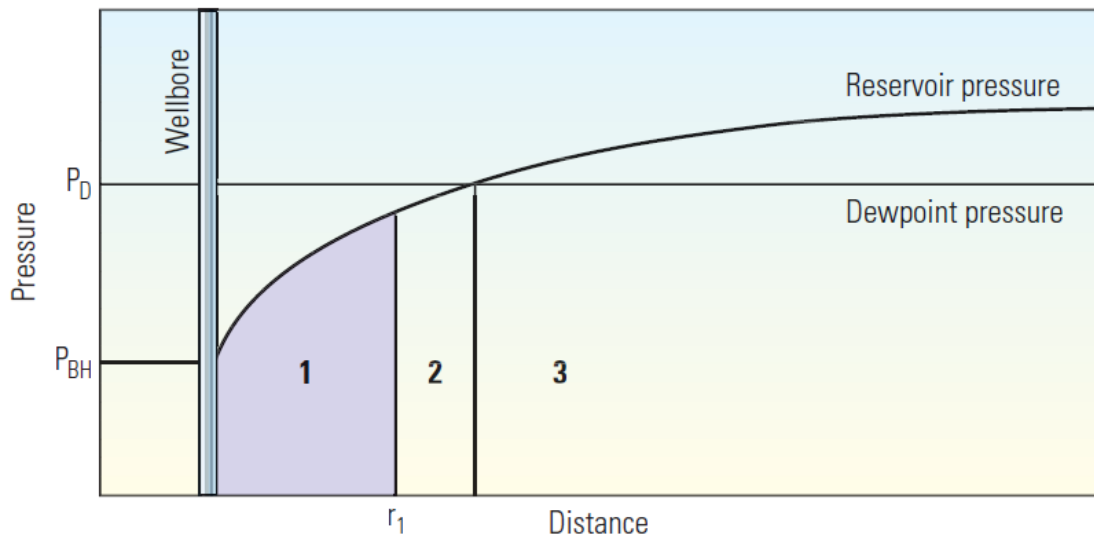


Figure 3.3: Pressure profile of a gas condensate reservoir illustrating flow region [1]

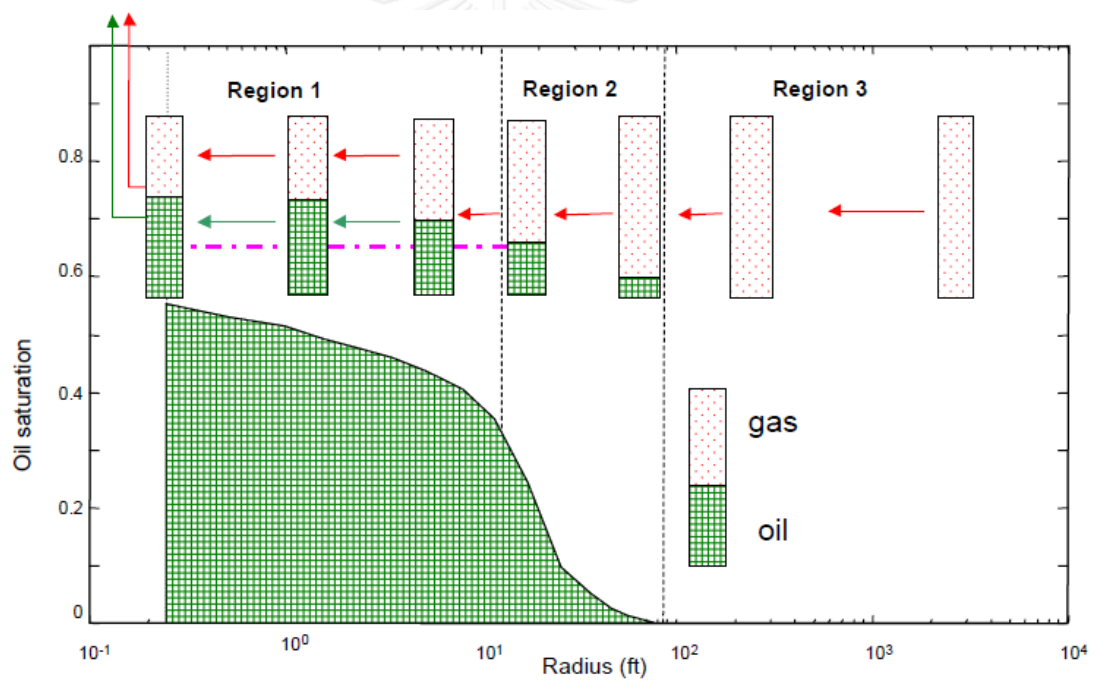


Figure 3.4: Oil saturation profile of a gas condensate reservoir illustrating flow region [13]

3.1.3 Fluid Composition Change by Condensation Process

Between the original reservoir condition (point B) and dewpoint pressure (point B1) as illustrated in Figure 3.5, the fluid remains single phase gas as the original fluid. Due to depletion of the gas condensate reservoir, the pressure declines until it is below

the dewpoint pressure of the original fluid (point B1). Then, intermediate and heavier components start to condense in the reservoir and only the gas phase is flowing and produced at low condensate saturations. Thus, produced fluid contains less fractions of intermediate and heavy components compared to original reservoir fluid. The composition of the reservoir fluid subsequently becoming richer in intermediate and heavy components. This transformation of the fluid composition can be demonstrated by a shift of the phase envelope as shown in Figure 3.5. It is important to note that more and more condensate will drop out until the pressure reaches point B'2 where the condensate saturation is the maximum for a given composition of the reservoir fluid. After that, further depletion of the pressure will result in revaporization of the condensate and a second dewpoint may be encountered eventually.

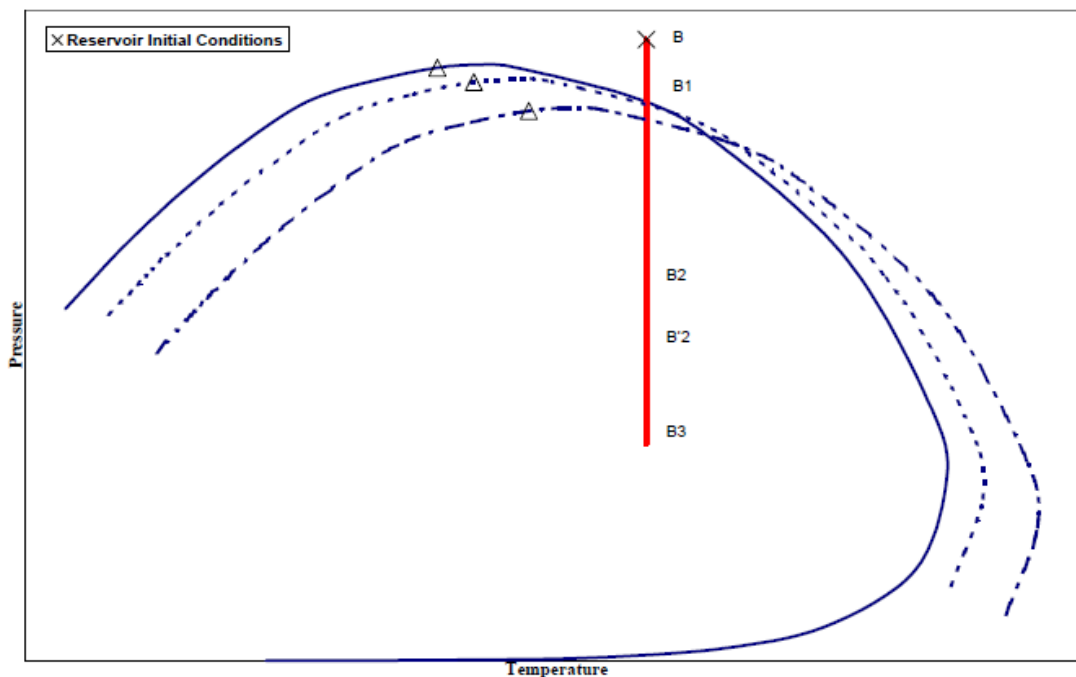


Figure 3.5: Shift of phase envelope with composition change [13]

3.2 CO₂ Flooding in Gas Condensate Reservoir

In natural depletion, a gas condensate reservoir is produced and condensate will later drop out when the dewpoint pressure is reached resulting in condensate blockage. This phenomenon will consequently obstruct productivity of the gas

condensate reservoir. The condensate recovery factor of natural depletion is only 20 - 40% [12] as a result of this effect.

Repressurizing the condensate reservoir is a common method for maintaining the reservoir pressure above the dewpoint pressure and preventing condensate blockage. CO₂ flooding by injection or dumpflood is one of the techniques for repressurization of gas condensate reservoirs. A positive point of CO₂ flooding is revaporization of condensate contents in the reservoir and therefore yielding higher condensate recovery than that of natural depletion approach.

3.2.1 Flooding Patterns

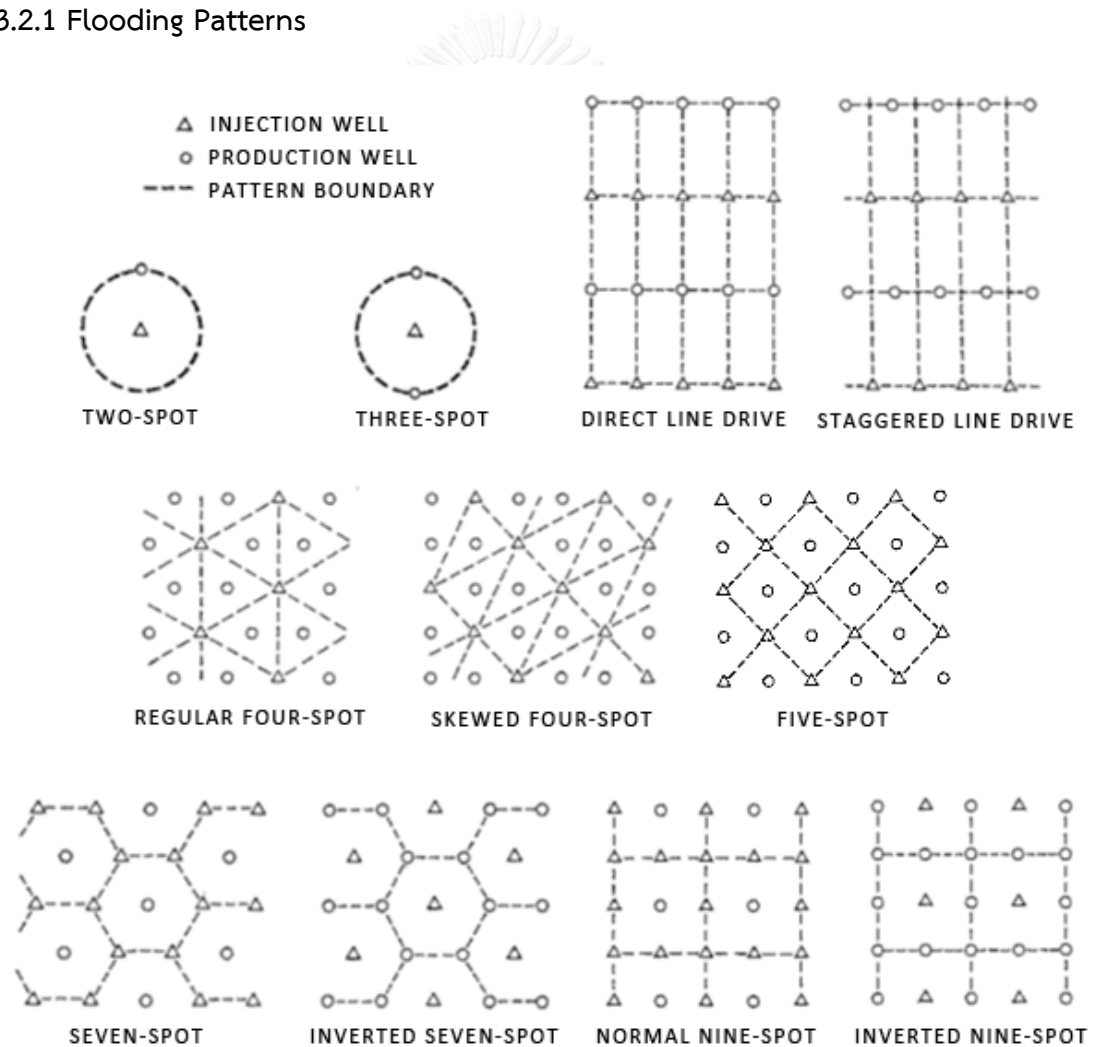


Figure 3.6: Flooding patterns [14]

A flow regime of a fluid in a reservoir is controlled by arrangement of production wells and injection wells. There are several patterns of arrangements as depicted in Figure 3.6. The difference between “normal” and “inverted” well arrangement is that the patterns termed “inverted” have only one injection well per pattern. It is worth to note that the inverted seven-spot and the regular four-spot patterns are identical.

Different flooding patterns will result in different areal sweep efficiencies. Various experimental techniques were developed to determine areal sweep efficiencies at mobility ratio of 1.0 as shown in Table 3.2. Invert seven-spot provides the highest areal sweep efficiency at breakthrough of 82.2%.

In this study, isolated flooding pattern is applied in the reservoir model because the area of reservoir is quite small in order to imitate multi-stack thin layers of small size reservoirs in the Gulf of Thailand. Comparing between isolated two-spot and three-spot patterns, the isolated three-spot pattern can increase areal sweep efficiency at breakthrough around 24.7% – 26.0% from the isolated two-spot pattern. Therefore, the selected flooding pattern is isolated three-spot.

Table 3.2: Areal sweep efficiencies for various flooding patterns [14]

Flooding pattern	Mobility ratio	Areal sweep efficiency at breakthrough (%)
Isolated two-spot	1.0	52.5 – 53.8
Isolated three-spot	1.0	78.5
Skewed four-spot	1.0	55.0
Inverted five-spot	1.0	80.0
Normal seven-spot	1.0	74.0 – 82.0
Invert seven-spot	1.0	82.2

3.2.2 Overall Sweep Efficiency

The overall sweep efficiency is a measure of competence of displacement process by flooding fluids. It depends on the volume of the original reservoir fluids displaced by flooding fluids. The overall sweep efficiency can be affected by injection pattern, mobility ratio, reservoir thickness, permeability, fractures, position of gas-oil and oil-water contacts, and areal and vertical heterogeneity. As expressed in Equation (3.1), the overall sweep efficiency is defined as a combination of three efficiencies which are areal sweep efficiency (E_A), invasion or vertical sweep efficiency (E_I), and displacement efficiency (E_D). The volumetric sweep efficiency (E_V) or a combination of areal sweep efficiency and vertical sweep efficiency is the volumetric fraction of the reservoir displaced by the flooding fluids as shown in Equation (3.2) - (3.4). The displacement efficiency (E_D) is fraction of movable fluids that is displaced in the swept zone of the reservoir as shown in Equation (3.5).

$$E = E_A \times E_I \times E_D \quad (3.1)$$

$$E_V = E_A \times E_I \quad (3.2)$$

$$E_A = \frac{\text{Displaced area of the pattern}}{\text{Total area of the pattern}} \quad (3.3)$$

$$E_I = \frac{\text{Displaced crosssectional area}}{\text{Total crosssectional area}} \quad (3.4)$$

$$E_D = \frac{\text{Displaced movable fluids}}{\text{Total movable fluids}} \quad (3.5)$$

where

E = overall sweep efficiency

E_A = areal sweep efficiency

E_V = volumetric sweep efficiency

E_I = invasion or vertical sweep efficiency

E_D = displacement efficiency

3.2.3 Fluid Composition Change by Flooding Process

Drying effect is the result from CO₂ mixing with gas condensate fluids which is explained by the shrinking of two-phase envelope. Ramharak et al [15] investigated the impact of CO₂ on gas condensate reservoir and found that drying effect can affect the phase diagram of gas condensate as shown in Figure 3.7. The shrinking of the two-phase envelope is reduction of cricondentherm and cricondenbar when CO₂ concentration increases. This indicates partial revaporization of the condensate into the gas phase. When the concentration of CO₂ is continuously increasing, this shrinking will be more and more pronounced. Once the cricondentherm of the two-phase envelope is lower than reservoir temperature, only single gas phase is allowed to present in this condition.

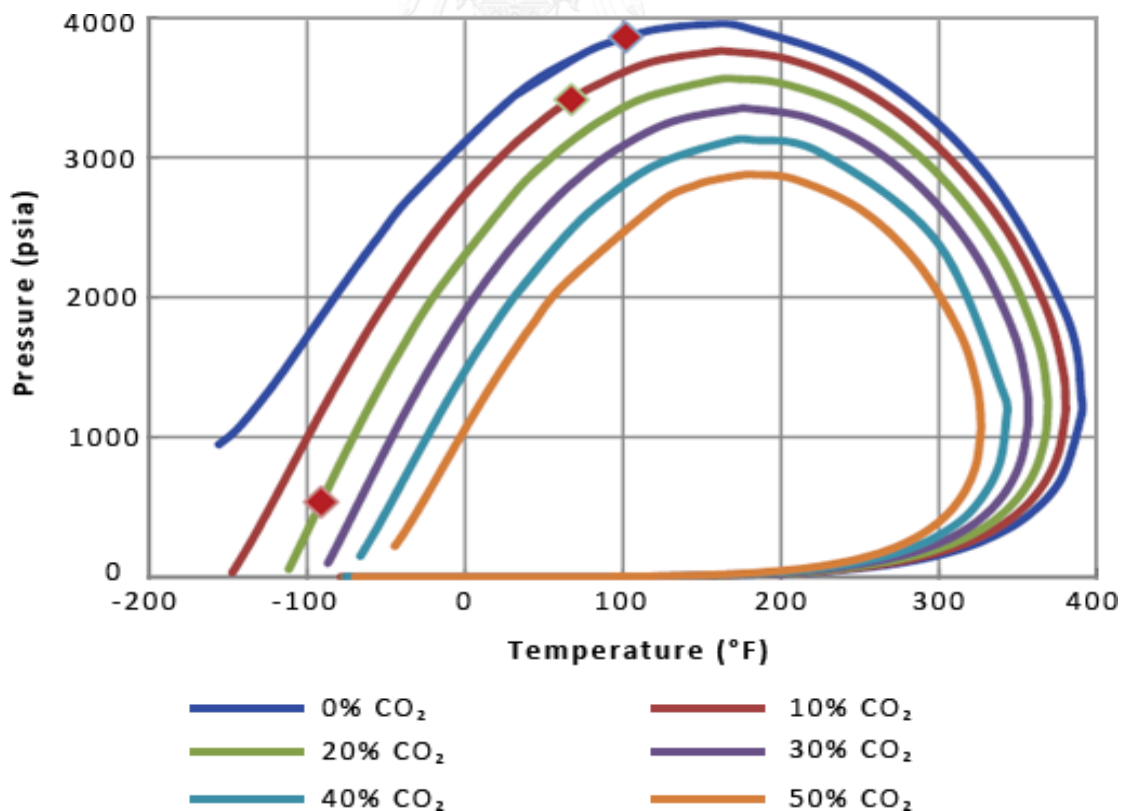


Figure 3.7: Drying effects of CO₂ concentration in mole percent on two-phase envelope for a CO₂-Gas Condensate Mixture [15]

3.2.4 Fracture Pressure

In order to avoid fracturing of the reservoir, injection or dumpflood of fluid into the target reservoir should be operated at pressure below the fracture pressure. The correlations as defined in Equations (3.6) and (3.7) are used to calculate the fracture pressure of the M field in Gulf of Thailand [16].

$$p_f = \frac{\left(\frac{dp}{dx}\right)_f \times TVD}{10.2} \quad (3.6)$$

$$\left(\frac{dp}{dx}\right)_f = 1.22 + (TVD \times 1.6 \times 10^{-4}) \quad (3.7)$$

where

p_f	=	fracture pressure of the reservoir, bar
$\left(\frac{dp}{dx}\right)_f$	=	fracturing pressure gradient, bar/meter
TVD	=	true vertical depth, meter

3.3 Recovery Calculation

Gas and condensate recoveries in this study are converted to barrel of oil equivalent (BOE) in order to simplify the analysis. The BOE is a unit of energy defined as 5.8 million BTU [17] which approximately equals to the higher heating value of 1.0 STB of crude oil. Because of this reason, 1.0 STB of condensate in this study simply equals to 1.0 BOE.

In case of gas, the higher heating value per standard cubic feet of gas mixture is used to convert a volume of gas to be barrel of oil equivalent. It can be evaluated from gas composition and higher heating values of each component [11] as shown in Table 3.3 [18] by Equation (3.8).

$$L_c = \sum_j y_j L_{cj} \quad (3.8)$$

where

$$L_c = \text{higher heating value of gas mixture, BTU/SCF}$$

$$y_j = \text{mole fraction in gas of component } j$$

$$L_{cj} = \text{higher heating value of component } j, \text{ BTU/SCF}$$

Table 3.3: The higher heating values of each gas composition [18]

Components	Higher heating value (BTU/SCF)
Methane	1010.0
Ethane	1769.7
Propane	2516.2
Isobutane	3252.0
Normal butane	3262.4
Isopentane	4000.9
Normal pentane	4008.7
Hexane	4756.0
Heptane	5502.5
Carbon dioxide	0.0
Nitrogen	0.0

3.4 Two Phase Vertical Flow Regimes

Typically, fluid inside a production well of a gas condensate reservoir is two phase consisting of both gas and condensate. They have different physical properties, resulting in many possible flow regime as depicted in Figure 3.8 [19].

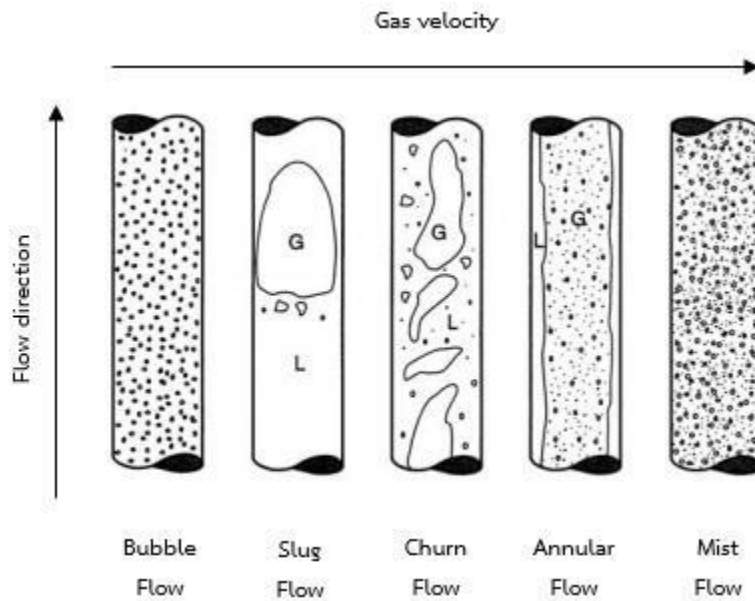


Figure 3.8: Two phase vertical flow regimes [19]

Bubble flow is appeared when gas velocity is very low and only tiny bubbles of gas phase are suspended in a continuous liquid phase.

Slug flow is defined by a series of liquid slugs separated by a relatively large gas bubbles. There are small bubbles within the liquid phase as well. Nevertheless, many of these small bubbles are coalesced to form the large bubbles until they expand as large as the diameter of the pipe.

Churn flow have a large gas bubbles with irregular shape moving up at the center of the pipe. Usually they carry droplets of liquid phase with them. Most of the remaining liquid flows up along the pipe walls. Churn flow is also known as transition flow or intermediate flow condition between slug flow and mist flow.

Annular flow is defined by flowing on the pipe wall of the liquid phase and on the center of the pipe of the gas phase.

Mist Flow is flow regime in which liquid phase exists as very small distributed droplets in the continuous gas phase.

CHAPTER 4

RESERVOIR SIMULATION MODEL

The hypothetical reservoir model that was investigated in this study and also the detail of methodology are presented in this chapter. ECLIPSE office was used as a tool to create the reservoir model, and ECLIPSE 300 specializing in compositional modeling was used as a simulator to predict gas and condensate production under different sensitivity cases.

The reservoir model can be divided into five main sections including case definition, grid, fluid properties, special core analysis, and production schedule. The input details of each section of the base-case dumpflood model are described separately.

4.1 Case Definition

Simulator:	Compositional
Unit:	Field
Model dimensions:	Number of cells in the x-direction 45
	Number of cells in the y-direction 15
	Number of cells in the z-direction 34
Grid type:	Cartesian
Geometry type:	Block centered
Oil-Gas-Water options:	Water and gas condensate
Number of components:	11
Pressure saturation options:	Adaptive Implicit [20]

4.2 Grid

The hypothetical reservoir model consists of a gas-condensate reservoir with four thin-layered high carbon-dioxide gas reservoirs using Cartesian coordinate under simple geometry and homogeneous conditions. The porosity, horizontal and vertical permeability, initial water saturation, and pressure and temperature gradient of the gas-condensate and the source gas reservoirs were obtained from average values of a gas field in the Gulf of Thailand. The geometries and properties of the base-case models are summarized in Table 4.1 and Table 4.2. The illustration of the hypothetical reservoir model is shown as the three-dimensional view in Figure 4.1.

4.2.1 Target Gas-Condensate Reservoir

The top depth of the target gas condensate reservoir is 6,000 ft. with the area of $4,500 \times 1,500 \text{ ft}^2$ and thickness of 50 ft. The target reservoir has 45×15 grids in the x-y plane and 10 grids in z-direction.

Table 4.1: Geometries and properties of the target gas-condensate reservoir

Parameter	Target gas-condensate reservoir
Top depth (ft.)	6000
K-Layer in the model	1 - 10
Number of grid	$45 \times 15 \times 10$
Grid size (ft. \times ft. \times ft.)	$100 \times 100 \times 5$
Reservoir dimension (ft. \times ft. \times ft.)	$4500 \times 1500 \times 50$
Porosity (%)	21.50
Horizontal permeability (mD)	126.0
Vertical permeability (mD)	12.6

4.2.2 Source Gas Reservoirs

The porosity of the top underlying reservoir is equal to that of the target reservoir. For the rest three underlying reservoir, the porosities are varied in order to maintain the same original gas in place as the first underlying reservoir at 5,192.35 MMSCF.

Table 4.2: Geometries and properties of the source gas reservoirs

Parameter	Source reservoir	Source reservoir	Source reservoir	Source reservoir
	1	2	3	4
Top depth (ft.)	7050	7275	7500	7725
K-Layer in the model	12 - 16	18 - 22	24 - 28	30 - 34
Number of grid	45 × 15 × 5	45 × 15 × 5	45 × 15 × 5	45 × 15 × 5
Grid size (ft. × ft. × ft.)	100 × 100 × 5	100 × 100 × 5	100 × 100 × 5	100 × 100 × 5
Reservoir dimension (ft. × ft. × ft.)	4500 × 1500 × 25	4500 × 1500 × 25	4500 × 1500 × 25	4500 × 1500 × 25
Porosity (%)	21.50	21.23	20.99	20.76
Horizontal permeability (mD)	126.0	126.0	126.0	126.0
Vertical permeability (mD)	12.6	12.6	12.6	12.6
Shale above the reservoir				
Thickness (ft.)	1000	200	200	200
K-Layer in the model	11	17	23	29

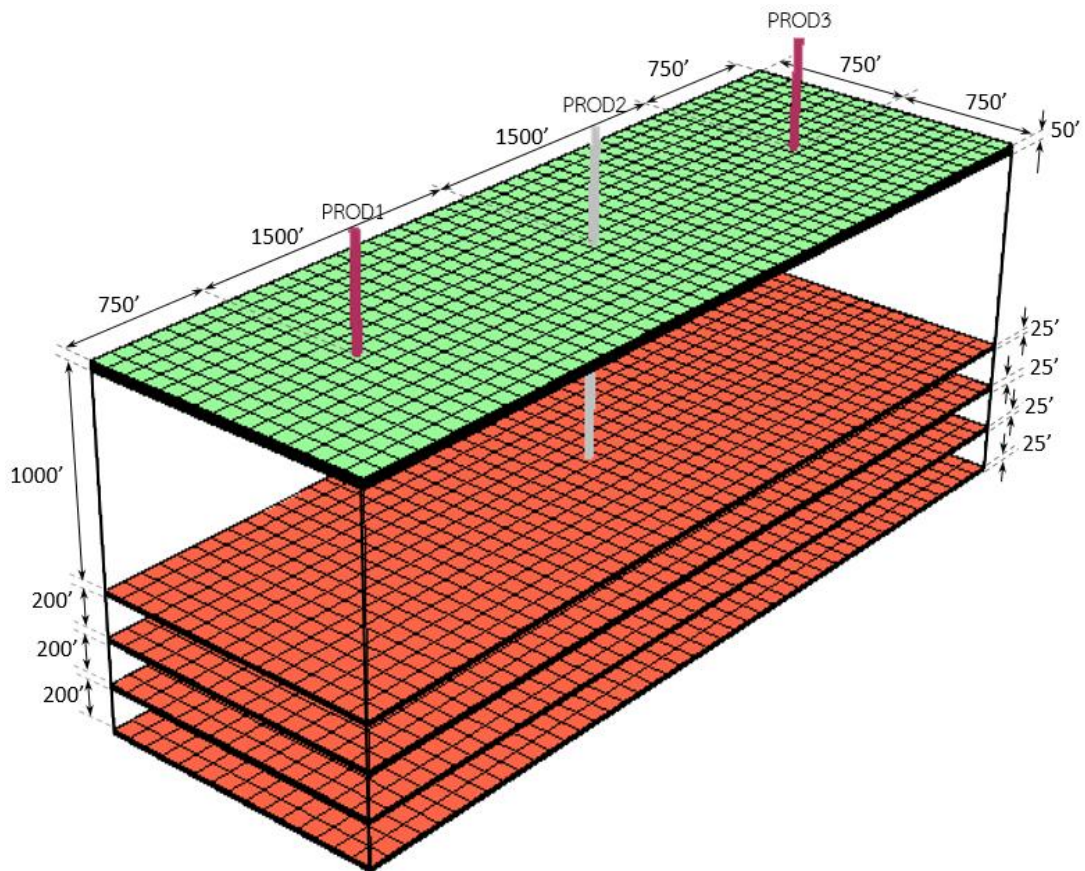


Figure 4.1: Three-dimensional view of the reservoir model

4.2 Fluid Properties

This section contains pressure and saturation dependent properties of the reservoir fluids including condensate, gas, and water. The properties of water were specified in PVT table while the properties of condensate and gas were determined using physical properties of each component via equation of state calculation.

4.3.1 Water Properties

The properties of water were calculated using sets of correlations provided in ECLIPSE 300 with the input shown in Table 4.3. The temperatures and pressures of formations in this study were obtained from the typical temperature and pressure gradients in the Gulf of Thailand [16] as illustrated in Equations (4.1) and (4.2). Correlated properties obtained from ECLIPSE 300 are shown in Table 4.4.

Formation pressure

$$p_R = TVD \times 0.3048 \times 1.462 + 14.7 \quad (4.1)$$

Formation temperature

$$T_R = TVD \times 0.3048 \times 0.059 + 21.38 \quad (4.2)$$

where

P_R = reservoir pressure, psia

T_R = reservoir temperature, °C

TVD = true vertical depth, ft.

Table 4.3: Input parameters used to calculate the properties of water

Parameter	Target reservoir	Source reservoir 1	Source reservoir 2	Source reservoir 3	Source reservoir 4
Reference depth (ft.)	6000	7050	7275	7500	7725
Temperatures at reference depth (°F)	264.70	298.69	305.97	313.23	320.54
Pressures at reference depth (psia)	2688.41	3156.30	3256.57	3356.83	3457.10
Salinity (ppm)			5,000		
Rock type		Consolidated sandstone			
Standard temperature			60 °F		
Standard pressure			14.7 psia		

Table 4.4: Water properties resulting from using correlations provided in ECLIPSE 300

Parameter	Target reservoir	Source reservoir 1	Source reservoir 2	Source reservoir 3	Source reservoir 4
Water density	62.42811 lb/ft ³ at standard condition				
p _{ref} (psia)	2688.41	3156.30	3256.57	3356.83	3457.10
Water FVF at p _{ref} (RB/STB)	1.0478583	1.0633183	1.0668728	1.0705021	1.0742430
Water compressibility (psi ⁻¹)	3.55 × 10 ⁻⁰⁶	3.89 × 10 ⁻⁰⁶	3.97 × 10 ⁻⁰⁶	4.06 × 10 ⁻⁰⁶	4.15 × 10 ⁻⁰⁶
Water viscosity at P _{ref} (cP)	0.220995	0.192044	0.186885	0.182047	0.177461
Water viscosibility (psi ⁻¹)	8.03 × 10 ⁻⁰⁶	9.19 × 10 ⁻⁰⁶	9.40 × 10 ⁻⁰⁶	9.57 × 10 ⁻⁰⁶	9.72 × 10 ⁻⁰⁶

4.3.2 Gas and Condensate Properties

The properties of gas and condensate were calculated using equation of state provided in ECLIPSE 300. A typical composition of gas-condensate found in the Gulf of Thailand was used for the gas-condensate reservoir [10] while a binary-component system was used for the source reservoirs. Two compositions yielding low CGR and high CGR of the fluid in gas condensate reservoir are shown in Table 4.5. The composition of injected fluids in conventional gas injection scenario are similar to initial composition of four source reservoirs as expressed in Table 4.6.

Table 4.5: The initial composition of the target-reservoir fluid [10]

Component	Mole fraction	
	High CGR	Low CGR
Methane	0.6481	0.5999
Ethane	0.0527	0.0843
Propane	0.0623	0.0640
Isobutane	0.0167	0.0341
Normal butane	0.0309	0.0390
Isopentane	0.0137	0.0143
Normal pentane	0.0131	0.0140
Hexane	0.0159	0.0727
Heptane	0.1339	0.0654
Carbon dioxide	0.0106	0.0123
Nitrogen	0.0021	0.0000

Table 4.6: The initial composition of gas in the source reservoirs and the injected fluids

Component	Mole fraction
Methane	0.20
Carbon dioxide	0.80

Peng Robinson [21] equation of state was used in order to determine the reservoir fluid properties at different reservoir pressures. The physical properties of each component were acquired from Engineering Data Book [18] as shown in Table 4.7.

Table 4.7: Physical properties of each component [18]

Component	Critical Pressure (psia)	Critical Temp. ($^{\circ}$ R)	Critical Volume ($\text{ft}^3/\text{lbmole}$)	Molecular Weight	Acentric Factor
C1	667.0	343.34	1.580137	16.042	0.0115
C2	706.6	549.92	2.330348	30.069	0.0994
C ₃	615.5	665.92	3.210189	44.096	0.1529
i-C ₄	527.9	734.41	4.155723	58.122	0.1865
n-C ₄	550.9	765.55	4.085977	58.122	0.2003
i-C ₅	490.4	829.00	4.942207	72.149	0.2284
n-C ₅	488.8	845.80	4.877272	72.149	0.2515
C ₆	436.9	913.80	5.928840	86.175	0.2993
C ₇	396.8	972.90	6.833776	100.202	0.3483
CO ₂	1070.0	547.76	1.509543	44.010	0.2239
N ₂	492.5	227.47	1.431490	28.014	0.0372

The binary interaction coefficients of this system were determined by PVTi program. The results are shown in Table 4.8.

Table 4.8: Binary interaction coefficient between components

	C ₁	C ₂	C ₃	i-C ₄	n-C ₄	i-C ₅	n-C ₅	C ₆	C ₇	CO ₂
C ₂	0.0000									
C ₃	0.0000	0.0000								
i-C ₄	0.0196	0.0100	0.0100							
n-C ₄	0.0196	0.0100	0.0100	0.0000						
i-C ₅	0.0238	0.0100	0.0100	0.0000	0.0000					
n-C ₅	0.0238	0.0100	0.0100	0.0000	0.0000	0.0000				
C ₆	0.0288	0.0100	0.0100	0.0000	0.0000	0.0000	0.0000			
C ₇	0.0343	0.0100	0.0100	0.0000	0.0000	0.0000	0.0000	0.0000		
CO ₂	0.0153	0.0100	0.0100	0.0000	0.0000	0.0000	0.0000	0.0000	0.0000	
N ₂	0.0106	0.0100	0.0100	0.0000	0.0000	0.0000	0.0000	0.0000	0.0000	0.0000

4.4 Special Core Analysis

Special core analysis or SCAL section allows users to enter relative permeability of active phases which are gas, oil, and water into the model. Corey's correlation [22] was used in this study to construct water, gas, and oil relative permeability as functions of water or oil saturation. The parameters used in Corey relative permeability correlation for the base case are shown in Table 4.9 and the graphical relative permeabilities resulting from Corey's correlation are illustrated in Figure 4.2 and Figure 4.3.

Table 4.9: Parameters used in Corey correlation

Corey Water	4	Corey Gas/Oil	3	Corey Oil/Water	3
S_{wmin}	0.2	S_{gmin}	0	Corey Oil/Gas	3
S_{wcr}	0.2	S_{gcr}	0.15	S_{org}	0.2
S_{wi}	0.2	S_{gi}	0.15	S_{orw}	0.2
S_{wmax}	1	$k_{rg}(S_{org})$	0.6	$k_{ro}(S_{wmin})$	0.8
$k_{rw}(S_{orw})$	0.3	$k_{rg}(S_{gmax})$	0.6	$k_{ro}(S_{gmin})$	0.8
$k_{rw}(S_{wmax})$	1				

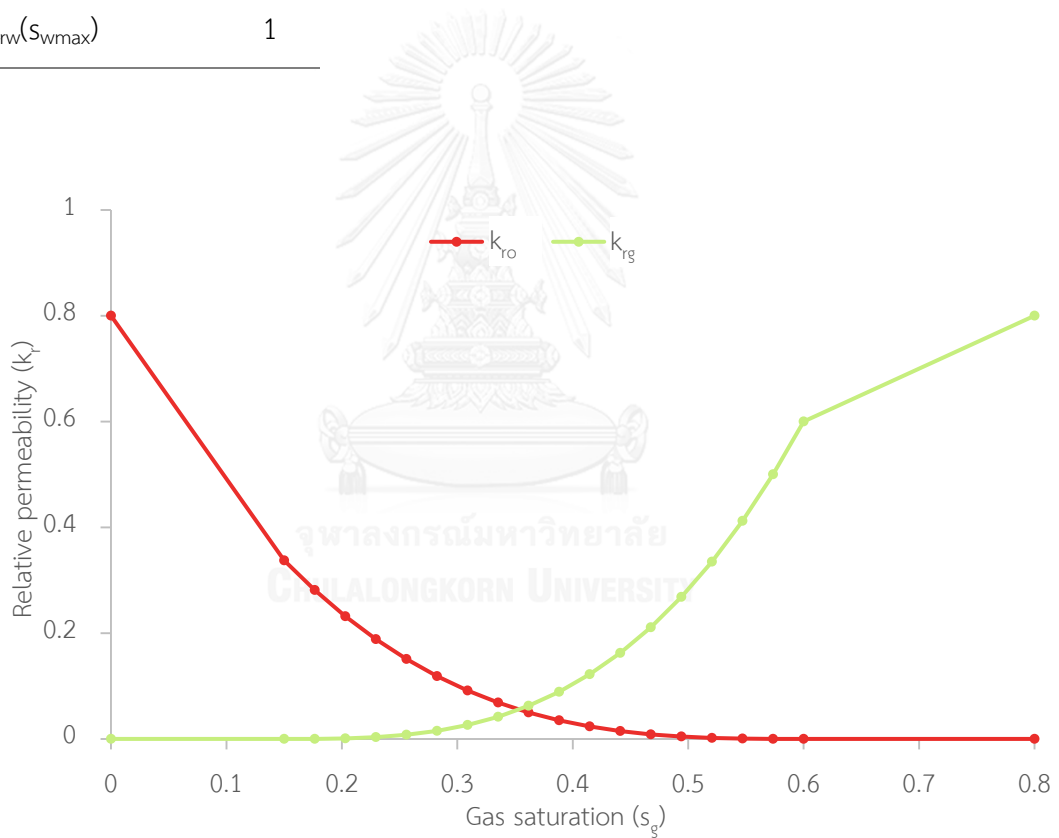


Figure 4.2: Two-phase relative permeabilities of gas/oil system

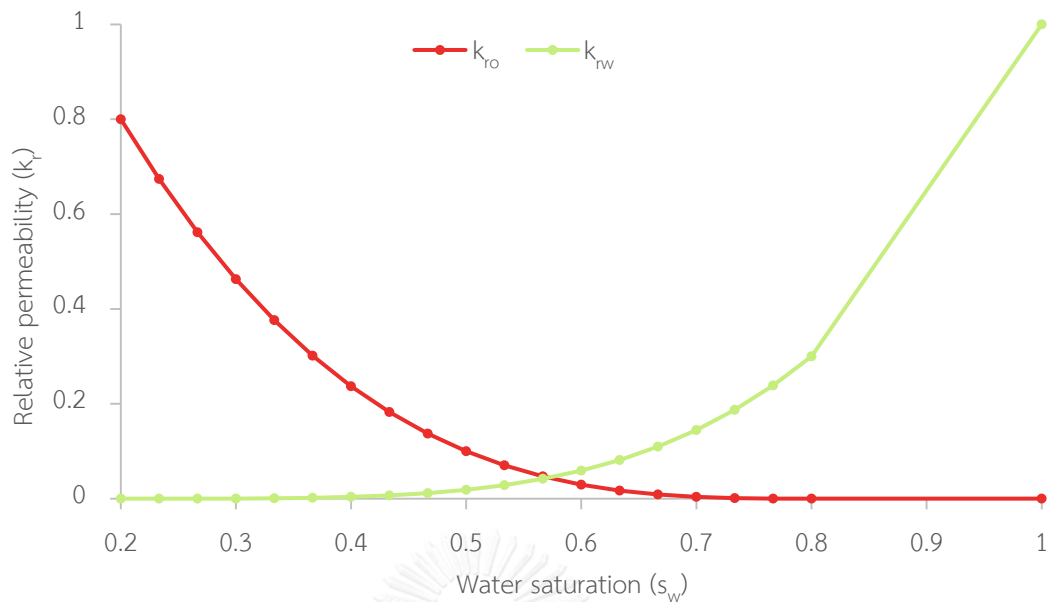


Figure 4.3: Two-phase relative permeabilities of water/oil system

4.5 Production Schedule

The schedule section specifies the operations to be simulated such as production and injection control. All three wells have the same wellbore diameter of 6-1/8 in. and tubing outside diameter of 2-7/8 in. The perforation interval is from the top to the bottom of the reservoir. The detail of input well specification and VFP can be found in Appendix A. Our production strategy is to drill three wells in which the well pattern is shown in Figure 4.1. For natural depletion case, the three wells were used as producers. For conventional gas injection case, the middle well was used as a gas injector. For the dumpflood case, the middle well was used to produce hydrocarbon at early times and then converted to gas dumping well at late times. Dumping was started when the production reached the triggering condition as described in operational constraints. Since the dumping well is connected to multiple reservoirs, multi-segment well option needs to be applied. The detailed input data for each keyword are summarized in Appendix A. Well production control data and constraints are summarized in Table 4.10 and Table 4.11 respectively.

Table 4.10: Production control data for all production wells

Parameters	All production well
Control	Gas rate
Gas rate (MSCF/D)	10000
THP target (psia)	200

Table 4.11: Operational constraints of the production well

Operation	Constraints
Starting production	All production wells are started simultaneously at the beginning
Field abandonment	All production wells are abandoned simultaneously when field net gain BOE production rate less than 83.33 BOE/D/production well which is equivalent to 0.5 MMSCFD * or the CO ₂ content in producing gas is more than 80.0% which is assumed to be facility limitation for the field in this study.

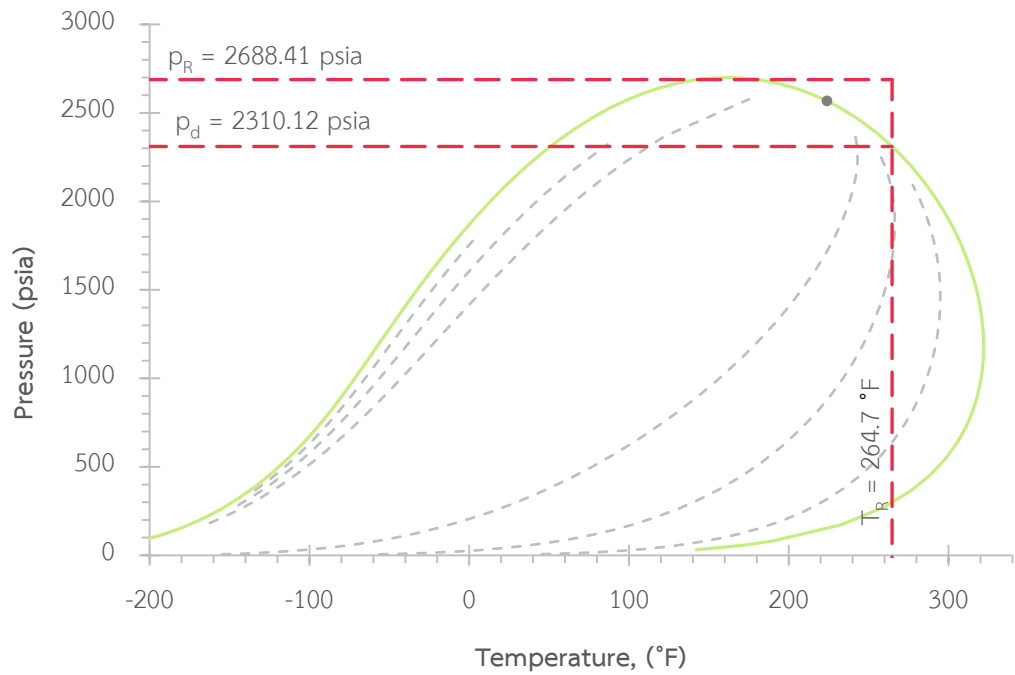
Note: * The details of the calculations are illustrated in Appendix B

Table 4.12: Operational constraints of the middle well or the dumping well for dumpflood scenario and the injector for conventional gas injection scenario

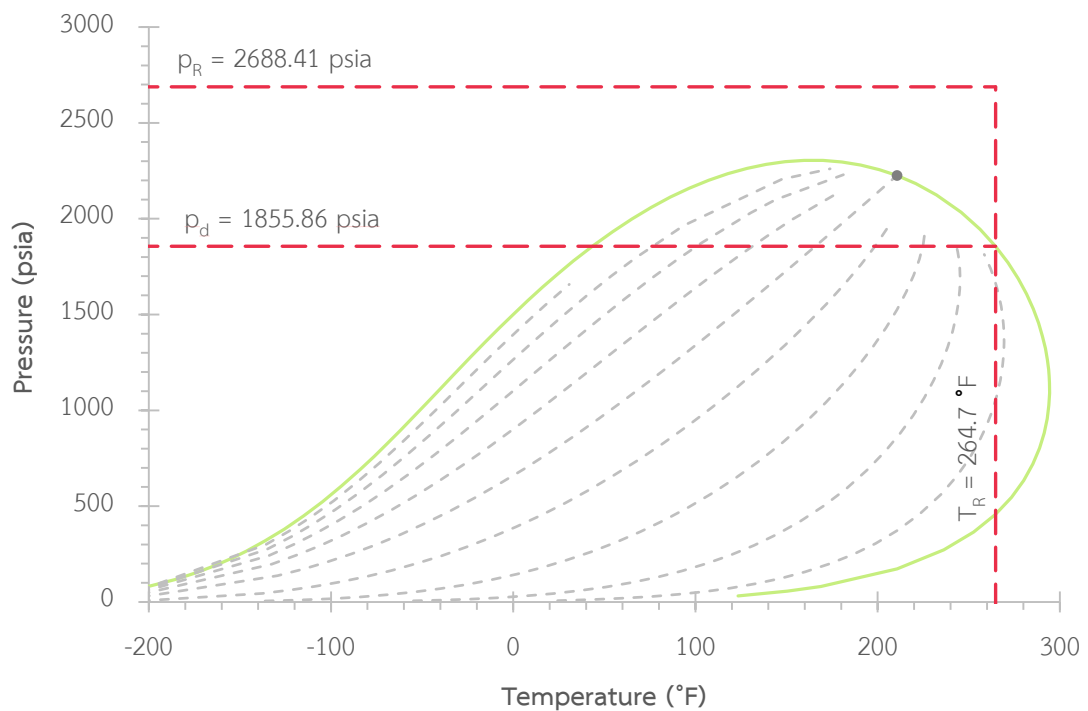
Operation	Constraints
Starting production	Before dumpflood or gas injection operation, the middle well is used as a production well until the condition for starting dumpflood or gas injection is triggered. Except for the cases that gas dumpflood or gas injection is started at the beginning, the middle well is not used as a production well.
Starting gas dumpflood or gas injection	<p>Reservoir pressure is triggering condition for starting gas dumpflood or gas injection and varied from case to case.</p> <p>(1) At beginning of the production</p> <p>(2) When the average reservoir pressure declines below the dewpoint pressure</p> <p>(3) When the average reservoir pressure declines more than 500 psi below the dewpoint pressure</p> <p>After the condition is triggered, the middle well which is used as production well is shut for 30 days. Then, gas dumpflood or gas injection is performed at the middle well depending on scenarios. Except for the cases that gas dumpflood or gas injection is started at the beginning, the middle well is performed as gas dumpflood or gas injection since the beginning.</p>
Stopping gas injection	The middle well stops injecting gas and is abandoned when the revenue from produced condensate cannot compensate with the cost of gas injection which is illustrated in Appendix B. After stopping the gas injection, two production wells are continuously operated until the constraint for well abandonment is reached.
Stopping gas dumpflood	The gas dumpflood is stopped when the production wells are abandoned.

4.5 Details of Methodology

1. Construct a base-case model and perform simulation of hydrocarbon production using three techniques:
 - 1.1 Natural depletion
 - 1.2 Conventional gas injection
 - 1.3 Gas dumpflood from multiple-gas reservoirs into a condensate reservoir
2. Perform three strategies for two different fluid compositions yielding different condensate to gas ratios as shown in Table 4.5. Phase behavior of initial gas condensate composition for each case generated from PVTi program is demonstrated in Figure 4.4.
3. Simulate conventional gas injection models with different gas injection rates and starting time of gas injection in order to evaluate the optimal condition.
 - 3.1 Gas injection rate
 - Gas injection rate equals to target field gas rate
 - Gas injection rate equals to 80% of target field gas rate
 - Gas injection rate equals to 60% of target field gas rate
 - Gas injection rate equals to 40% of target field gas rate
 - Gas injection rate equals to 20% of target field gas rate
 - Gas injection rate equals to 5% of target field gas rate
 - 3.2 Starting time of gas injection
 - At beginning
 - When the reservoir pressure declines below the dewpoint pressure
 - When the reservoir pressure declines more than 500 psi below the dewpoint pressure



(a) high CGR



(b) low CGR

Figure 4.4: Phase behaviors of initial gas condensate composition for two fluid compositions used in this study including (a) high CGR and (b) low CGR

4. Simulate gas dumpflood model with different system parameters in order to determine the optimal condition for gas dumpflood scenario.
 - 4.1 Size of multiple source reservoirs for dumping
 - 4 layers of 25-ft source gas reservoirs
 - 4 layers of 50-ft source gas reservoirs
 - 4.2 Perforation sequence of dumping well
 - Simultaneously perforate four source reservoirs
 - Perforate two lower source gas reservoirs first then the remaining two upper reservoirs after the reservoir pressure decline below 300 psi from the first perforation or bottom up
 - Perforate only two upper gas reservoirs
 - Perforate only two lower gas reservoirs
 - 4.3 Starting time of gas dumpflood
 - At beginning
 - When the reservoir pressure declines below the dewpoint pressure
 - When the reservoir pressure declines more than 500 psi below the dewpoint pressure
5. Analyze the results from the simulations and discuss the results
6. Conclude the performance of the gas condensate reservoir for natural depletion techniques.
7. Summarize the effect of each parameter on performance of the gas condensate reservoir for conventional gas injection and gas dumpflood from multiple-gas reservoirs.
8. Suggest the optimum condition for each production scenario and compare the performance of multiple-gas source dumpflood over the conventional gas injection and natural depletion.

9. Express recommendations for further study

All the simulation cases in this study are depicted as the flowchart diagram in Figure 4.5 to Figure 4.7 for natural depletion, conventional gas injection and gas dumpflood scenarios, respectively.

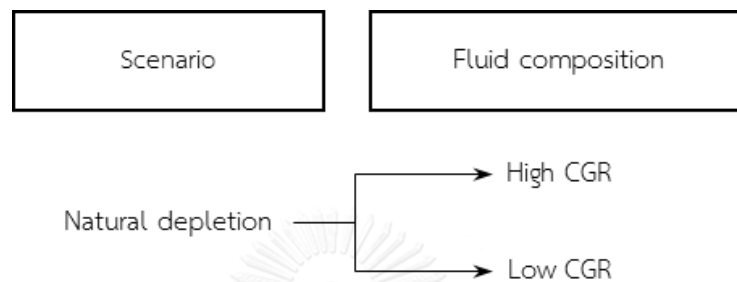


Figure 4.5: Diagram of simulation cases for natural depletion scenario

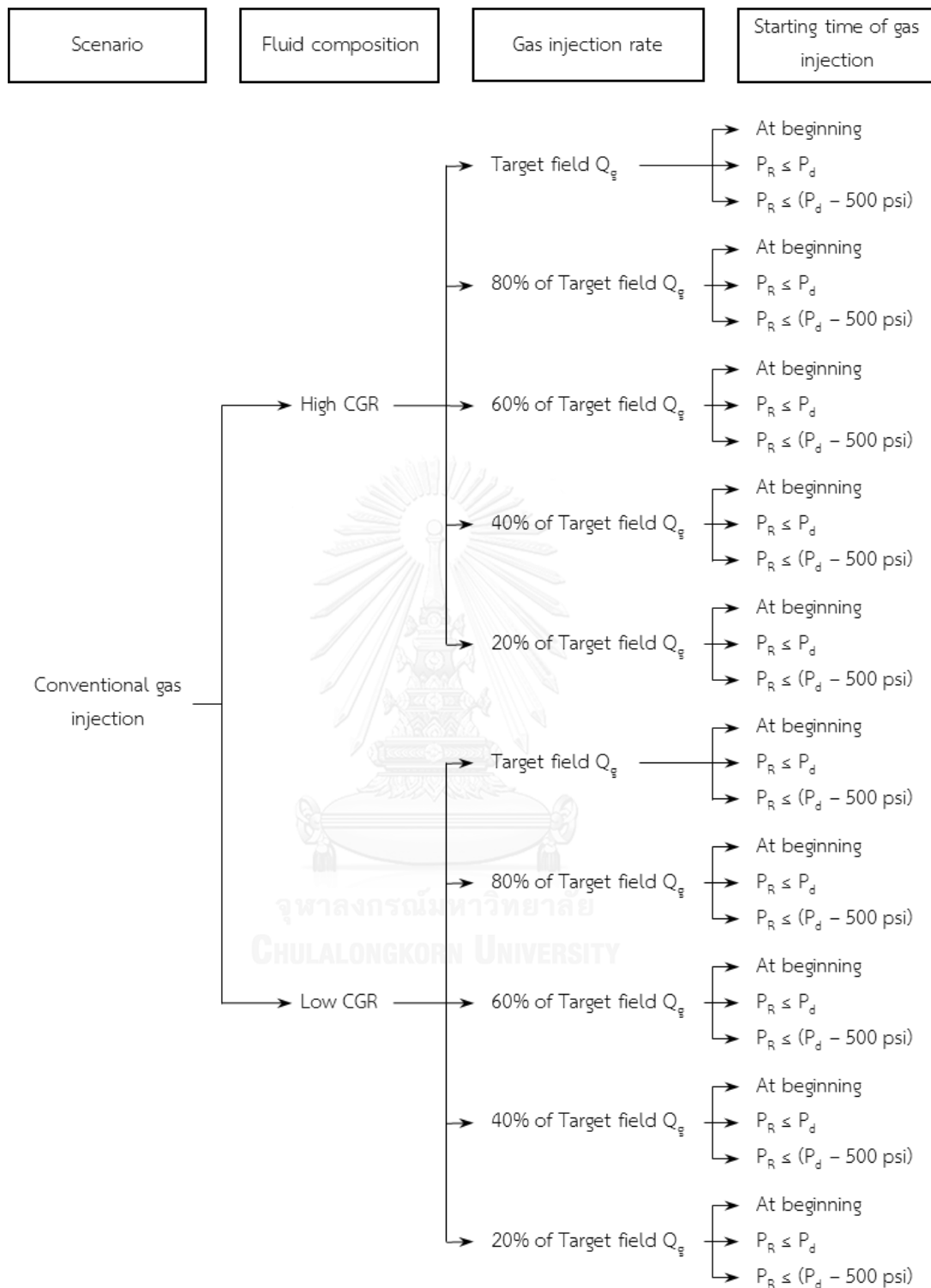


Figure 4.6: Diagram of simulation cases for conventional gas injection scenario

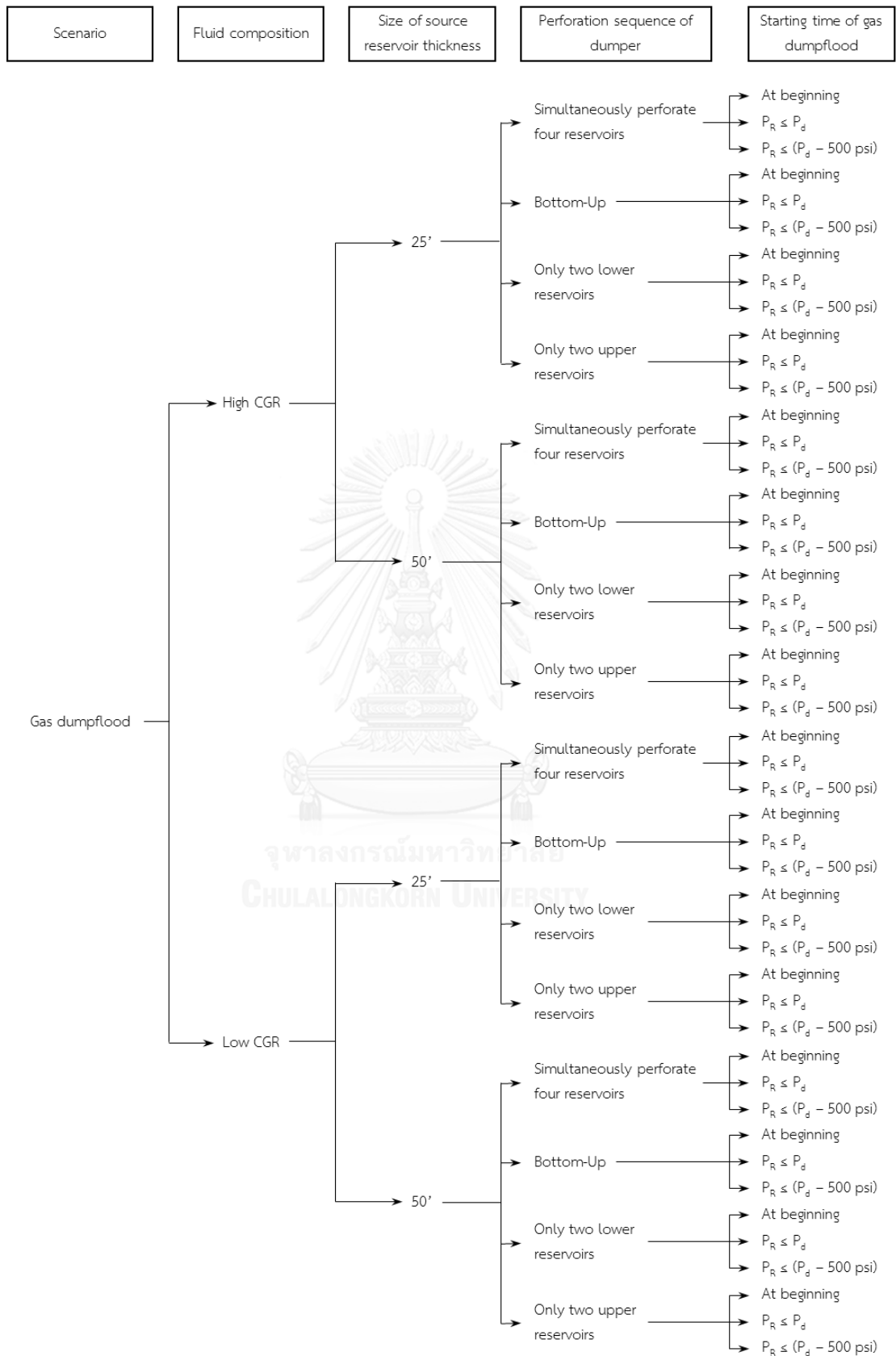


Figure 4.7: Diagram of simulation cases for conventional gas dumpflood scenario

CHAPTER 5

SIMULATION RESULTS AND DISSUSION

The results from simulation models of all cases as described in Section 4.5 are discussed and summarized in this chapter. The discussions of all simulation cases are mainly separated into each section by three production scenarios.

Firstly, results of natural depletion scenarios including two types of fluid composition yielding different condensate to gas ratio are discussed in order to emphasize the fluid flow behavior and primary problems of the gas condensate reservoir. The comparison between different fluid compositions is also shown in this section. Then, all results of the cases with gas injection are shown in Section 5.2 which is divided into two subsections for different fluid compositions. After that, all four parameters in gas dumpflood scenario including fluid composition, size of source reservoirs, perforation sequence, and starting time of dumpflood operation are analyzed in order to investigate the effect of each parameter on the performance of gas dumpflood.

Last of all, the optimal case of each scenario from all previous sections are selected in order to compare the performance of each scenario in the last section. The results of the optimal cases from different fluid compositions are individually discussed in subsections 5.4.1 and 5.4.2 for fluid composition yielding low and high condensate to gas ratio, respectively.

5.1 Natural Depletion

The natural depletion scenario was performed in order to investigate the production from a gas condensate reservoir encountering condensate banking which is the primary problem of a gas condensate reservoir. Two different initial fluid compositions yielding different condensate to gas ratios of the gas condensate reservoirs were modelled with the same production strategy. In the simulation runs, the gas condensate reservoir was depleted by three production wells with the specified plateau rate of 10.0 MMSCFD for each, minimum wellhead pressure of 200 psia, and distance of 1,500 ft. between wells. Since there are three production wells in this case, the abandonment condition is 250.0 BOE/D (83.33 BOE/D/well).

The gas and oil production rates are plotted in Figure 5.1 and Figure 5.2 respectively. Initially, gas is produced at a plateau rate of 10.0 MMSCFD/well for almost half a year before the beginning of the decline period. High CGR case initially provides higher condensate production rate because the reservoir fluid contains more heavy and intermediate hydrocarbon.

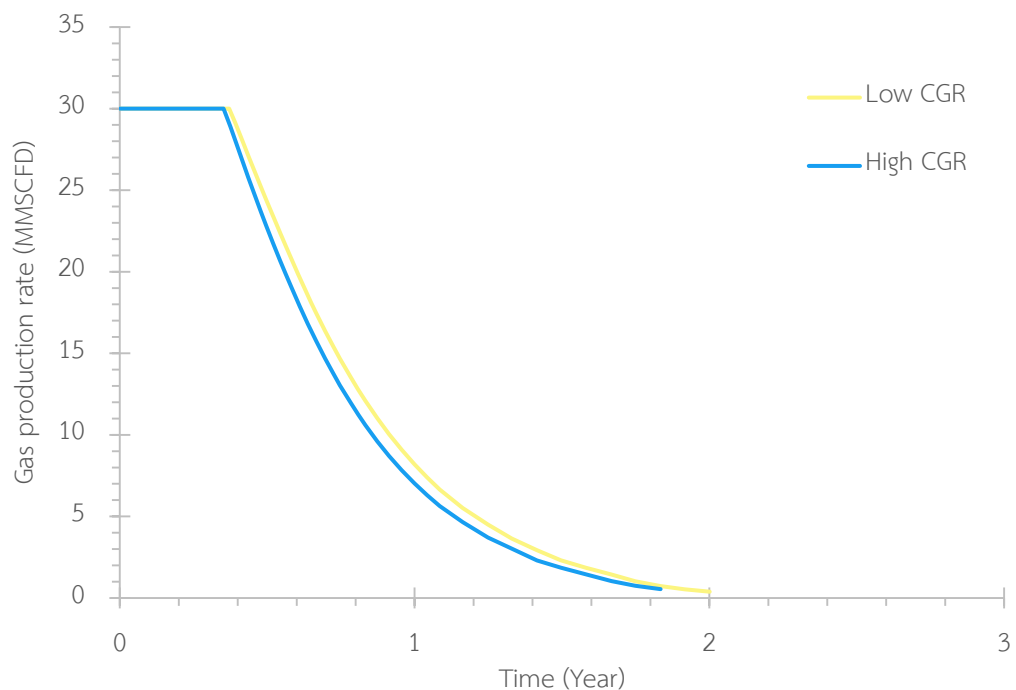


Figure 5.1: Field gas production rate profiles of different composition cases of natural depletion scenarios

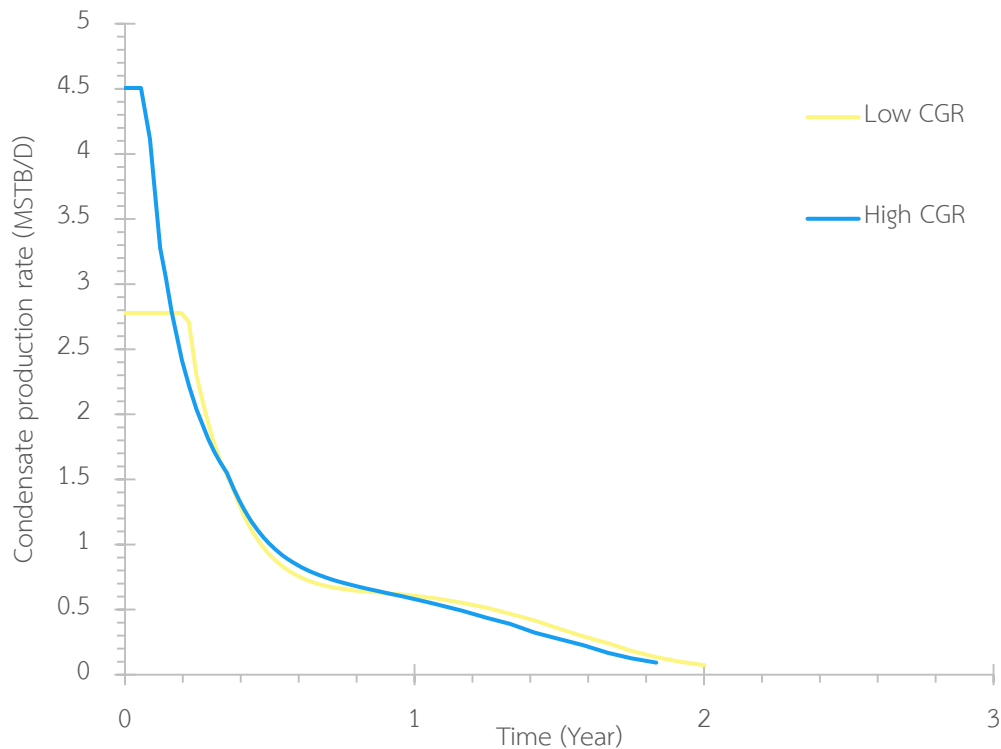


Figure 5.2: Field oil production rate profiles of different composition cases of natural depletion scenarios

During the gas plateau period of both cases, condensate production rates begin declining. This indicates the condensate dropout phenomenon in the near wellbore regions as illustrated in Figure 5.3 to Figure 5.6. This phenomenon happens sooner in high CGR case because the dewpoint pressure is higher comparing to low CGR case since high CGR fluid contain more heavy and intermediate component than low CGR fluid. This, hence, results in faster appearance of condensate banking at 31 days of production for high CGR case and 90 days of production for low CGR case by the fact that the BHP of high CGR case reaches the dewpoint pressure before low CGR case.

The condensate banking effect causes abrupt reductions of condensate production rate because, when condensate forms in the near well bore region, only part of condensate above the critical condensate saturation of 20% can flow. The rest is trapped in the pore of the reservoir. As condensate banking occurs sooner in high CGR case, the condensate production rate abruptly drops until it is less than that of low CRG case for a certain period of time. After that period, the condensate production

rate in high CGR case is slightly higher again because low CGR case encounters the same phenomenon that causes the decline of condensate as happens in high CGR case.

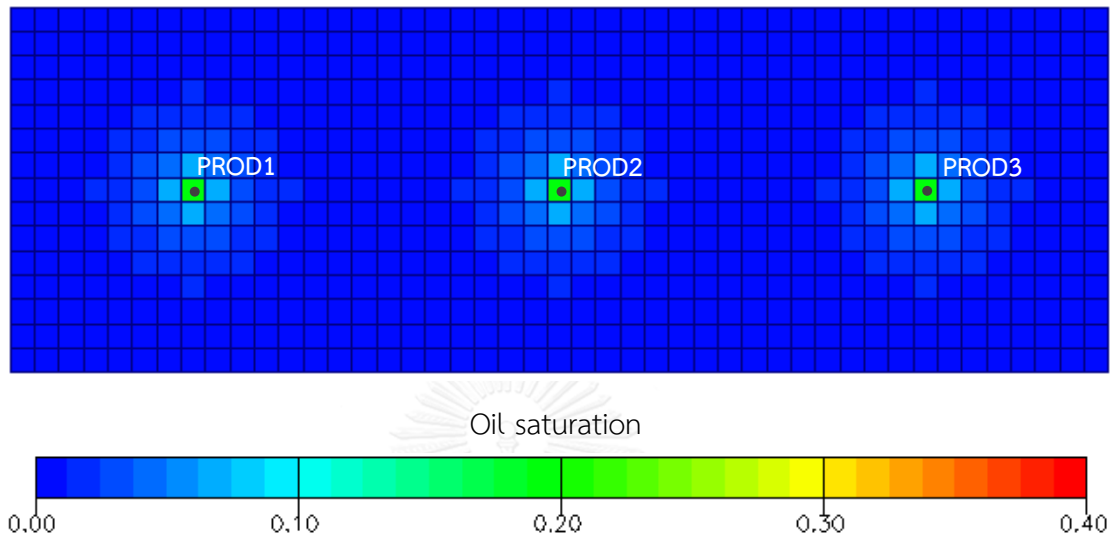


Figure 5.3: Oil saturation distribution of natural depletion scenario with high CGR reservoir fluid when condensate production rate starts to decline (i.e. 31 days of production)

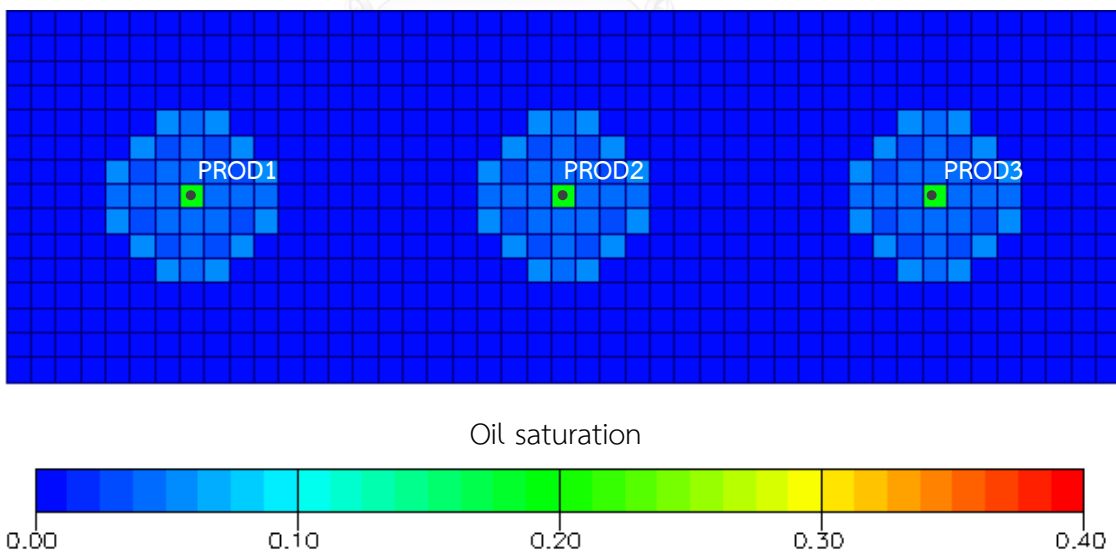


Figure 5.4: Oil saturation distribution of natural depletion scenario with low CGR reservoir fluid when condensate production rate starts to decline (i.e. 90 days of production)

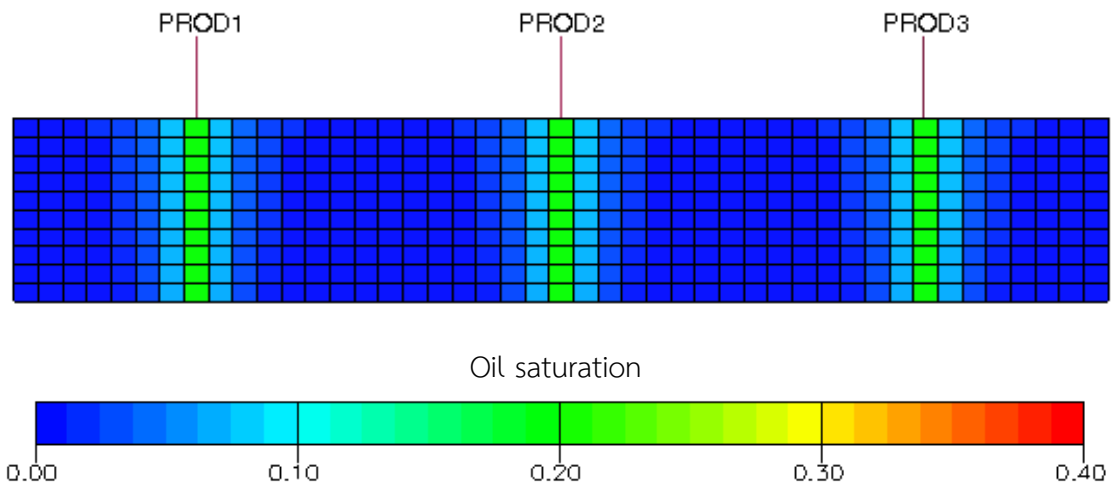


Figure 5.5: Oil saturation distribution at layer $j = 8$ of natural depletion scenario with high CGR reservoir fluid when condensate production rate starts to decline (i.e. 90 days of production)

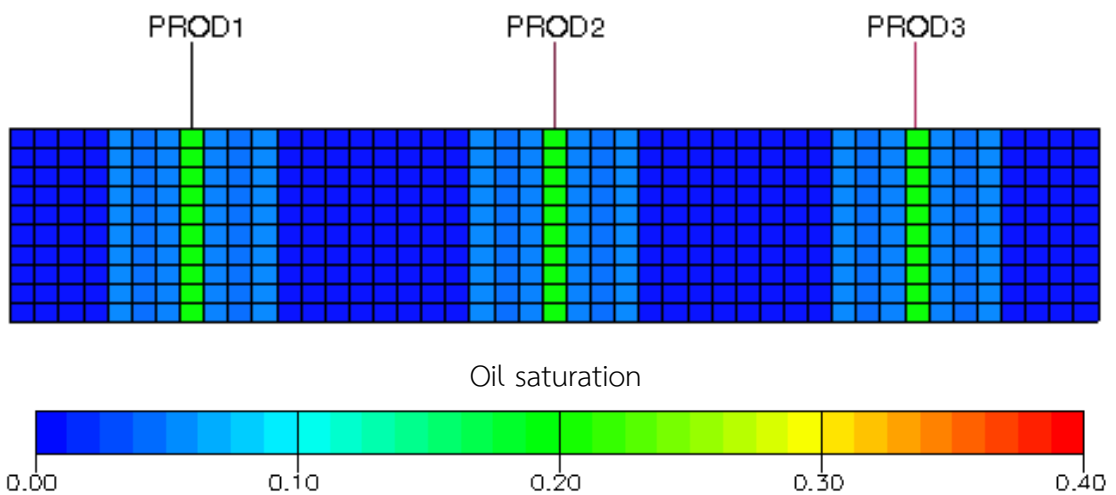


Figure 5.6: Oil saturation distribution at layer $j = 8$ of natural depletion scenario with low CGR reservoir fluid when condensate production rate starts to decline (i.e. 90 days of production)

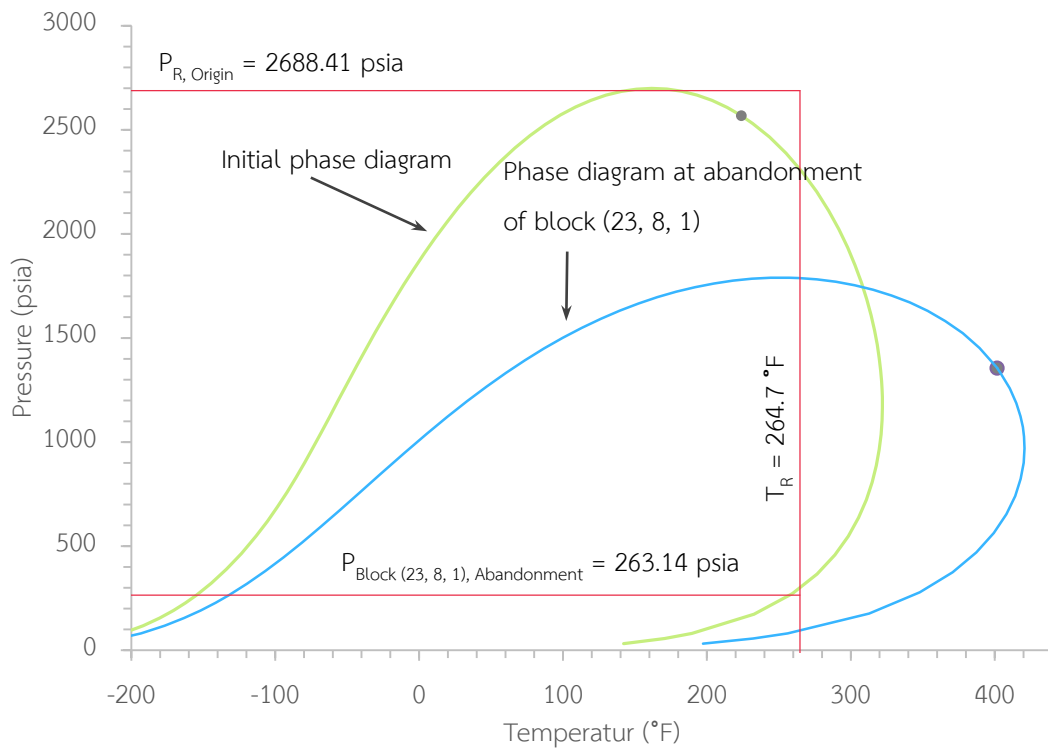


Figure 5.7: Phase behaviors of gas condensate composition for high CGR case

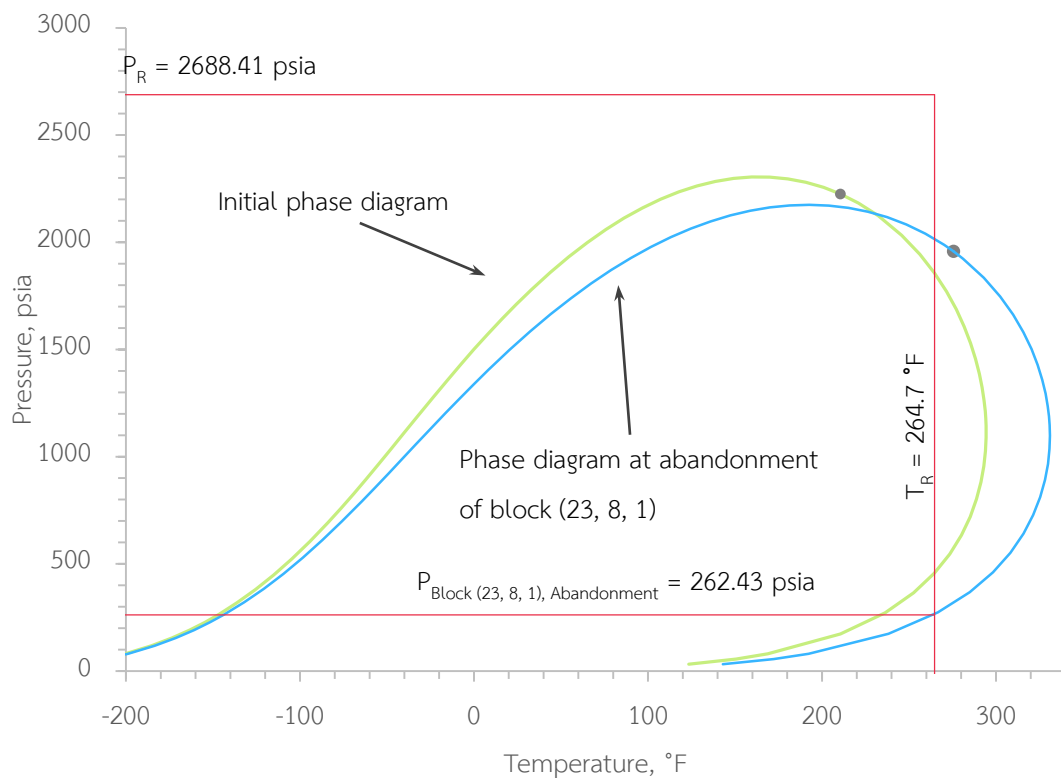


Figure 5.8: Phase behaviors of gas condensate composition for low CGR case

However, at late time which is near abandonment condition, the low CGR case has slightly higher condensate production rate due to the higher effect of revaporization in this case. Figure 5.7 and Figure 5.8 illustrate the phase diagram at near abandonment condition of block (28, 8, 1) which is the top layer of the center of the reservoir. The deviated phase diagrams result from fluid composition change. As seen in the illustrated phase diagram, the high CGR case has partial revaporization while the low CGR case has complete revaporization resulting in slightly lower condensate production rate for high CGR case comparing to low CGR case at late time.

The high CGR case result in higher condensate recovery of 0.647 MMSTB while only 0.618 MMSTB can be recovered in the low CGR case as depicted in Table 5.1. The main reason is the original condensate in place in the high CGR case is more than that of the low CGR case.

Nevertheless, if we consider in term of percentage from original fluids in place, the high CGR case can recovery 47.1% of condensate and 92.0% of gas. Both are lower than those of the low CGR case which can recovery 69.0% of condensate and 92.7% of gas. This is because the condensate dropout partially revaporizes in the case of high CGR at average reservoir pressure of 266.35 psia at abandonment date. As depicted in Figure 5.7, there is remaining condensate in block (28, 8, 1) at the abandonment condition. The oil saturation profile of high CGR case at abandonment date as illustrated in Figure 5.9 shows some amount of condensate remaining in the reservoir. In contrast, the low CGR case results in completed revaporization of condensate banking at average reservoir pressure of 264.63 psia at abandonment date. Figure 5.8 shows that the condensate of block (28, 8, 1) is completely revaporized at the abandonment. The oil saturation profile of low CGR case at abandonment date as illustrated in Figure 5.10 shows insignificant condensate remaining in the reservoir.

Table 5.1: Summarized results for different composition cases of natural depletion scenario

Cases	High CGR	Low CGR
Cumulative condensate production (MMSTB)	0.647	0.618
Original condensate in place (MMSTB)	1.374	0.896
Condensate recovery factor (%)	47.1%	69.0%
Cumulative gas production (BCF)	8.416	8.970
Original gas in place (BCF)	9.149	9.673
Gas recovery factor (%)	92.0%	92.7%
Cumulative HC gas production (BCF) *	8.294	8.850
HC gas recovery factor (%) **	90.7%	91.5%
Cumulative gas production (MMBOE)	2.179	2.612
Cumulative total BOE production (MMBOE)	2.826	3.230
Original BOE in place (MMBOE)	4.496	4.186
Total BOE recovery factor (%)	62.9%	77.2%

Note: * HC gas is produced gas deducted by nitrogen and carbon dioxide content

** Percentage of HC gas production gas production compared to original gas in place

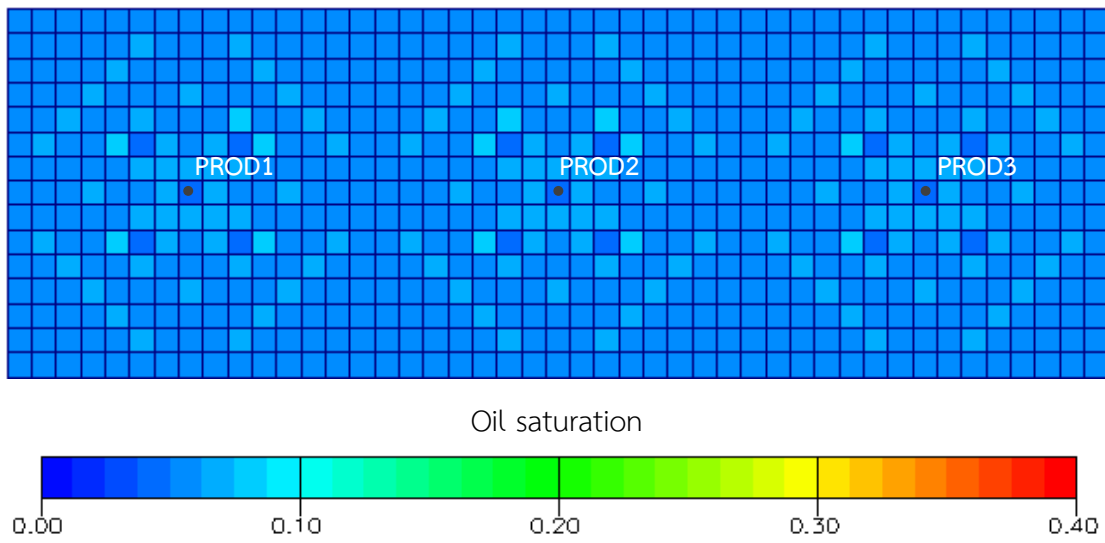


Figure 5.9: Oil saturation distribution of natural depletion scenario with high CGR reservoir fluid at abandonment date (i.e. 670 days of production)

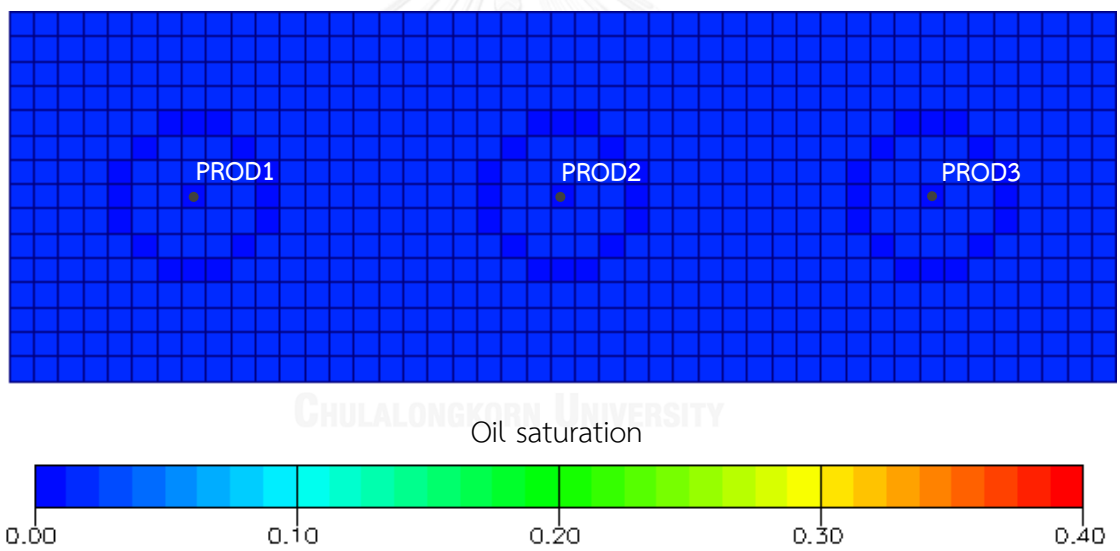


Figure 5.10: Oil saturation distribution of natural depletion scenario with low CGR reservoir fluid at abandonment date (i.e. 731 days of production)

5.2 Conventional Gas Injection

Conventional gas injection scenarios were performed in order to compare with the new technique proposed in this study, which is gas dumpflood. The same well pattern and reservoir as in the case of natural depletion scenario were used. In order to be comparable, high carbon dioxide content gas consisting of 20% mole methane and 80% mole carbon dioxide as same as the composition of original gas in place of source reservoirs in dumpflood scenario was injected into the target reservoir.

Two different initial fluid compositions yielding different condensate to gas ratios of the gas condensate reservoir were modelled with the same production strategy. The effects of compositions are individually discussed in Section 5.2.1 and 5.2.2 for high CGR and low CGR composition, respectively.

The gas condensate reservoir was depleted by three production wells with a specified plateau rate of 10.0 MMSCFD for each, minimum wellhead pressure of 200 psia, and distance of 1,500 ft. as in the case of natural depletion scenario. Since there are two production wells in this scenario, the abandonment condition is 166.7 BOE/D (83.33 BOE/D/well). After the condition for starting gas injection is triggered, the middle well will be shut for 30 days and converted to gas injection well with varying gas injection rates from 1.0 to 20.0 MMSCFD in order to determine the optimal condition for gas injection. The triggering condition for starting gas injection was varied as follows:

1. At beginning of the production
2. When the reservoir pressure declines below the dewpoint pressure
3. When the reservoir pressure declines more than 500 psi below the dewpoint pressure

In case of starting gas injection at the beginning of the production, the middle well was not used as production well but used as injection well since first day of the production.

Table 5.2: Economic condensate rate for different gas injection rates

Injection rate (MMSCF/D)	Economic condensate rate (STB/D)
20.0	87.1
16.0	69.7
12.0	52.2
8.0	34.8
4.0	17.4
1.0	4.4

Gas injection was performed as long as the revenue of the produced condensate can afford the gas injection cost, resulting in different conditions to stop gas injection for different gas injection rates as demonstrated in Table 5.2. Note that the production wells was still kept producing until their economic limit after the injection well is shut in. The detail of the calculation of these economic condensate rates can be found in Appendix B.2.

Gas recovery factor, HC gas recovery factor, and total BOE recovery factor in this scenario were calculated based on net recovery. This was done by subtracting the reported production by the cumulative gas injection. The net gain recovery factor was analyzed instead of normal recovery that considers only production because it is the net recovery that we gain from the reservoir after some amount of gas is injected, and this net gain recovery is the benefit that needs to be maximized.

5.2.1 Composition Yielding High CGR of Original Reservoir Fluid

Different gas injection rate cases having the same starting point of gas injection at the beginning are discussed first in order to describe the effect of gas injection rate. Figure 5.11 illustrates the gas production profiles for different gas injection rates. Initially, gas production rate is constant at 10.0 MMSCFD/well (i.e. 20.0 MMSCFD total) for all cases but the gas injection rate is different from case to case. The cases with gas injection rate of 4.0 and 8.0 MMSCFD have two decline trends while the other cases have only one. The first decline is caused by insufficient pressure support of the reservoir and the second decline results from stopping gas injection due to economic condensate production rate limit as shown in Table 5.2. After the second decline or the shut in of gas injection well, gas and condensate are continuously producing until the production well is abandoned at the economic rate of 83.33 BOE/D/well.

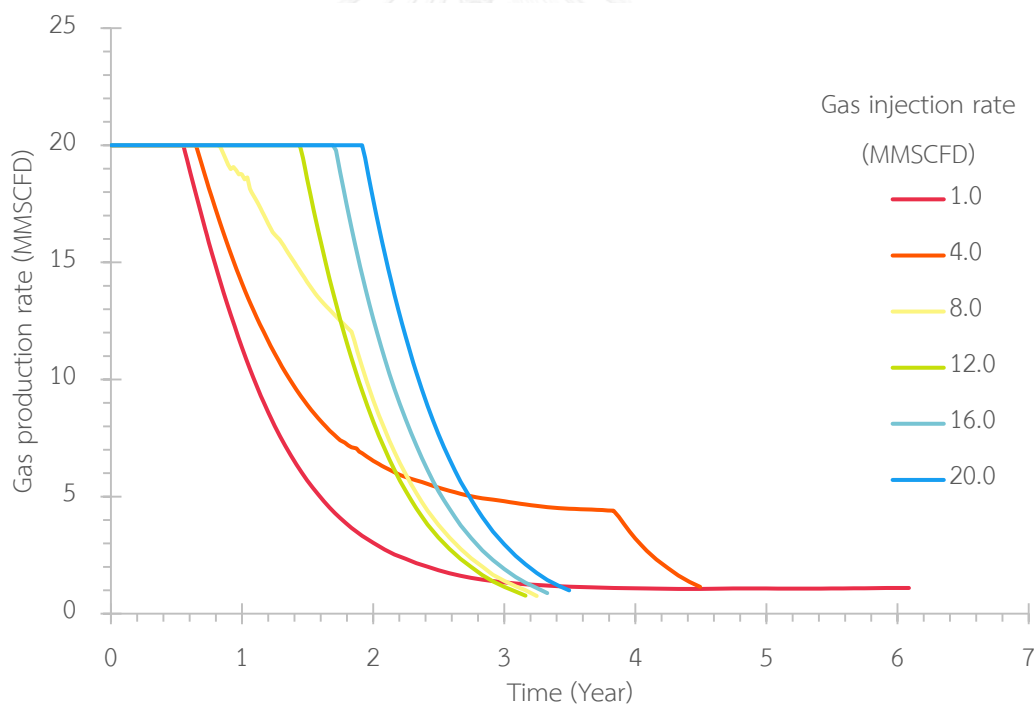


Figure 5.11: Field gas production rate profiles for different gas injection rates of conventional gas injection scenario with high CGR composition of original reservoir fluid

For the lower gas injection rate case, 1.0 MMSCFD, comparing to the cases that have two decline trends, the drop of gas production rate is mainly because of

insufficient reservoir pressure support and there is no second decline due to the fact that this case never reaches the condensate economic limit of 4.4 STB/D to stop gas injection. For the higher gas injection rate from 12.0 to 20.0 MMSCFD, the reservoir pressure is maintained by high gas injection rate and can support the plateau of the gas production rate at 10.0 MMSCFD/well until the gas injection is stopped due to the economic condensate production rate limit.

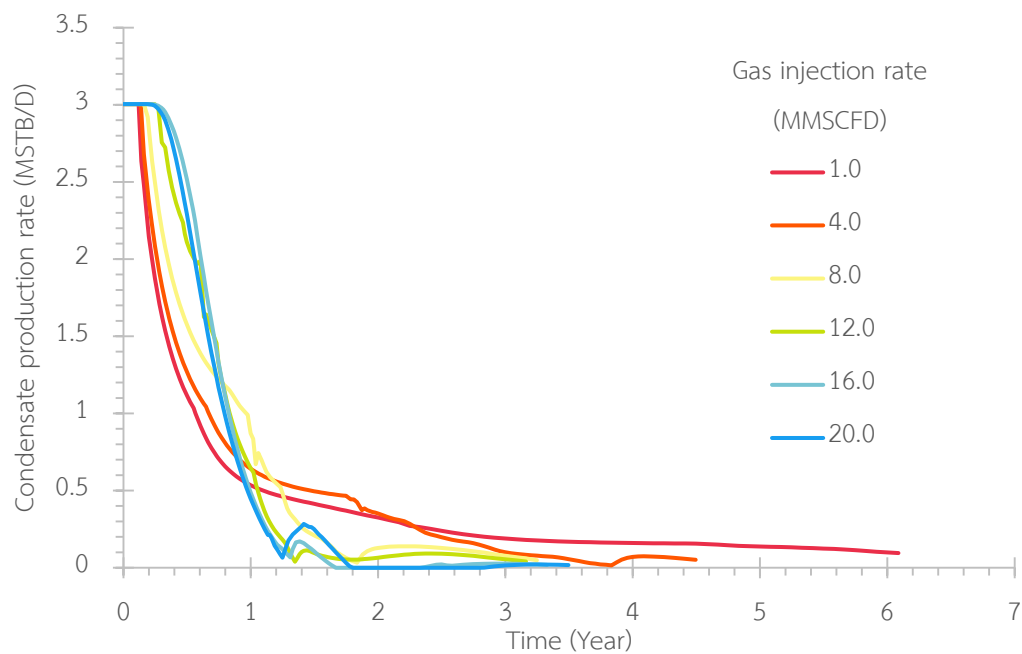


Figure 5.12: Field condensate production rate profiles for different gas injection rates of conventional gas injection scenario with high CGR composition of original reservoir fluid

In prospect of condensate production rate as depicted in Figure 5.12, all cases show abrupt drop of condensate production rates at early time of production. However, the cause of the decline of condensate production can be categorized into two reasons. The first one is for cases with low gas injection rate (1.0 to 12.0 MMSCFD). There are sudden falls of condensate production rates as happened in natural depletion scenario which result from condensate banking near the producers as demonstrated in Figure 5.13 to Figure 5.16. This is because these low gas injection rates cannot maintain the reservoir pressure above the dewpoint pressure. This

phenomenon induces a faster decline of condensate production rate when the gas injection rate is lower by the fact that the lower gas injection rate, the lower capability to maintain the reservoir pressure.

On the other hand, the abrupt drops of the condensate production rates for high gas injection rate (16.0 and 20.0 MMSCFD) are caused by carbon dioxide breakthrough. Condensate banking phenomenon does not occur near the producers in these cases because high gas injection rate can maintain the reservoir pressure above the dewpoint pressure until carbon dioxide breaks through. This phenomenon is influenced by the shrinking effect near the producers by the breakthrough of the gas injection. The shrinking effect of phase diagram causes the two-phase envelope to be smaller or, in another word, less amount of condensate. Hence, this results in condensate production rate decline faster at late time when gas injection rate is higher. This is opposite to low injection rate cases where carbon dioxide breaks through later and causes condensate to drop slower at late time. After the breakthrough, condensate banking occurs in area along the edges of the reservoir which have less amount of carbon dioxide as illustrated in Figure 5.17 and Figure 5.18.

Although higher gas injection rate cases can maintain longer condensate plateau period at early time, the condensate production rate of higher injection rate cases falls quickly and eventually becomes lower than that of the lower gas injection rate cases at late time. This is because of the higher carbon dioxide content near the producers for high injection rate cases. Consequently, the phase envelope continuously shrinks resulting in less amount of condensate. Also, due to higher cumulative condensate production of high injection rate cases at early times, less and less heavy and intermediate components are left inside the reservoir.

After reaching the economic limit of condensate production rates, gas injection is stopped. Then, condensate production rate gradually increases for a while as there is less and less carbon dioxide content near the producer as demonstrated as produced carbon dioxide content in Figure 5.19. After that, due to less and less reservoir pressure, slightly increasing of carbon dioxide content, and less amount of

remaining condensate, the condensate production rate declines until the abandonment conditions.

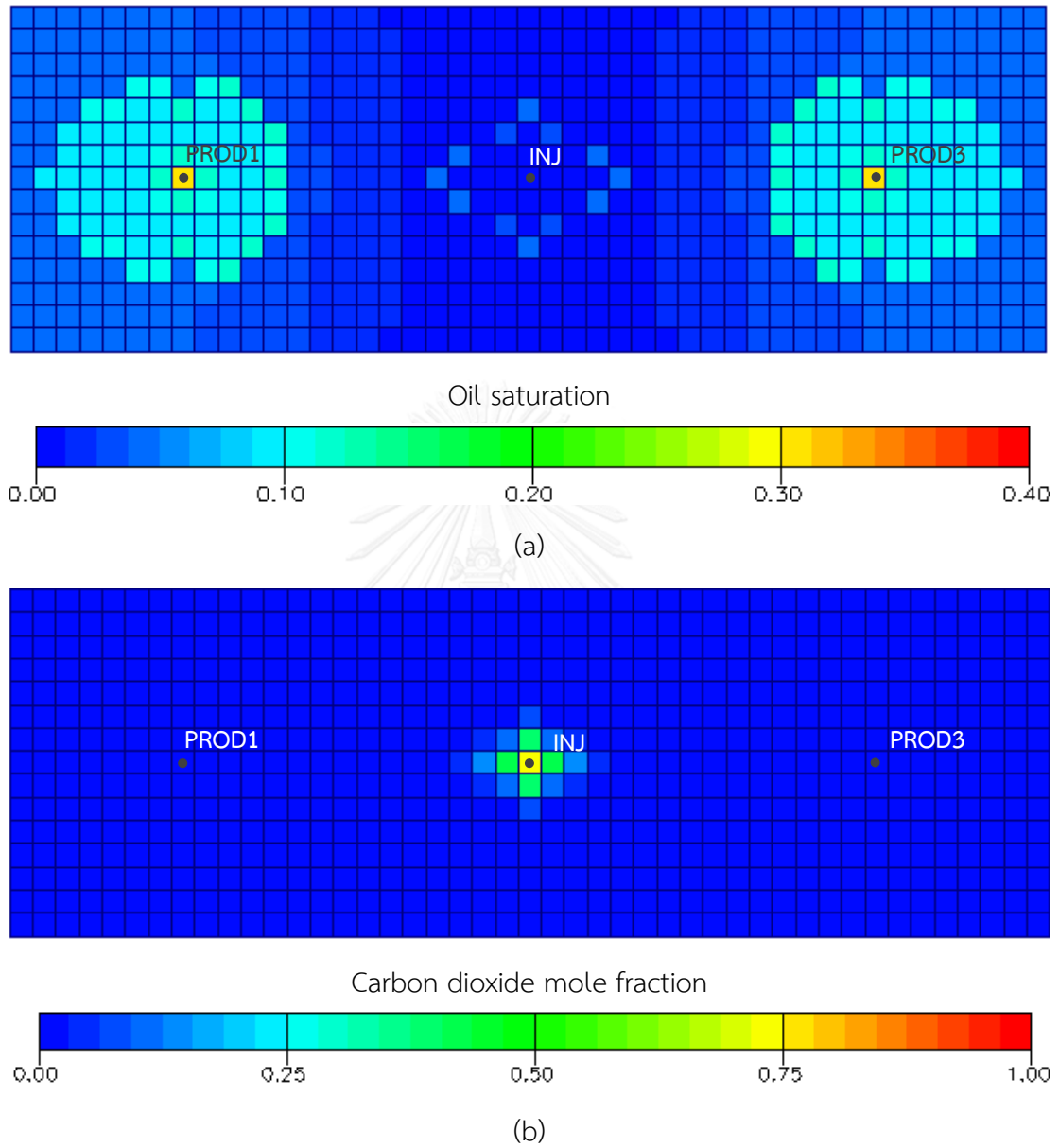


Figure 5.13: (a) Oil saturation distribution and (b) Carbon dioxide mole fraction distribution of case with injection rate of 1.0 MMSCFD of conventional gas injection scenario with high CGR composition of original reservoir fluid when condensate starts to dropout (i.e. 58 days of production)

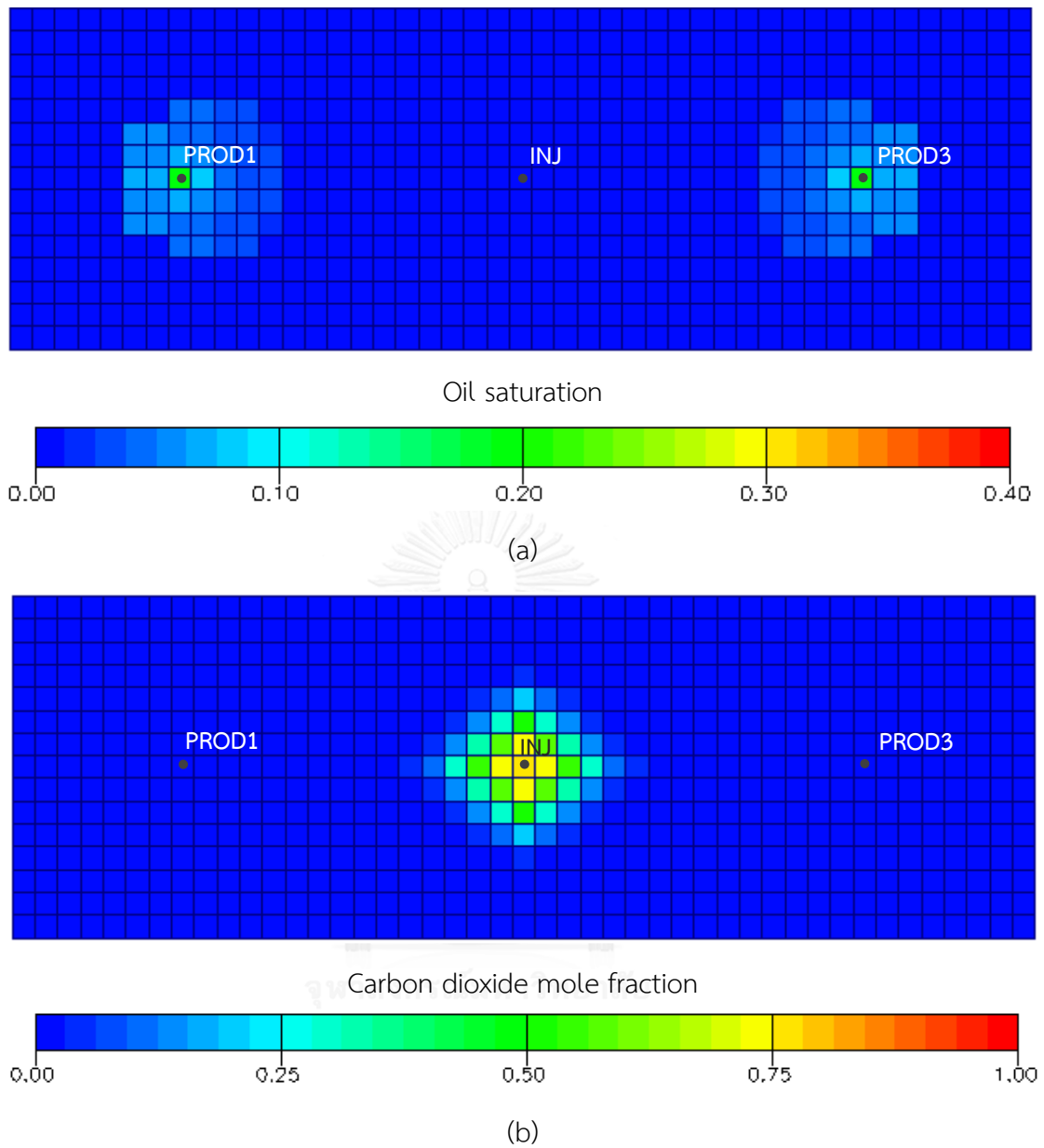


Figure 5.14: (a) Oil saturation distribution and (b) Carbon dioxide mole fraction distribution of case with injection rate of 4.0 MMSCFD of conventional gas injection scenario with high CGR composition of original reservoir fluid when condensate starts to dropout (i.e. 58 days of production)

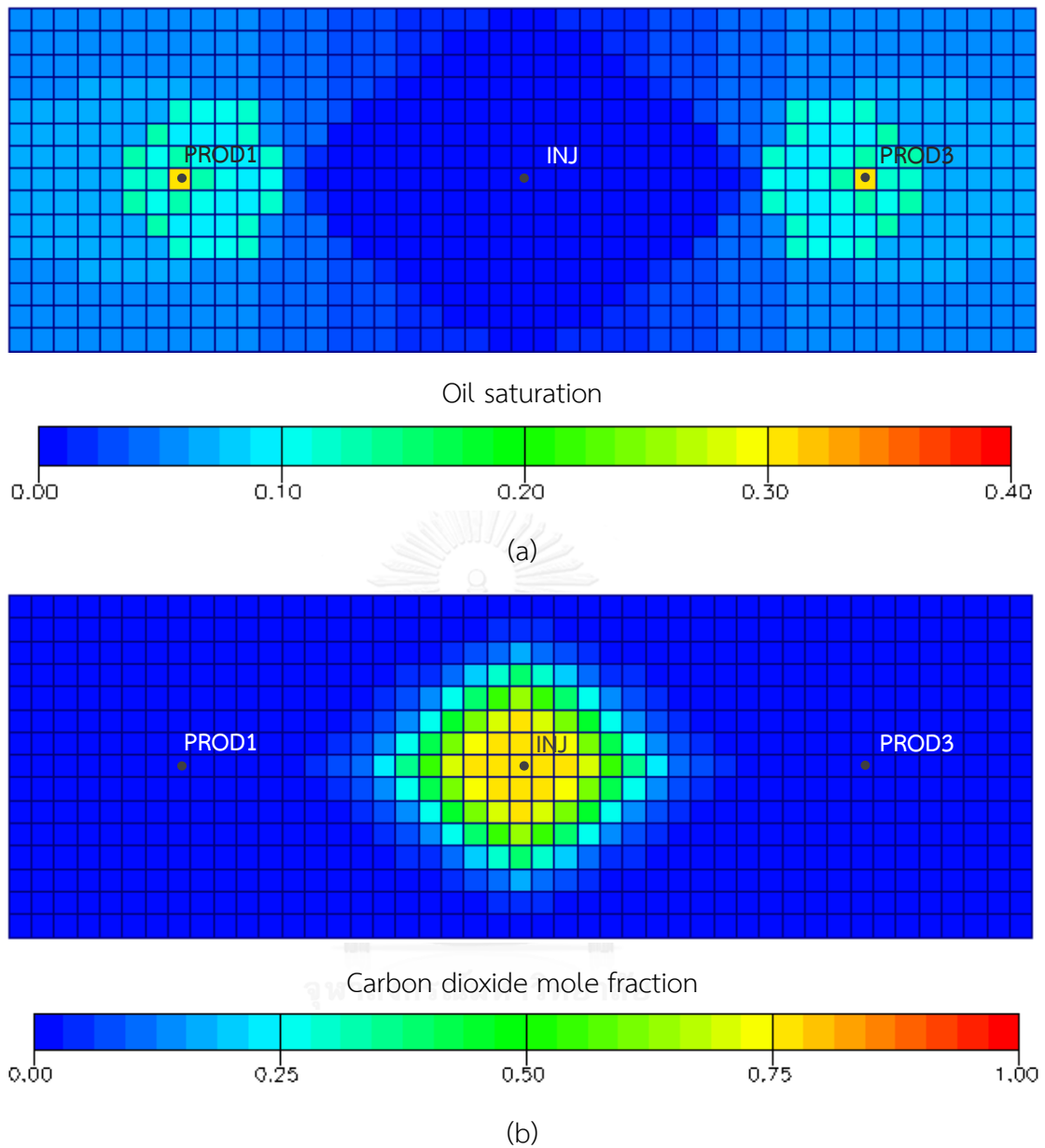


Figure 5.15: (a) Oil saturation distribution and (b) Carbon dioxide mole fraction distribution of case with injection rate of 8.0 MMSCFD of conventional gas injection scenario with high CGR composition of original reservoir fluid when condensate starts to dropout (i.e. 90 days of production)

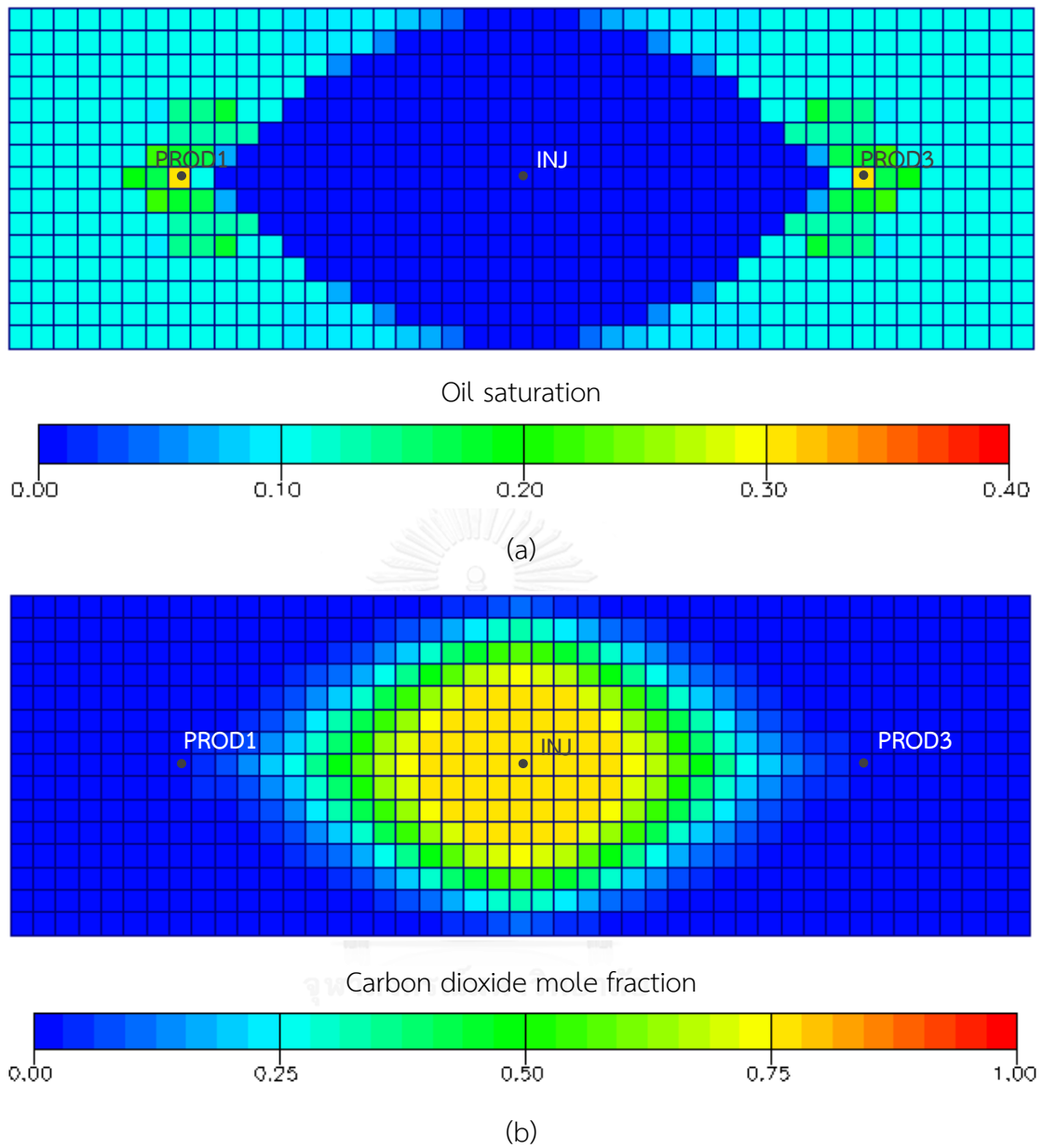


Figure 5.16: (a) Oil saturation distribution and (b) Carbon dioxide mole fraction distribution of case with injection rate of 12.0 MMSCFD of conventional gas injection scenario with high CGR composition of original reservoir fluid when condensate starts to dropout (i.e. 140 days of production)

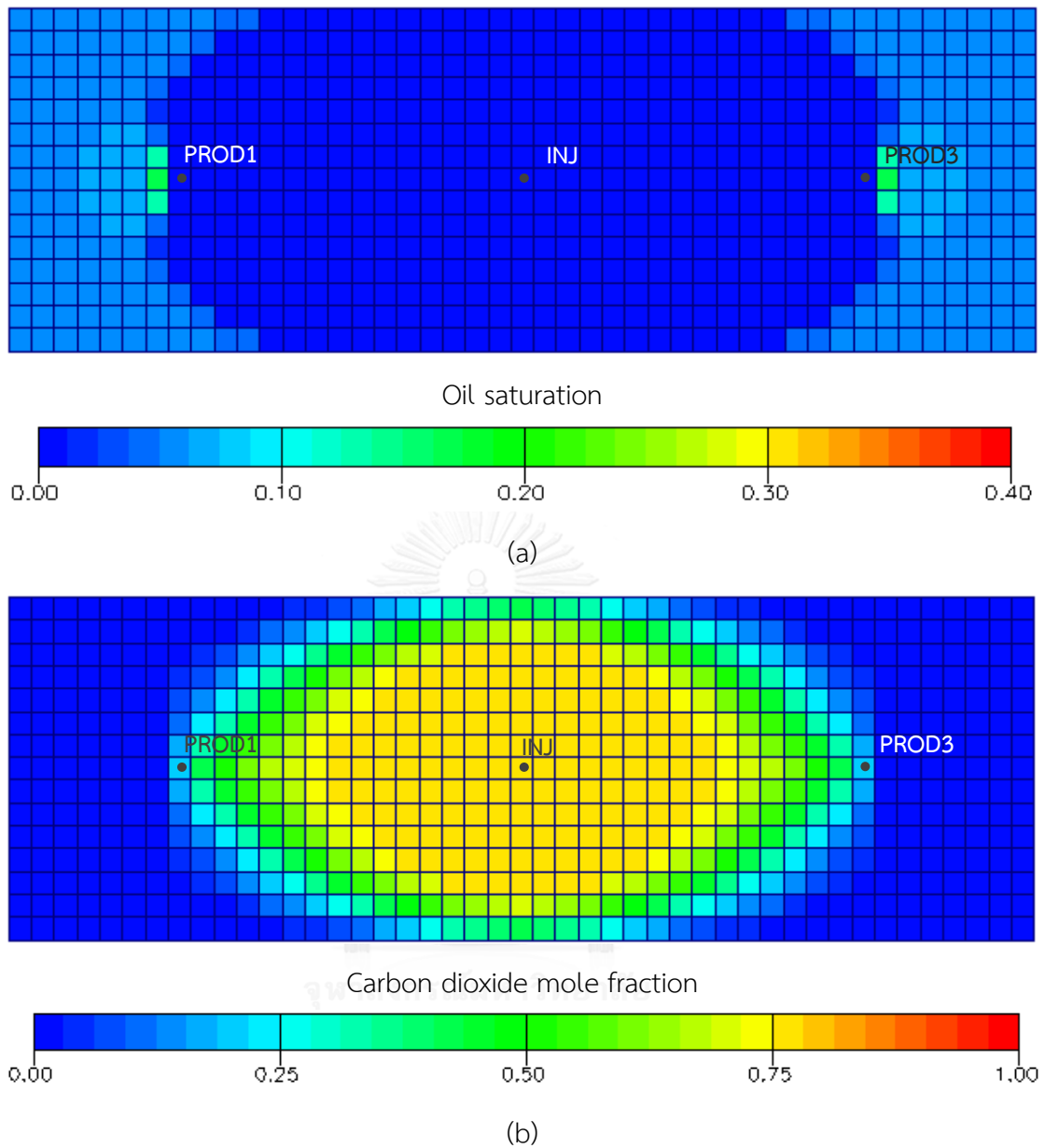


Figure 5.17: (a) Oil saturation distribution and (b) Carbon dioxide mole fraction distribution of case with injection rate of 16.0 MMSCFD of conventional gas injection scenario with high CGR composition of original reservoir fluid when condensate starts to dropout (i.e. 272 days of production)

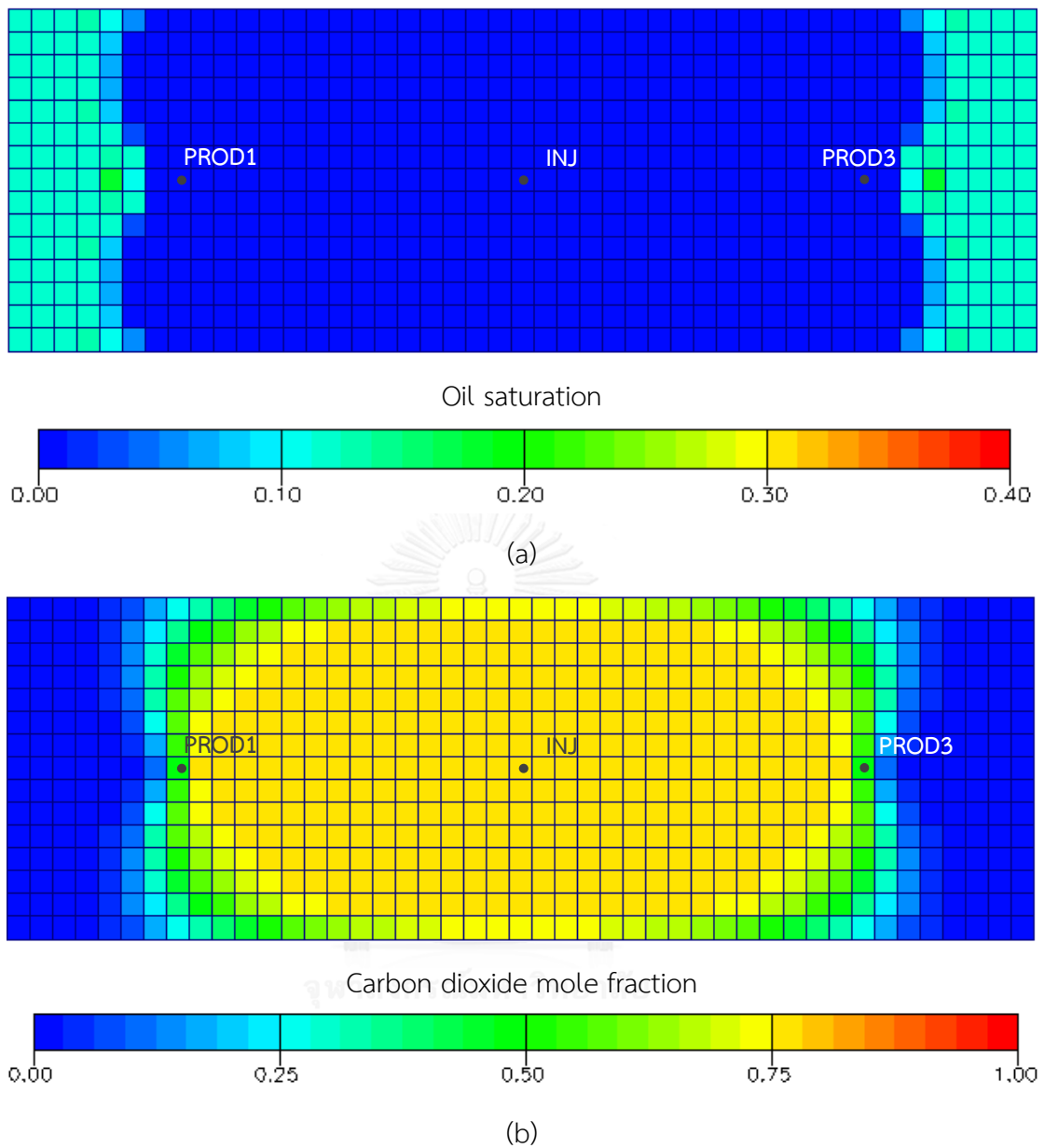


Figure 5.18: (a) Oil saturation distribution and (b) Carbon dioxide mole fraction distribution of case with injection rate of 20.0 MMSCFD of conventional gas injection scenario with high CGR composition of original reservoir fluid when condensate starts to dropout (i.e. 546 days of production)

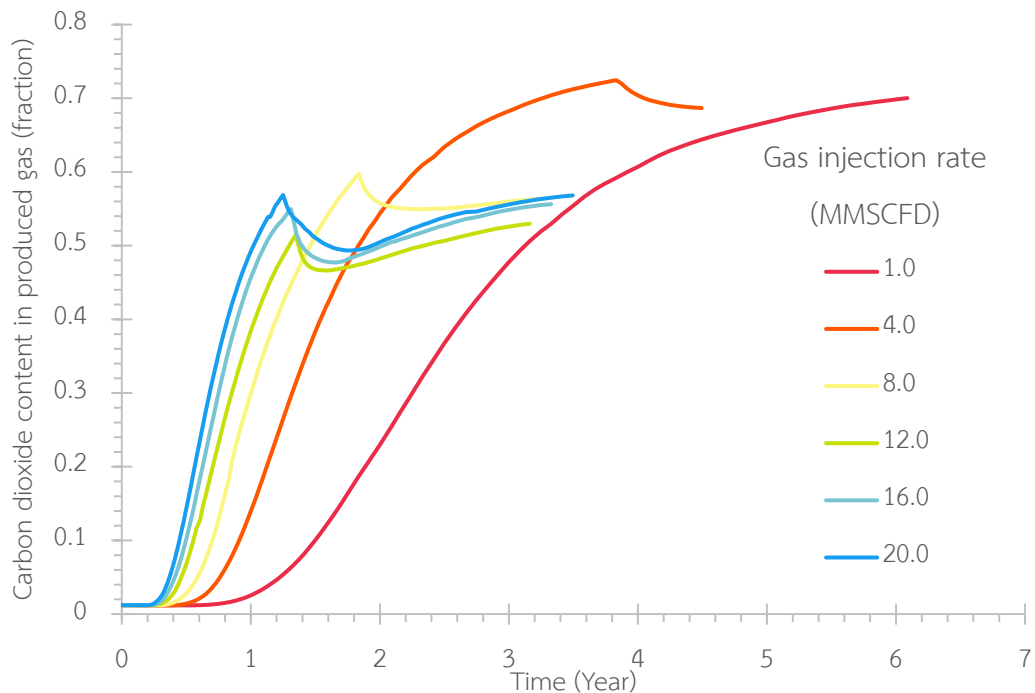


Figure 5.19: Carbon dioxide content of produced gas for different gas injection rates of conventional gas injection scenario with high CGR composition of original reservoir fluid

Figure 5.20 shows that cases with low injection rate (1.0 and 4.0 MMSCFD) can recover less condensate at early time but have a longer production life resulting in higher condensate recovery at field abandonment date. Although less gas injection rate results in condensate banking near the producers and cause less condensate production at early time, excessive amount of carbon dioxide in high injection rate cases severely shrinks the phase envelope of the reservoir fluids and results in quick falling of condensate production rate at late time, reaching the economic condensate rate limits for gas injection sooner. Less pressure support at late time and prior severe shrinking effect in the cases with high gas injection rate is due to stopping gas injection sooner, and higher carbon dioxide content near the producers leads to rapid decline of total BOE production reaching economic limit earlier. This results in less cumulative condensate production at abandonment and shorter production time in high gas injection case. Consequently, low gas injection rate case is attractive in term of condensate recovery. However, low injection rate case provides slightly lower HC gas recovery comparing to high injection rate cases and requires longer production time.

In summary, the less injection rate is, the more condensate recovery as shown in Table 5.3. However, the lowest injection rate causes very long production time as well.

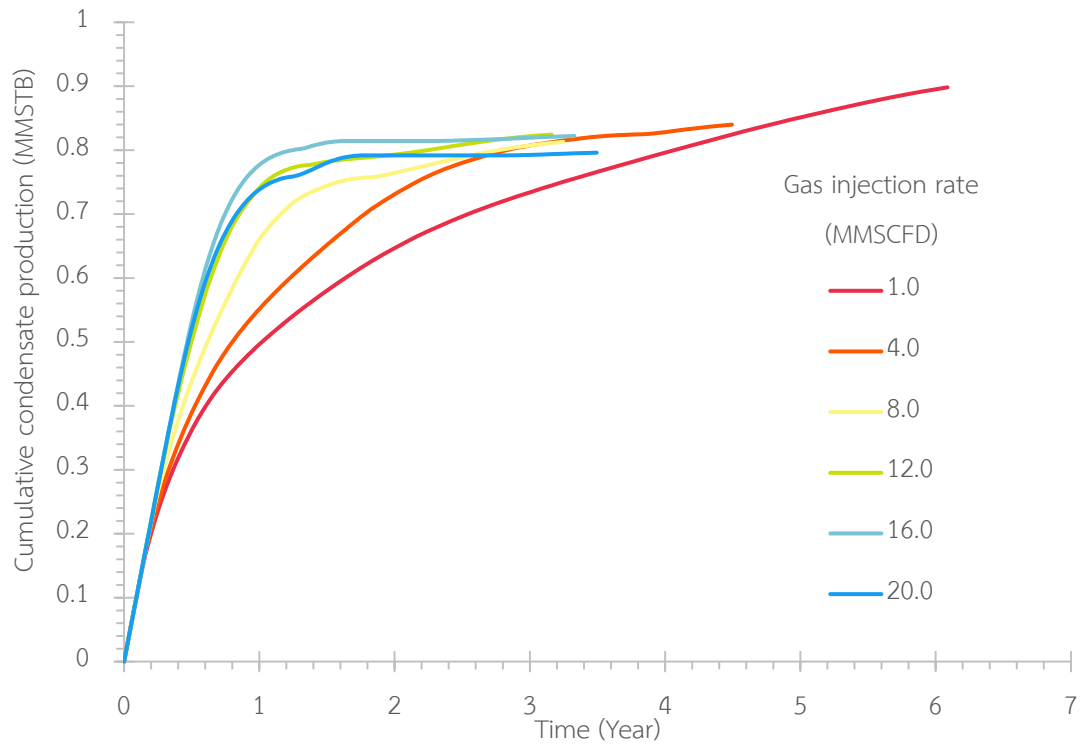


Figure 5.20: Cumulative oil production versus time for different gas injection rates of conventional gas injection scenario with high CGR composition of original reservoir fluid

Table 5.3: Summarized results of different gas injection rates of conventional gas injection scenario with high CGR composition of original reservoir fluid

Cases	20.0	16.0	12.0	8.0	4.0	1.0
Cumulative condensate production (MMSTB)	0.796	0.822	0.824	0.813	0.840	0.898
Original condensate in place (MMSTB)	1.374	1.374	1.374	1.374	1.374	1.374
Condensate recovery factor (%)	57.9%	59.8%	60.0%	59.1%	61.1%	65.4%
Cumulative gas production (BCF)	17.883	16.374	14.563	13.990	14.201	10.649
Original gas in place (BCF)	9.149	9.149	9.149	9.149	9.149	9.149
Gas recovery factor (%)	95.7%	95.3%	94.6%	94.3%	94.0%	92.1%
Cumulative HC gas production (BCF) *	10.938	10.590	10.160	10.045	10.172	9.311
HC gas recovery factor (%) **	99.6%	99.0%	98.1%	98.1%	98.9%	96.9%
Cumulative gas production (MMBOE)	2.989	2.889	2.760	2.723	2.763	2.492
Cumulative total BOE production (MMBOE)	3.785	3.711	3.584	3.536	3.603	3.390
Original BOE in place (MMBOE)	4.496	4.496	4.496	4.496	4.496	4.496
Total BOE recovery factor (%)	77.1%	76.6%	75.1%	74.5%	75.8%	73.7%

Note: * HC gas is produced gas deducted by nitrogen and carbon dioxide content

** Percentage of HC gas production gas production compared to original gas in place

The starting time of gas injection was varied by three different triggering conditions for all gas injection rates. Figure 5.21 and Figure 5.22 show condensate recovery and HC gas recovery factor for all cases of conventional gas injection scenario, respectively. Delaying starting time does not have significant effect in HC gas recovery.

Condensate recovery factor is reduced for cases with high gas injection rate when the gas injection is delayed due to condensate banking and rapid blend between reservoir fluid and injected gas resulting in drying out of condensate faster. However, the reduction of condensate recovery by delaying gas injection tends to decrease as injection rate decreases until the opposite manner appears at very low gas injection rate of 1.0 to 4.0 MMSCFD. With these low gas injection rates, the condensate production slightly increases by starting gas injection at late time. This is because more condensate are produced earlier. Moreover, slowly blending the fluids inside the target reservoir by low gas injection rate does not dry out the condensate by severe shrinking effect and can maintain condensate production until abandonment.

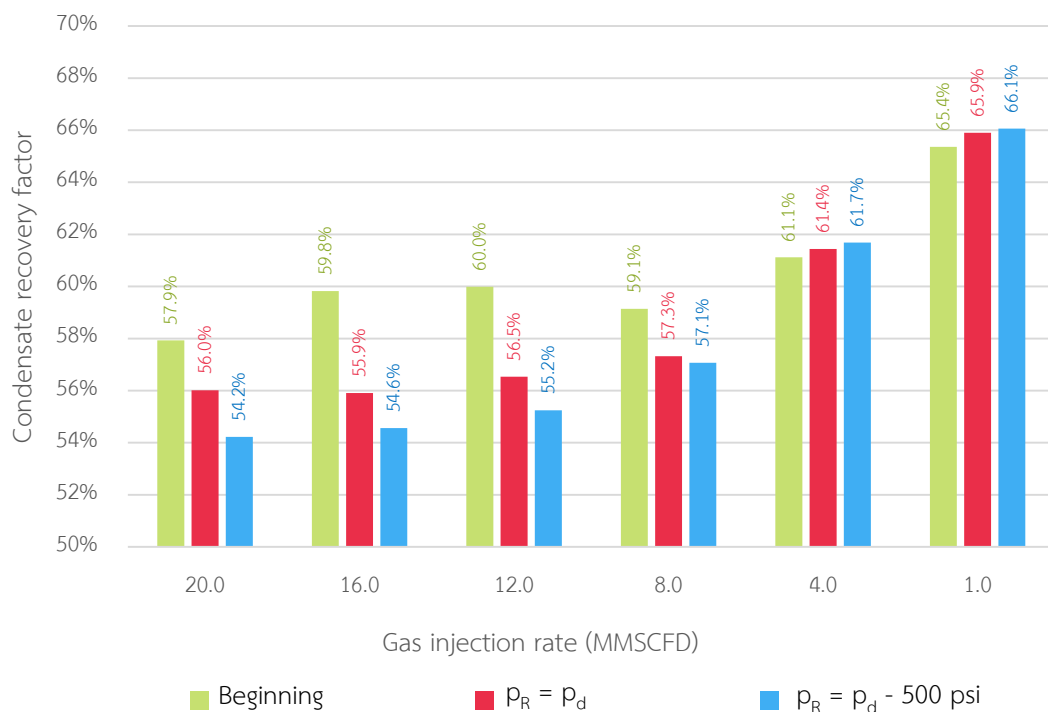


Figure 5.21: Condensate recovery factor for different starting times of gas injection with high CGR composition of original reservoir fluid

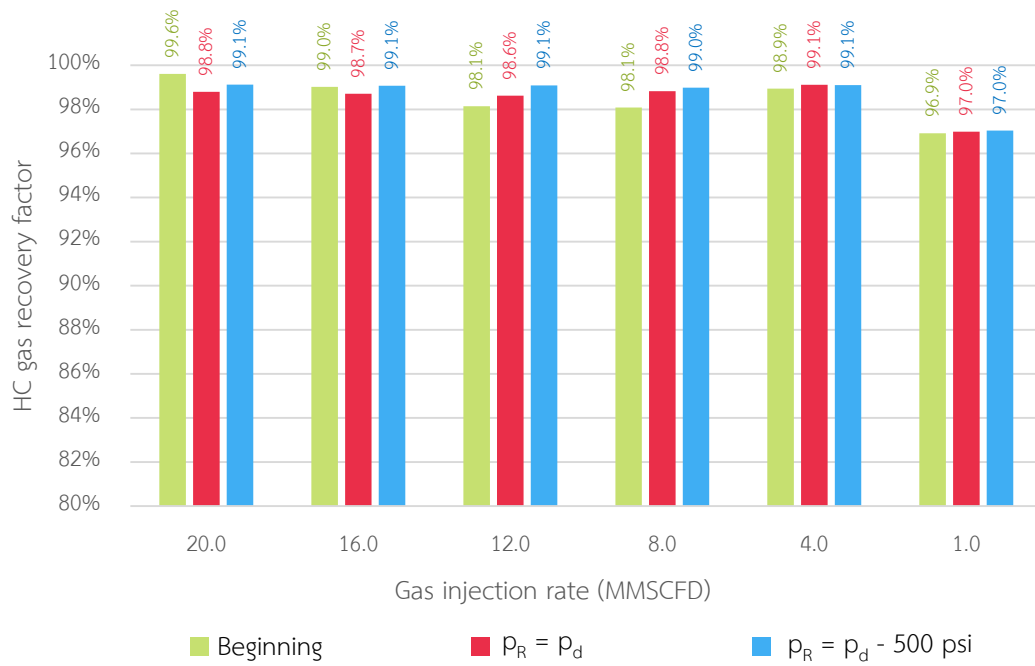


Figure 5.22: HC gas recovery factor for different starting times of gas injection with high CGR composition of original reservoir fluid



5.2.2 Composition Yielding Low CGR of Original Reservoir Fluid

The first part of this section mainly focuses on the effect of gas injection rate on reservoirs fluid yielding low CGR. The cases with varied gas injection from 1.0 to 20.0 MMSCFD starting gas injection since the beginning are discussed first. Although all cases initially produce the same gas production rate at 10.0 MMSCFD/well, each case began its decline period at different times depending on gas injection rate as demonstrated in Figure 5.23.

The case of the lowest injection rate of 1.0 MMSCFD encounters decline period earliest by the fact that this low injection rate results in less capability to maintain the reservoir pressure. Nevertheless, this low injection rate has lower condensate production rate limit of 4.4 STB/D. Consequently, the gas injection is continued until abandonment as the economic condensate production rate limit for gas injection is not reached.

For cases with injection rate of 4.0 to 8.0 MMSCFD, these have two decline trends which are (1) the first decline as a result of insufficient pressure support of the reservoir and (2) the second decline caused by stopping gas injection due to economic condensate production rate limit. For the higher gas injection rate cases from 12.0 to 20.0 MMSCFD, the reservoir pressure maintained by high injection rate can support the gas production at plateau rate as long as gas injection is operating. However, the economic condensate production rate limits for gas injection are reached earlier in case of higher gas injection rates. After reaching the condensate rate limits, gas injection is stopped and the gas production is sustained at plateau rate for a while before it declines due to less pressure support.

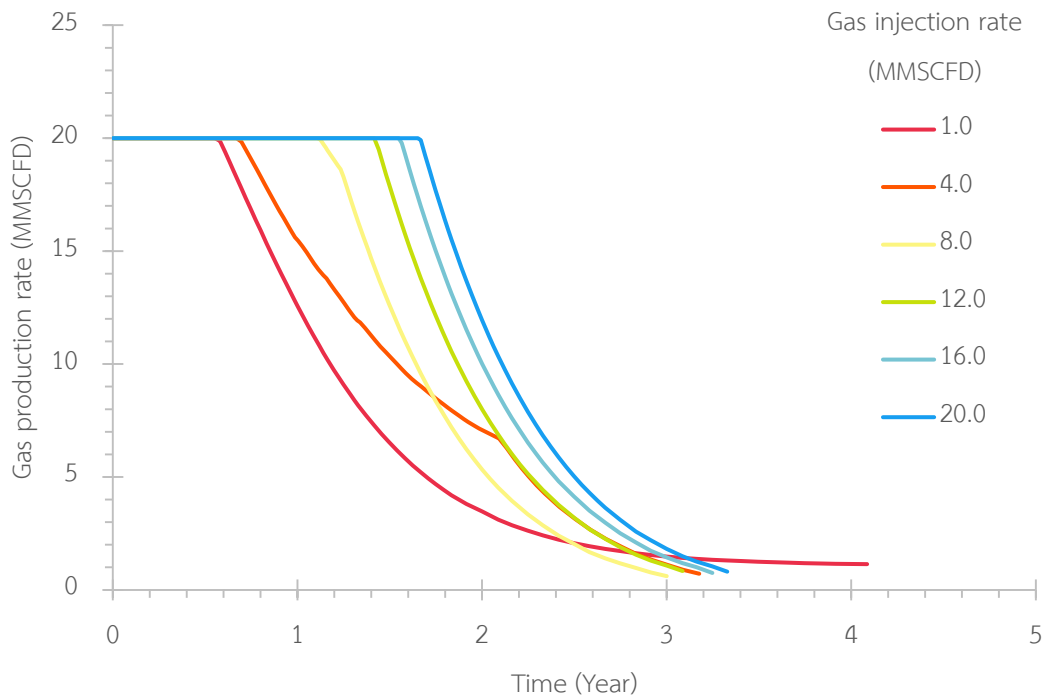


Figure 5.23: Field gas production rate profiles for different gas injection rates of conventional gas injection scenario with low CGR composition of original reservoir fluid

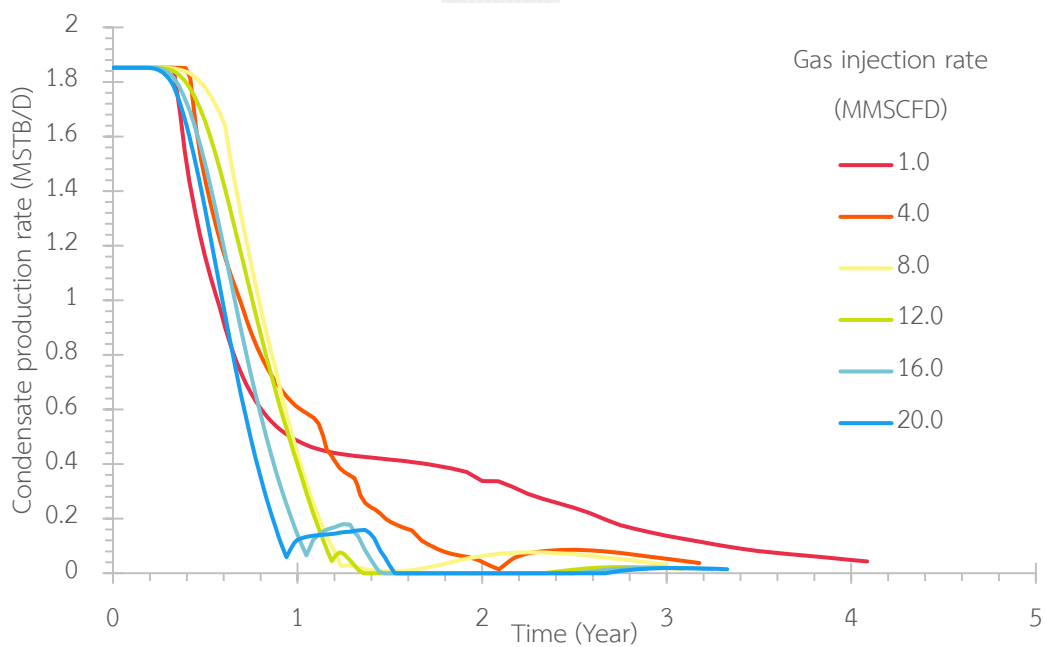


Figure 5.24: Field condensate production rate profiles for different gas injection rates of conventional gas injection scenario with low CGR composition of original reservoir fluid

As seen in Figure 5.24, all the cases initially provide the same condensate production rate of 1.85 MSTB/D as they all have the same original reservoir fluid composition. During the same period of time, condensate production rates of all cases start falling from the plateau rate because of two determinants. The first one is condensate banking near the producers. This phenomenon happens for the cases with low gas injection rate (1.0 and 4.0 MMSCFD) which have less capability to sustain the reservoir pressure. Due to less capability to maintain the pressure, condensate production of 1 MMSCFD gas injection declines faster than that of 4.0 MMSCFD.

The second determinant is shrinking effect by high carbon dioxide content near the production wells. This happens in higher injection rate cases from 8.0 to 20.0 MMSCFD which have capability to maintain the pressure to be above the dewpoint pressure until the carbon dioxide breaks through. After that, the phase envelope shrinks due to higher carbon dioxide content, resulting in less condensate. From Figure 5.25, the higher gas injection rate, the faster carbon dioxide breaks through resulting in faster drop of condensate production rate. This phenomenon causes the severe shrinking effect, influencing quick drop of condensate production rates until they are lower than those of the cases having condensate banking at the producers (1.0 and 4.0 MMSCFD cases).

The economic condensate limit for gas injection is reached quicker for cases with higher gas injection rate because of the shrinking effect. Therefore, the time to stop gas injection is quite early for higher gas injection rate cases. After stopping the injection, condensate production rate gradually increases for a short period of time due to less carbon dioxide content as depicted in Figure 5.25 before it continuously declines until abandonment.

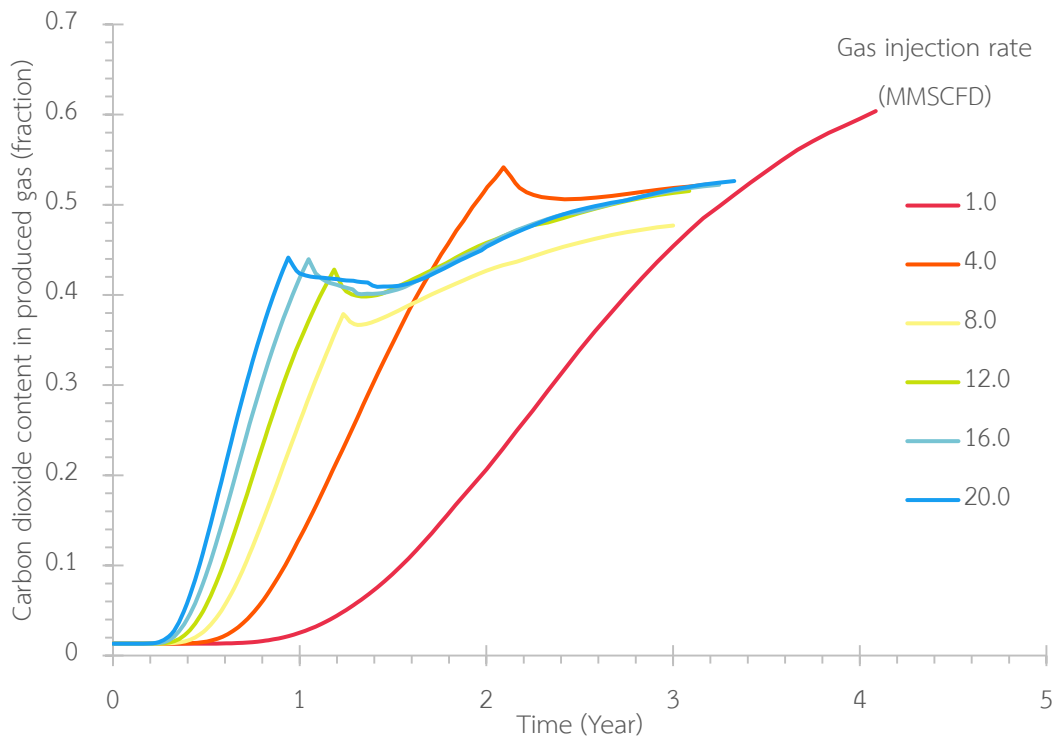


Figure 5.25: Carbon dioxide content of produced gas for different gas injection rates of conventional gas injection scenario with low CGR composition of original reservoir fluid

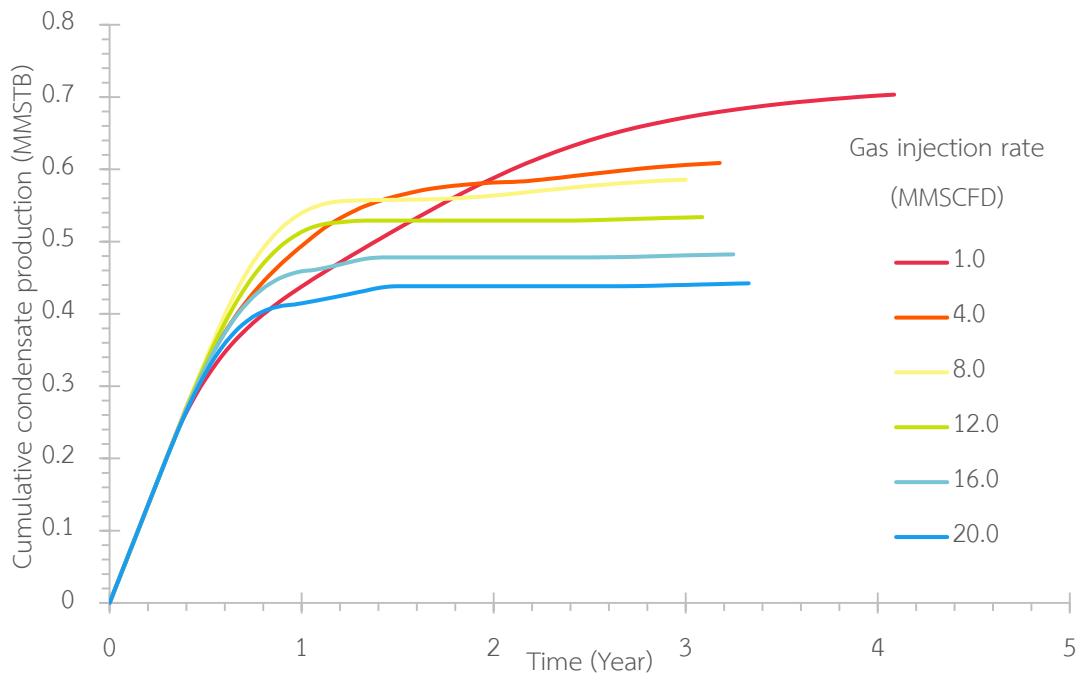


Figure 5.26: Cumulative condensate production for different gas injection rates of conventional gas injection scenario with low CGR composition of original reservoir fluid

As demonstrated in Figure 5.26, all cases have the same cumulative condensate production until condensate banking occurs at the producers in low gas injection rate cases (1.0 and 4.0 MMSCFD) and carbon dioxide breaks through in high gas injection cases (8.0 to 20.0 MMSCFD).

After occurrence of these phenomena, condensate banking at the producers results in lower condensate production rate at early time. However, severe shrinking effect drastically reduces condensate production rate until it less than that of cases with condensate banking at the producers and causes the condensate to dry out rapidly reaching the limit condensate rate for gas injection earlier. Less pressure support by stopping gas injection results in further reduction of both gas and condensate production rate until reaching the economic limit of 83.33 BOED/well faster than cases with condensate banking at producers. While cases with low gas injection rate of 1.0 and 4.0 MMSCFD, they can maintain condensate production due to gradual shrinking effect. This results in higher condensate recovery for lower gas injection rate as depicted in Table 5.4.

Although cumulative gas production mainly depends on gas production rate, after deducting cumulative gas injection, gas recovery is not much different among cases. The maximum difference of gas recovery is only 3.6% which is much smaller than the difference in condensate recovery in which the highest value is 29.1%.

Table 5.4: Summarized results of different gas injection rates of conventional gas injection scenario with low CGR composition of original reservoir fluid

Cases	20.0	16.0	12.0	8.0	4.0	1.0
Cumulative condensate production (MMSTB)	0.442	0.482	0.534	0.586	0.609	0.703
Original condensate in place (MMSTB)	0.896	0.896	0.896	0.896	0.896	0.896
Condensate recovery factor (%)	49.4%	53.9%	59.6%	65.4%	68.0%	78.5%
Cumulative gas production (BCF)	16.158	15.386	14.396	12.760	12.167	10.443
Original gas in place (BCF)	9.673	9.673	9.673	9.673	9.673	9.673
Gas recovery factor (%)	96.1%	95.8%	95.1%	94.6%	94.2%	92.5%
Cumulative HC gas production (BCF) *	10.991	10.804	10.559	10.157	10.040	9.614
HC gas recovery factor (%) **	99.4%	99.0%	98.4%	97.6%	97.5%	96.3%
Cumulative gas production (MMBOE)	3.316	3.255	3.175	3.051	3.012	2.865
Cumulative total BOE production (MMBOE)	3.758	3.738	3.709	3.637	3.620	3.568
Original BOE in place (MMBOE)	4.186	4.186	4.186	4.186	4.186	4.186
Total BOE recovery factor (%)	84.1%	84.2%	84.3%	83.9%	83.9%	84.0%

Note: * HC gas is produced gas deducted by nitrogen and carbon dioxide content

** Percentage of HC gas production gas production compared to original gas in place

The second part of this section mainly discusses about the effect of starting time of gas injection. Three different triggering conditions resulting in different starting

time were performed for all injection rate cases. From Figure 5.27, starting gas injection at late time tends to result in higher condensate recovery because of higher prior condensate production before carbon dioxide breakthrough. With respect to HC gas recovery, starting gas injection at different times insignificantly affects the results as depicted in Figure 5.28.

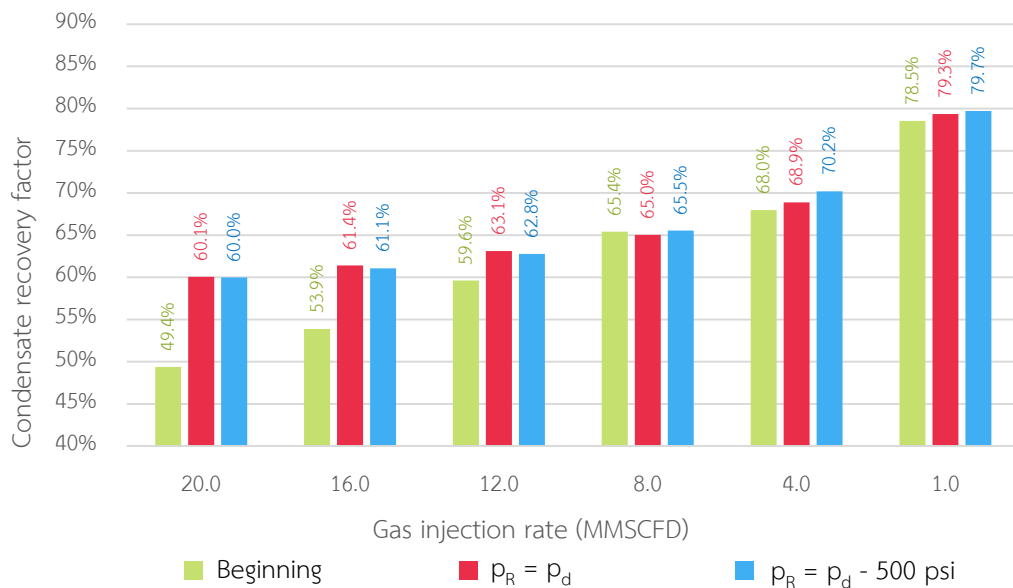


Figure 5.27: Condensate recovery factor for different starting times of gas injection with low CGR composition of original reservoir fluid

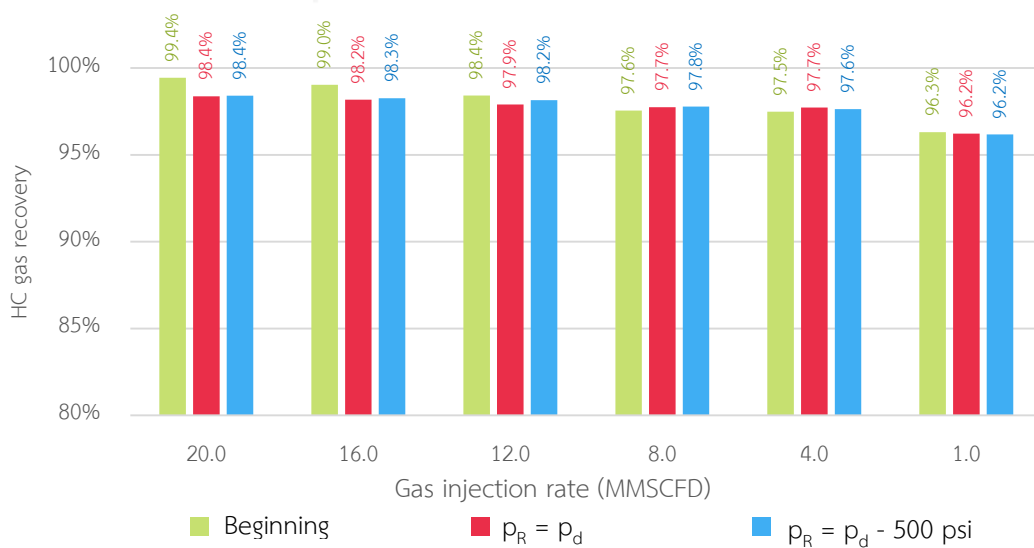


Figure 5.28: HC gas recovery factor for different starting times of gas injection with low CGR composition of original reservoir fluid

5.3 Gas Dumpflood from Multiple-Gas Reservoirs

In this scenario, the same condensate reservoir was modelled with existing of four underlying high carbon dioxide content gas source reservoirs. These reservoirs are used to represent typical contingent resource gas reservoirs in Gulf of Thailand where many gas reservoirs are multi-stack thin layers of small sizes contaminating high carbon dioxide. The gas source reservoirs in the model contain very high carbon dioxide content of 80% mole with the rest as methane, the same as injected gas in the conventional gas injection scenario. The same well pattern as the one in the natural depletion scenario is used.

In the simulation model, the gas condensate reservoir was depleted by two production wells with a specified plateau rate of 10.0 MMSCFD for each, minimum wellhead pressure of 200 psia, and distance of 1,500 ft. as in the natural depletion scenario. The middle well is used as production well at beginning and dumping well after condition for dumpflood is triggered. Since there are two production wells in this scenario, the abandonment condition is 166.7 BOE/D (83.33 BOE/D/well).

In order to determine the optimal operating condition for gas dumpflood, the studied parameters are divided as follows:

1. Reservoir parameters including
 - 1.1 Compositions yielding different CGR of original reservoir fluid
 - High CGR
 - Low CGR
 - 1.2 Size of multiple source reservoirs for dumping
 - 4 layers of 25-ft source gas reservoirs
 - 4 layers of 50-ft source gas reservoirs
2. Operating parameters including
 - 2.1 Perforation sequence of dumping well
 - Simultaneously perforate four source gas reservoirs

- Perforate two lower source gas reservoirs first then the remaining two upper reservoirs after the reservoir pressure declines by 300 psi from the first perforation or bottom up
- Perforate only two upper source gas reservoirs
- Perforate only two lower source gas reservoirs

2.2 Starting time of dumpflood

- At beginning
- When the reservoir pressure declines below the dewpoint pressure
- When the reservoir pressure declines more than 500 psi below the dewpoint pressure

The effects of reservoir and operating parameters for the two compositions yielding different condensate to gas ratios are separately discussed in Sections 5.3.1 and 5.3.2 for high CGR and low CGR composition, respectively. Both sections are separated into two subtopics for discussions of sizes of multiple source reservoirs including 25-ft versus 50-ft thickness. All operating parameters consisting of 12 cases as described in Table 5.5 are discussed in each subtopic of reservoir parameters.

Due to the same original gas in place of each source reservoir of 5,192 MMSCF for 25-ft thickness and 10,390 MMSCF for 50-ft thickness, cases 1-1 to 2-3 have the same amount of total original gas source in place which is those of four source reservoirs while cases 3-1 to 4-3 are perforated only two reservoirs and, therefore, have only half of total original gas source in place.

Table 5.5: Descriptions of all cases with varying operating and reservoir parameters

Cases	Starting time of dumpflood	Perforation sequence of dumping well
1-1	Beginning	Simultaneously perforate four source gas reservoirs
1-2	$p_R < p_d$	
1-3	$p_R < p_d - 500$ psi	
2-1	Beginning	Bottom up
2-2	$p_R < p_d$	
2-3	$p_R < p_d - 500$ psi	
3-1	Beginning	Perforate only two upper source gas reservoirs
3-2	$p_R < p_d$	
3-3	$p_R < p_d - 500$ psi	
4-1	Beginning	Perforate only two lower source gas reservoirs
4-2	$p_R < p_d$	
4-3	$p_R < p_d - 500$ psi	

5.3.1 Composition Yielding High CGR of Original Reservoir Fluid

5.3.1.1 25-ft Thickness of Source Gas Reservoirs

In order to describe the effect of perforation sequence, the result of cases with the same time of starting dumpflood at the beginning with different perforation sequences including cases 1-1, 2-1, 3-1, and 4-1 were investigated first. For these cases, gas is produced at plateau rate for a while before it declines due to the insufficient pressure support. As seen in Figure 5.29 and Figure 5.30, there is no significant difference between cases 1-1 and 2-1 for gas and condensate production as there is the same number of perforated gas layers. In the same manner, cases 3-1 and 4-1 have similar gas and condensate recovery as only two source reservoirs are perforated for both cases.

Because of higher dumped gas rates, cases 1-1 and 2-1 have longer production lives of the field and recover more gas comparing to cases 3-1 and 4-1 as illustrated in Figure 5.31. Cases 1-1 and 2-1, moreover, can recover slightly higher oil comparing to cases 3-1 and 4-1 as depicted in Figure 5.30 due to faster displacement by dumped gas consisting 80% carbon dioxide and higher sweep efficiency at abandonment as demonstrated in Figure 5.32 for case 1-1 and Figure 5.33 for case 3-1.

Although the cross-flowing gas rates between cases 1-1 and 2-1 are not the same at early times because of different sequences of perforation, this has very small effect on gas and condensate production rates. Hence, the gas and condensate recoveries of both cases are similar. For cases with less perforated gas layer, cases 3-1 and 4-1, the slight difference of cross-flowing gas rates between cases 3-1 and 4-1 in Figure 5.31 is caused by the difference in initial pressure of the perforated high carbon dioxide gas reservoirs.

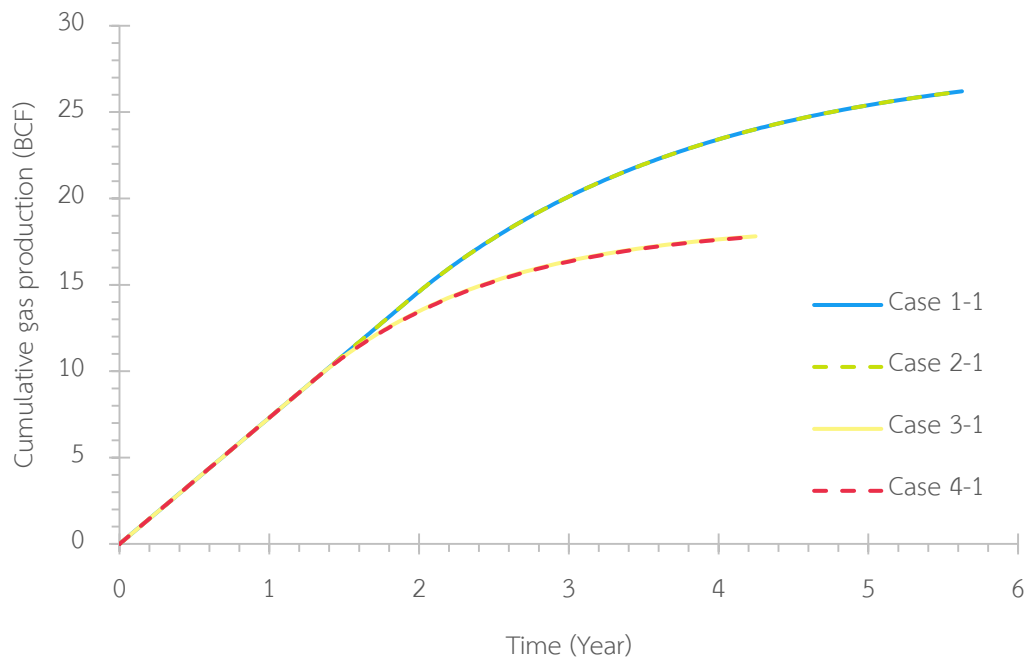


Figure 5.29: Cumulative gas production for different perforation sequences of gas dumpflood scenarios starting at the beginning with high CGR composition of original reservoir fluid and 25-ft thickness of the source gas reservoirs

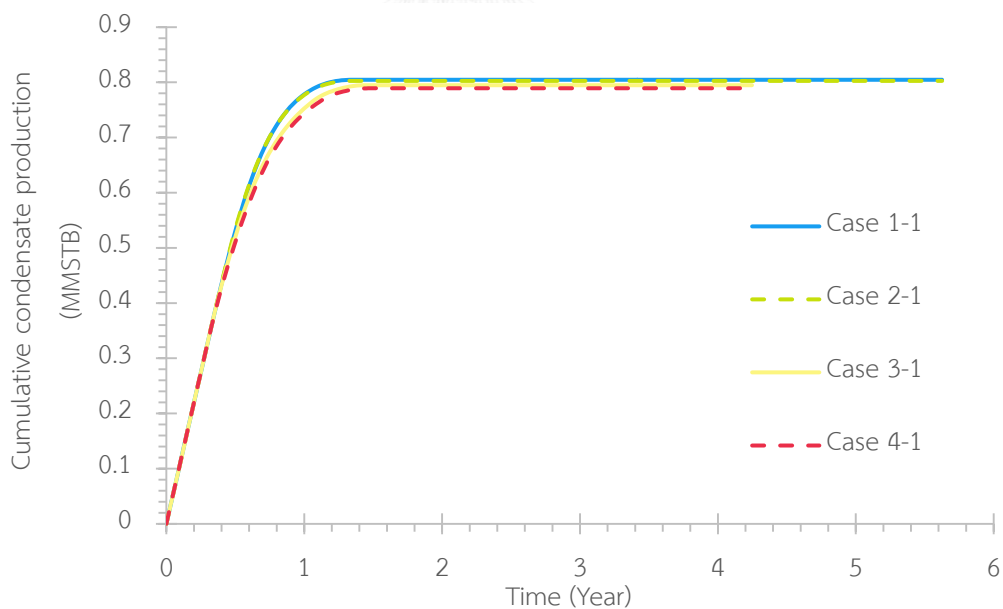


Figure 5.30: Cumulative condensate production for different perforation sequences of gas dumpflood scenarios starting at the beginning with high CGR composition of original reservoir fluid and 25-ft thickness of the source gas reservoirs

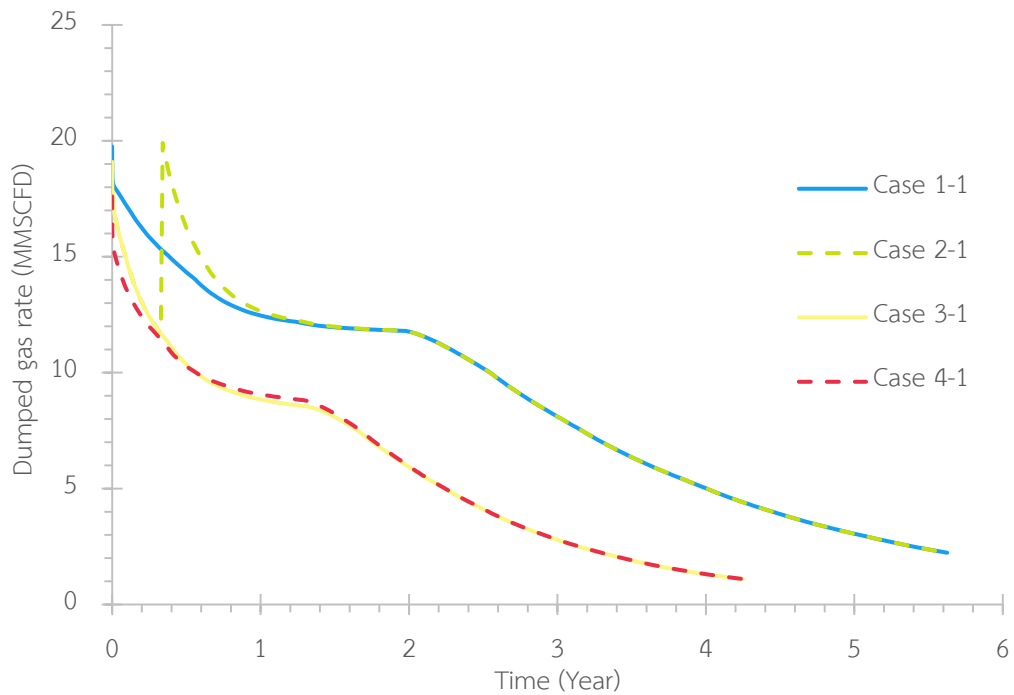


Figure 5.31: Dumped gas rate profiles for different perforation sequences of gas dumpflood scenarios starting at the beginning with high CGR composition of original reservoir fluid and 25-ft thickness of the source gas reservoirs

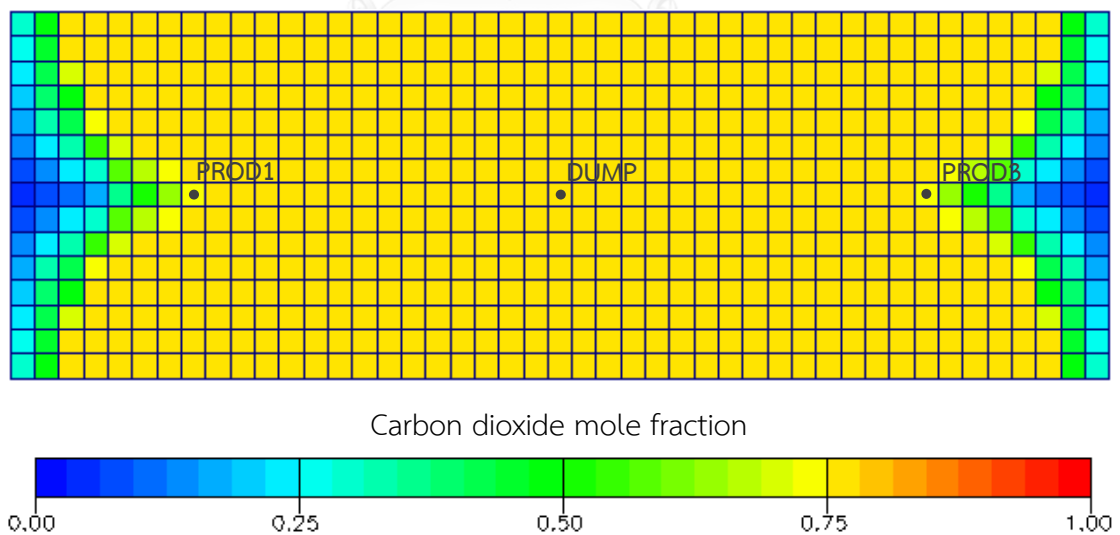


Figure 5.32: Carbon dioxide mole fraction distribution of simultaneously perforated all four source reservoirs at the beginning with high CGR composition of original reservoir fluid and 25-ft thickness of the source gas reservoirs when abandonment (i.e. 2053 days of production)

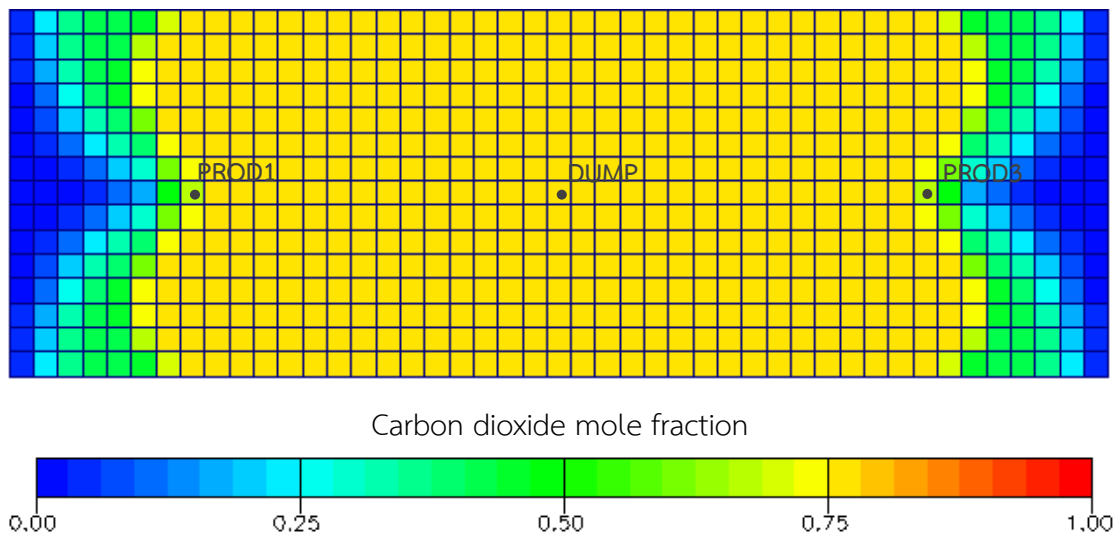


Figure 5.33: Carbon dioxide mole fraction distribution of simultaneously perforated two lower source reservoirs at the beginning with high CGR composition of original reservoir fluid and 25-ft thickness of the source gas reservoirs when abandonment (i.e. 1550 days of production)

From Table 5.6, perforating all high carbon dioxide reservoirs (i.e. cases 1-1 and 2-1) results in higher total barrels of oil-equivalent recovery since more HC gas and condensate can be recovered. With all four layers of source reservoirs being perforated (the same amount of gas available for dumping), cases 1-1 and 2-1, consequently, have insignificant differences of gas, HC gas, condensate, and total BOE recovery factors. Cases 3-1 and 4-1 provide similar amount of gas, HC gas, condensate, and total BOE recovery factors as the difference in initial pressures of the source reservoirs do not significantly impact the gas and condensate recovery because almost the same amount of carbon dioxide crosses flow from the high carbon dioxide reservoirs into the condensate reservoir.

HC gas recovery factors are more than 100% recovery in cases 1-1 and 2-1, indicating that there is another source of HC gas apart from the original HC gas in place and cross-flowing HC gas which is already subtracted for HC gas recovery factor calculation. That is the dried condensate by severe shrinking effect from excessive carbon dioxide content. The carbon dioxide content induces light end in condensate

to vaporize into gas phase, resulting in more amount of HC gas in the model meanwhile less amount of condensate in the contrary.

Table 5.6: Summarized results of different perforation sequences of gas dumpflood scenarios starting at the beginning with high CGR composition of original reservoir fluid and 25-ft thickness of the source gas reservoirs

Cases	1-1	2-1	3-1	4-1
Cumulative condensate production (MMSTB)	0.805	0.802	0.795	0.789
Original condensate in place (MMSTB)	1.374	1.374	1.374	1.374
Condensate recovery factor (%)	58.5%	58.4%	57.8%	57.4%
Cumulative gas production (BCF)	26.204	26.202	17.811	17.783
Original gas in place (BCF)	9.149	9.149	9.149	9.149
Gas recovery factor (%)	92.6%	92.7%	94.2%	94.2%
Cumulative HC gas production (BCF) *	12.743	12.744	10.972	10.969
HC gas recovery factor (%) **	100.5%	100.5%	99.8%	99.9%
Cumulative gas production (MMBOE)	3.349	3.350	2.986	2.987
Cumulative total BOE production (MMBOE)	4.153	4.152	3.780	3.776
Original BOE in place (MMBOE)	4.496	4.496	4.496	4.496
Total BOE recovery factor (%)	78.6%	78.6%	76.9%	76.9%

Note: * HC gas is produced gas deducted by nitrogen and carbon dioxide content

** Percentage of HC gas production gas production compared to original gas in place

Cases with the same perforation sequence of simultaneous perforation of four source reservoirs and different starting times of dumpflood including cases 1-1, 1-2,

and 1-3 are now discussed in order to describe the effect of starting time of dumpflood operation. As depicted in Figure 5.34 for gas production profiles and Figure 5.35 for condensate production profiles, cases 1-2 and 1-3 initially produce with higher gas and condensate production rate comparing to case 1-1 due to the fact that all three wells are production wells at beginning while the middle well in case 1-1 is a dumping well since the beginning. All three wells in cases of 1-2 and 1-3 produce for only a month before the BHPs reach the dewpoint pressure, and condensate drops out around the wellbores. Therefore, condensate production rate for both cases drastically decline and after that the middle well of case 1-2 is converted to dumping well as the reservoir pressure reaches the dewpoint which is the triggering condition. The middle well in case 1-3 produce for two months more and then is converted to dumping well when the reservoir pressure is 500 psi lower than the dewpoint pressure.

After performing a dumpflood operation, cases 1-2 and 1-3 have sudden falls of gas and condensate production rates because the middle well is converted to a dumping well. Gas production rates drops to the plateau rate of two production wells but condensate production rates drops below that of case 1-1 due to the fact that there is condensate banking for cases 1-2 and 1-3.

All three cases can maintain the plateau gas production rates until approximately two years of production before they decline as there is less and less pressure support. The later the starting time of dumpflood operation, the sooner the beginning of decline in gas production rate, resulting in a slight difference in gas recoveries among the three cases as shown in Figure 5.36. The gas production rates of all cases, then, continuously decline until the abandonment.

After dumpflood is started, condensate production rates continue declining with the original trend in cases 1-2 and 1-3 before they pick up because of condensate revaporization from gas dumpflood. After a while, condensate production rates decline again as less and less condensate is left inside the reservoir. Condensate recoveries for different cases are demonstrated in Figure 5.37.

Although cases 1-2 and 1-3 can recovery slightly higher condensate at very early time by the fact that there are more production wells in these case than that in case 1-1, condensate declines faster in cases 1-2 and 1-3 after condensate banking and beginning of gas dumpflood because the reservoir fluid quickly blends with dumped gas as less pressure in the target reservoir resulting in more pressure difference between the source and the target reservoirs. As seen in Figure 5.38, carbon dioxide content of the produced gas increases faster after breakthrough when gas dumpflood is started at late time, implying a quick blending between reservoir fluid and dumped gas. This phenomenon leads to rapid drying out of the condensate and causes less condensate production for the case with later starting time of gas dumpflood as happened in high gas injection rate cases.

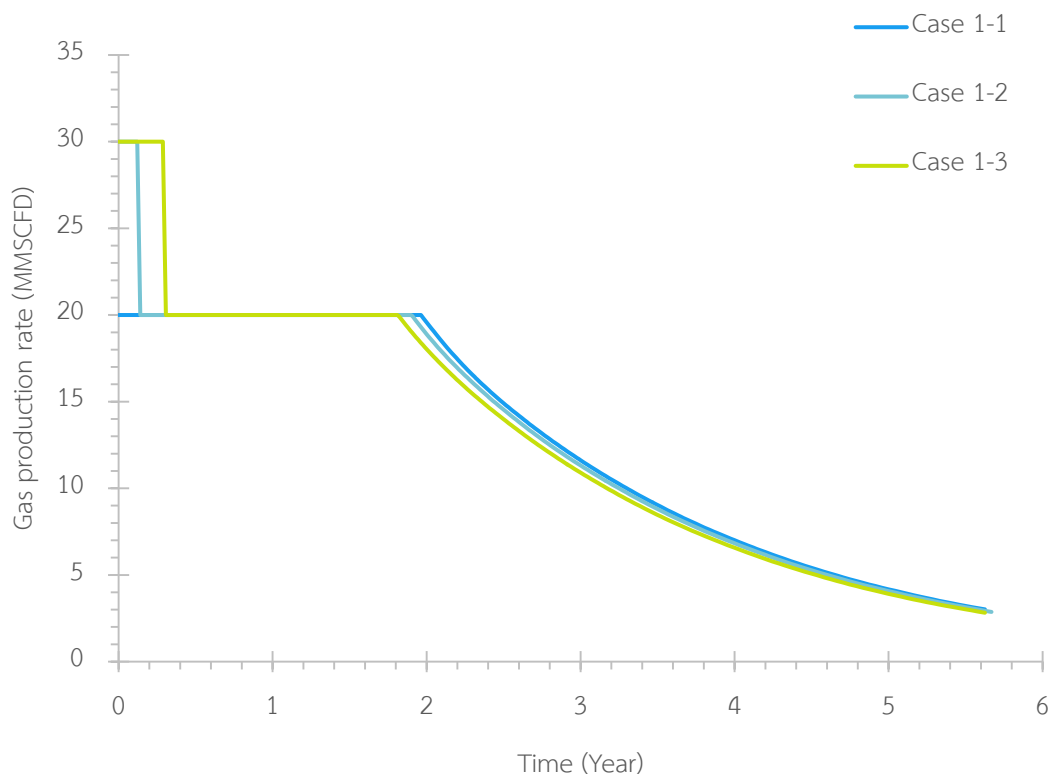


Figure 5.34: Gas production profiles for different starting times of dumpflood operation having simultaneous perforation all of source reservoirs with high CGR composition of original reservoir fluid and 25-ft thickness of the source gas reservoirs

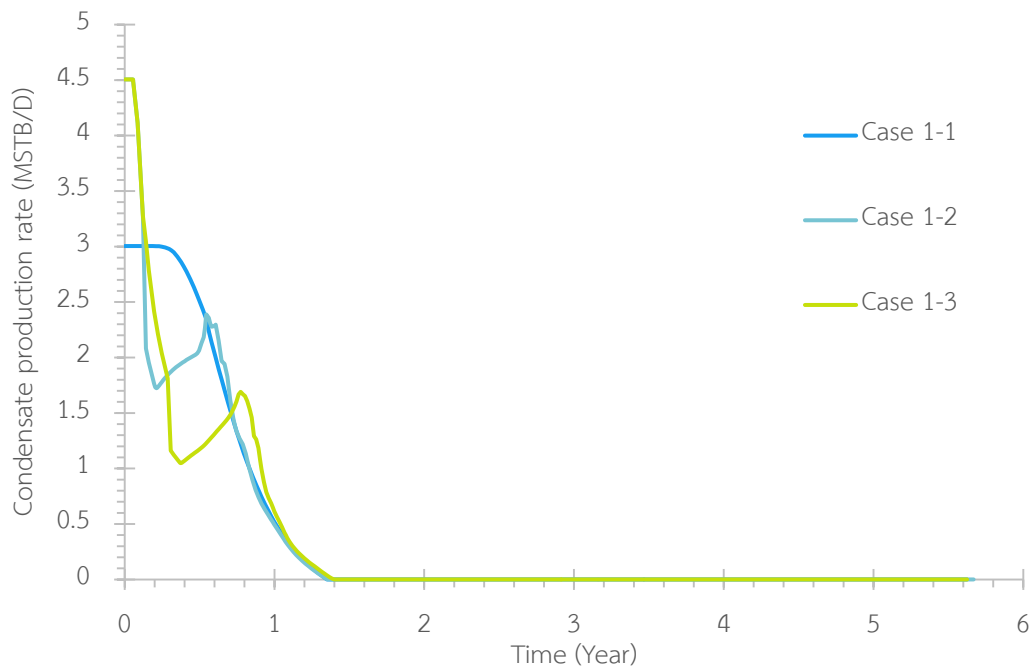


Figure 5.35: Condensate production for different starting times of dumpflood operation having simultaneous perforation all of source reservoirs with high CGR composition of original reservoir fluid and 25-ft thickness of the source gas reservoirs

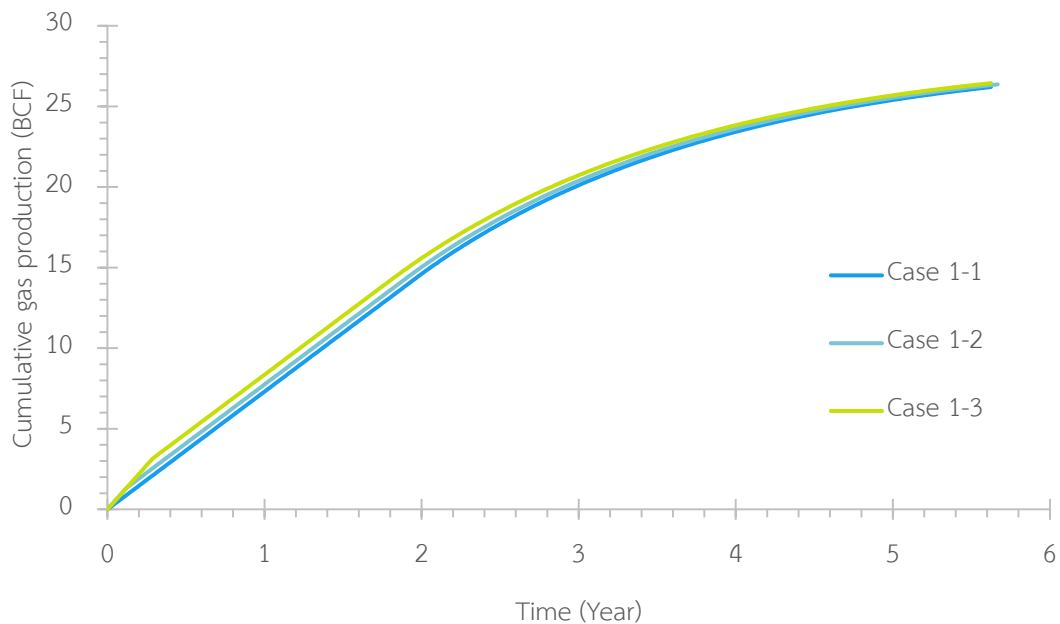


Figure 5.36: Cumulative gas production versus time for starting times of dumpflood operation having simultaneous perforation all of source reservoirs with high CGR composition of original reservoir fluid and 25-ft thickness of the source gas reservoirs

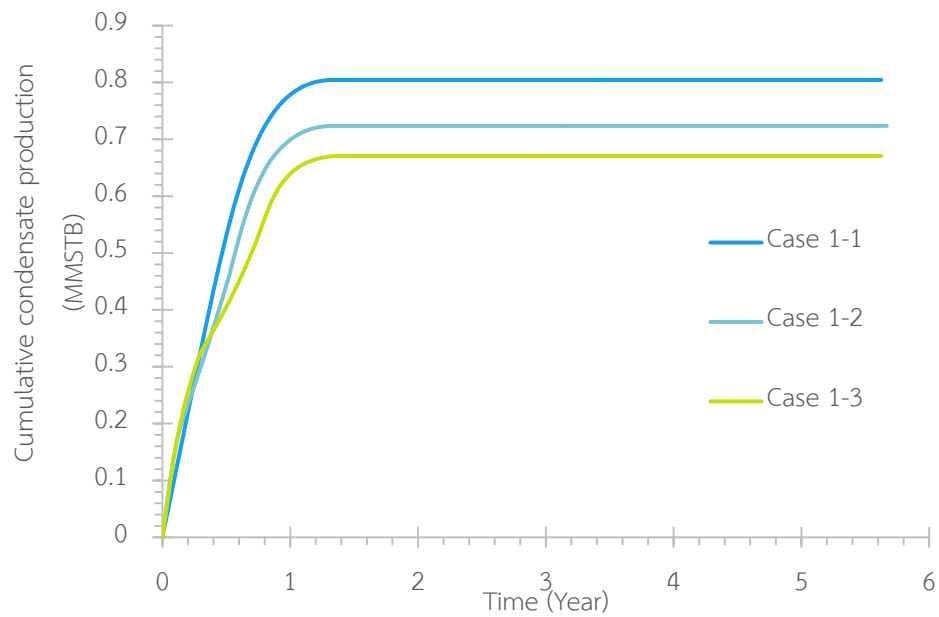


Figure 5.37: Cumulative oil production rates versus time for different starting times of dumpflood operation having simultaneous perforation all of source reservoirs with high CGR composition of original reservoir fluid and 25-ft thickness of the source gas reservoirs

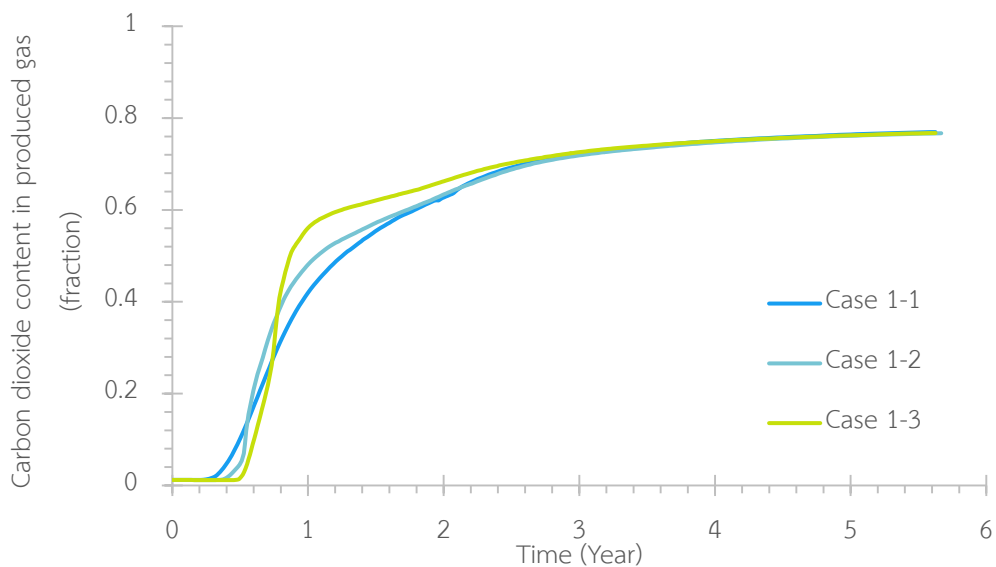


Figure 5.38: Carbon dioxide content in produced gas for different starting times of dumpflood operation having simultaneous perforation all of source reservoirs with high CGR composition of original reservoir fluid and 25-ft thickness of the source gas reservoirs

Among cases with different starting times of dumpflood operation including cases 1-1, 1-2, and 1-3, the highest total BOE recovery factor of 78.6% can be recovered in case 1-1 in which dumpflood operation is started since the beginning as shown in Table 5.7. Moreover, case 1-1 also provides the highest condensate recovery of 58.5% which is 5.8% and 9.7% more comparing to case 1-2 and 1-3 respectively.

Table 5.7: Summarized results of different starting times of dumpflood operation having simultaneous perforation all of source reservoirs with high CGR composition of original reservoir fluid and 25-ft thickness of the source gas reservoirs

Cases	1-1	1-2	1-3
Cumulative condensate production (MMSTB)	0.805	0.724	0.671
Original condensate in place (MMSTB)	1.374	1.374	1.374
Condensate recovery factor (%)	58.5%	52.7%	48.8%
Cumulative gas production (BCF)	26.204	26.368	26.442
Original gas in place (BCF)	9.149	9.149	9.149
Gas recovery factor (%)	92.6%	93.6%	94.1%
Cumulative HC gas production (BCF) *	12.743	12.827	12.877
HC gas recovery factor (%) **	100.5%	101.3%	101.8%
Cumulative gas production (MMBOE)	3.349	3.409	3.447
Cumulative total BOE production (MMBOE)	4.153	4.132	4.117
Original BOE in place (MMBOE)	4.496	4.496	4.496
Total BOE recovery factor (%)	78.6%	78.1%	77.8%

Note: * HC gas is produced gas deducted by nitrogen and carbon dioxide content

** Percentage of HC gas production gas production compared to original gas in place

Figure 5.39 shows condensate, HC gas and total BOE recoveries for all cases in this section. The descriptions of each case are specified in Table 5.5. Starting dumpflood operation at the beginning with four perforated source reservoirs in case 1-1 results in the highest both total BOE and condensate recovery of 78.6% and 58.5%, respectively. There is no significant difference for HC gas and total BOE recoveries among all cases. The main difference among cases is the condensate recovery.

For the higher amount of available source gas (perforating all four gas layers in cases 1-1 to 2-3), delaying gas dumpflood operation drastically decreases condensate recovery up to 9.7%. The reduction of condensate recovery by delaying gas dumpflood operation is decreased by less amount of cross-flowing gas in cases 3-1 to 4-3. In these cases, starting dumpflood when the reservoir pressure is more than 500 psi below the dewpoint pressure decreases condensate recovery up to 5.7%.

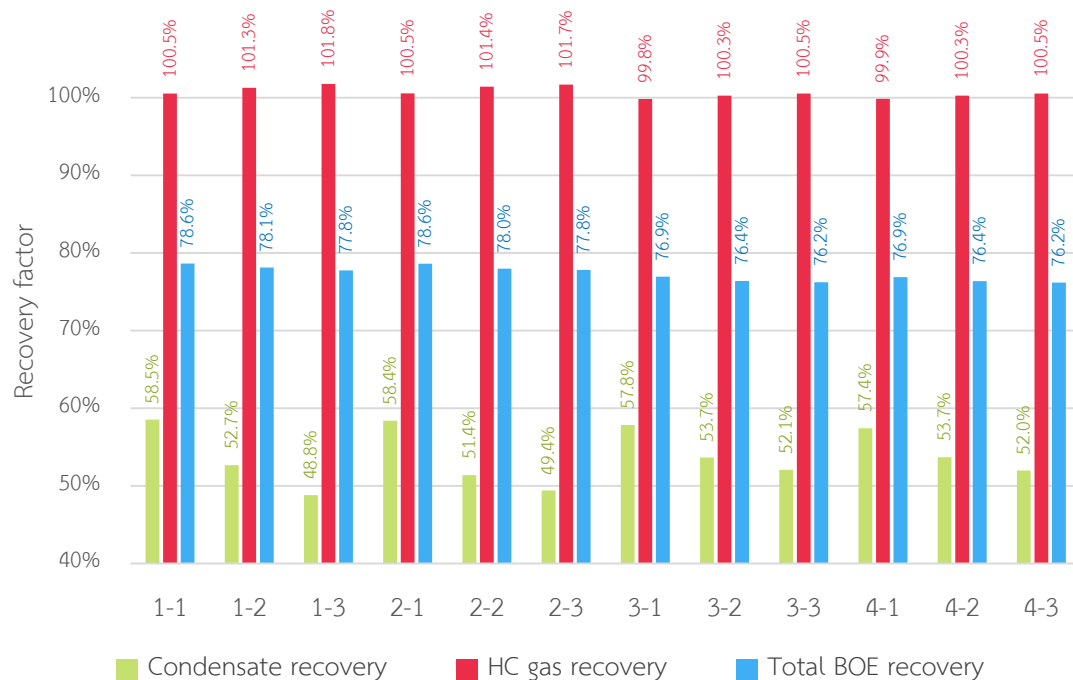


Figure 5.39: Condensate, HC gas, and total BOE recoveries for all cases with high CGR composition of original reservoir fluid and 25-ft thickness of the source gas reservoirs

5.3.1.2 50-ft Thickness of Source Gas Reservoirs

In the same manner as in Section 5.3.1.1, the results of cases 1-1, 2-1, 3-1, and 4-1 which have the same starting time of dumpflood and different perforation sequences are discussed first. Although the perforation sequences are different, the same perforated original gas of all four layers insignificantly leads to the difference of gas and condensate recoveries for cases 1-1 and 2-1 as depicted in Figure 5.40 and Figure 5.41. An additional 200.5 psi of average pressure of the perforated source gas reservoirs in case 4-1 comparing to case 3-1 does not result in significant difference of gas and condensate recoveries because they have the same original source gas in place.

As seen in Figure 5.40 and Figure 5.42, cumulative gas production and cumulative dumped gas have quite similar trends, implying that the cumulative gas production is mainly induced by the cumulative dumped gas. For the higher amount of dumped gas (cases 1-1 and 1-2), the production lives can be maintained longer, and more gas are produced comparing to cases 3-1 and 4-1. This is because the higher amount of dumped gas increases the ability to maintain the reservoir pressure and prolong the production period.

However, the difference in perforated source gas or perforation sequences does not cause a significant alteration of condensate recovery among these four cases. This is because all the cases have enough source gas to dry out all of the condensate within approximately one and a half years of the production. Also, during that period, the differences in dumped gas among four cases are still small. This leads to only tiny differences in condensate recovery of these cases.

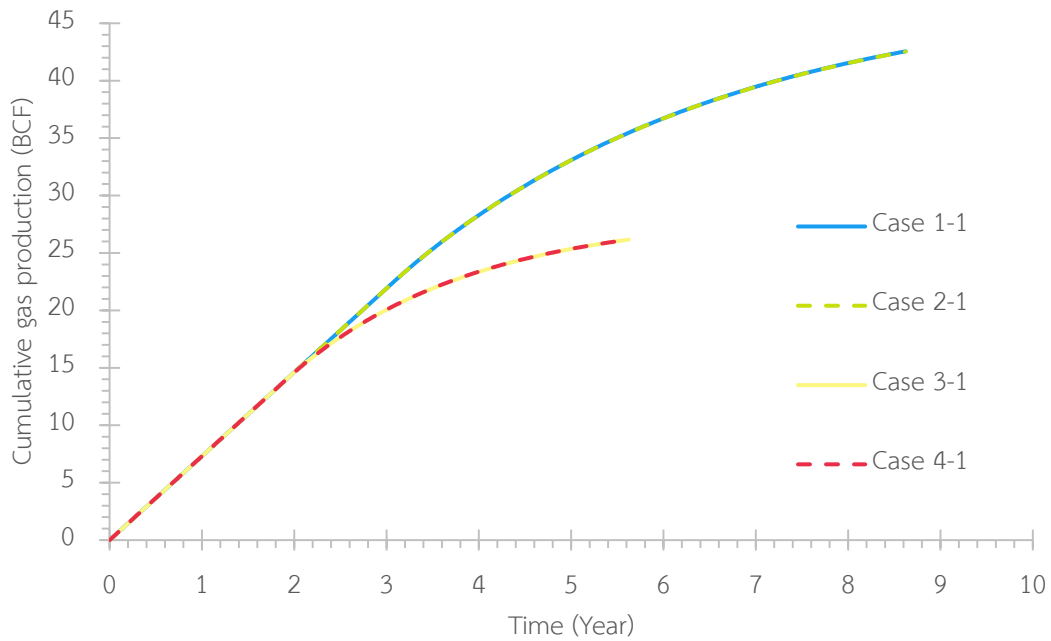


Figure 5.40: Cumulative gas production for different perforation sequences of gas dumpflood scenarios starting at the beginning with high CGR composition of original reservoir fluid and 50-ft thickness of the source gas reservoirs

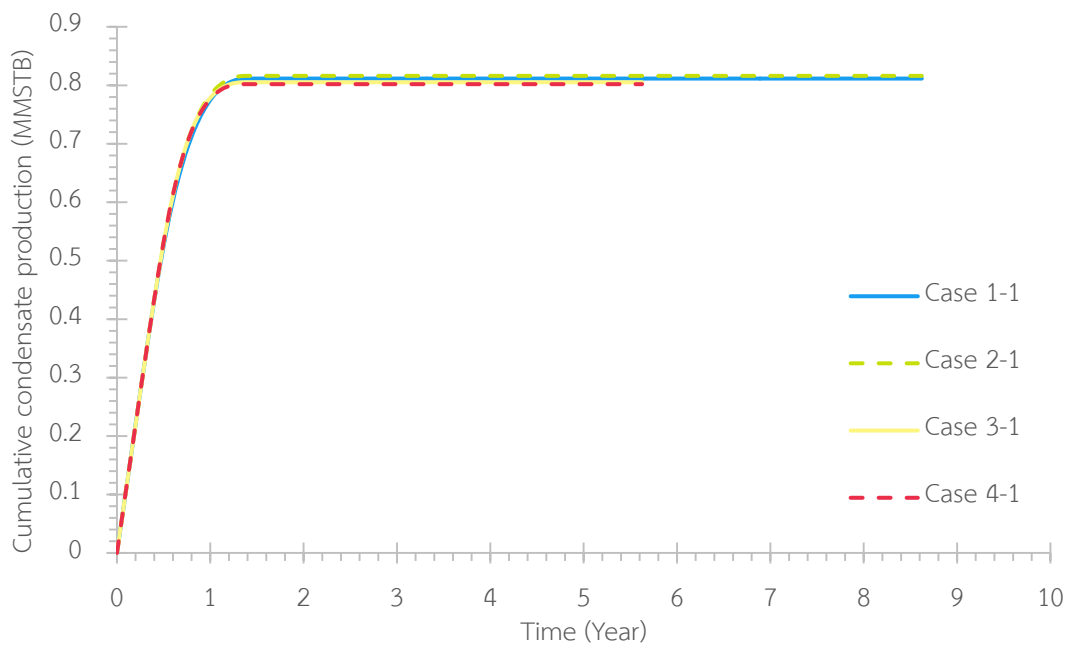


Figure 5.41: Cumulative condensate production for different perforation sequences of gas dumpflood scenarios starting at the beginning with high CGR composition of original reservoir fluid and 50-ft thickness of the source gas reservoirs

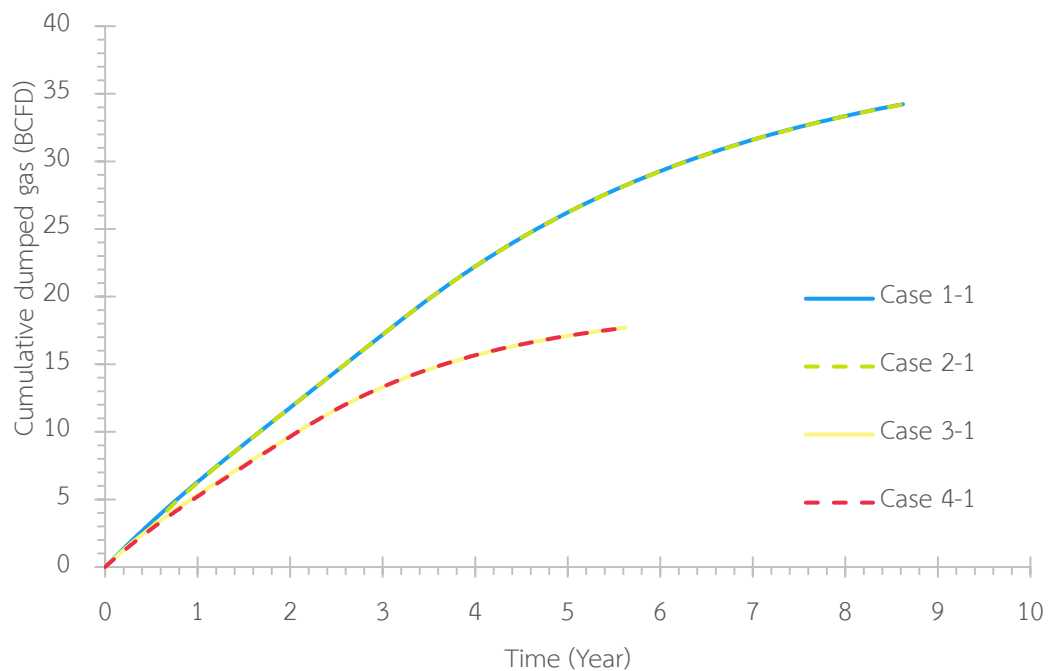


Figure 5.42: Cumulative dumped gas for different perforation sequences of gas dumpflood scenarios starting at the beginning with high CGR composition of original reservoir fluid and 50-ft thickness of the source gas reservoirs

From Table 5.8, the condensate recoveries of the four cases have small difference, varying within 1.0%. Although perforating all four reservoirs in cases 1-1 and 2-1 can induce much higher cumulative gas production than that of cases 3-1 and 4-1, after deduction of higher cumulative gas dumpflood, cases 1-1 and 2-1 have slightly lower gas recovery and approximately similar HC gas recovery comparing to cases 3-1 and 4-1. The higher amounts of cumulative total BOE production in cases 1-1 and 2-1 comparing to cases 3-1 and 4-1 are mainly caused by the higher amounts of cross-flowing gas. Although the perforation sequences are different, the same number of perforated source gas layers results in insignificant difference in condensate and gas production.

HC gas recovery factors are more than 100% recovery in all cases, indicating vaporized condensate by severe shrinking effect from excessive carbon dioxide content. The carbon dioxide in the gas phase induces light end in liquid phase to

vaporize into the gas phase. This results in more amount of HC gas meanwhile less amount of condensate.

Table 5.8: Summarized results of different perforation sequences of gas dumpflood scenarios starting at the beginning with high CGR composition of original reservoir fluid and 50-ft thickness of the source gas reservoirs

Cases	1-1	2-1	3-1	4-1
Cumulative condensate production (MMSTB)	0.812	0.816	0.805	0.802
Original condensate in place (MMSTB)	1.374	1.374	1.374	1.374
Condensate recovery factor (%)	59.1%	59.4%	58.6%	58.4%
Cumulative gas production (BCF)	42.557	42.541	26.169	26.167
Original gas in place (BCF)	9.149	9.149	9.149	9.149
Gas recovery factor (%)	91.1%	91.0%	92.5%	92.6%
Cumulative HC gas production (BCF) *	16.084	16.077	12.736	12.737
HC gas recovery factor (%) **	101.0%	100.9%	100.5%	100.5%
Cumulative gas production (MMBOE)	3.976	3.972	3.347	3.349
Cumulative total BOE production (MMBOE)	4.788	4.788	4.152	4.151
Original BOE in place (MMBOE)	4.496	4.496	4.496	4.496
Total BOE recovery factor (%)	80.0%	80.0%	78.6%	78.6%

Note: * HC gas is produced gas deducted by nitrogen and carbon dioxide content

** Percentage of HC gas production gas production compared to original gas in place

Delaying starting dumpflood operation yields less condensate recovery as demonstrated in Figure 5.43. For the cases with high CGR composition of original reservoir fluid and 50-ft thickness of the source gas reservoirs discussed in this section,

the highest condensate recovery of 59.4% and total BOE recovery of 80.0% can be recovered in case of bottom up perforation sequence starting dumpflood at the beginning (i.e. case 2-1). The severe reductions of condensate recovery of 8.2% and 10.4% occur when starting time of dumpflood operation is delayed in cases 2-2 and 2-3. The effects of starting time have the same trend for all perforation sequences.

Although cumulative gas production strongly depends on the cumulative dumped gas, HC gas recovery factor after deduction of dumped HC gas varies in small range of 100.5% to 102.5%. The large variations of condensate recovery among all cases slightly affect total BOE recovery by the fact that the majority of the production is gas, not condensate. Consequently, total BOE is reduced in small amount when the starting time of gas dumpflood is delayed.

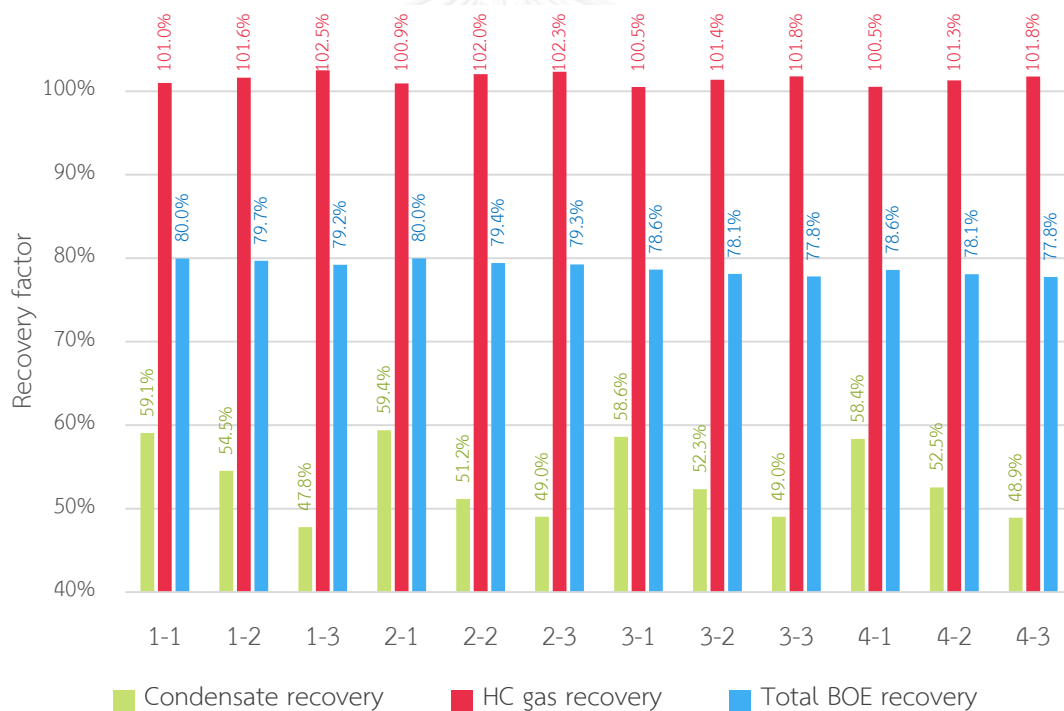


Figure 5.43: Condensate, HC gas, and total BOE recoveries for all cases with high CGR composition of original reservoir fluid and 50-ft thickness of the source gas reservoirs

5.3.1.3 Comparison between 25-ft and 50-ft Thickness of Source Gas Reservoirs

The cases with simultaneous perforations of all four layers and two lower gas source reservoirs at the beginning (i.e. 1-1 and 3-1) of 25-ft and 50-ft thickness of the source reservoirs are discussed in this section. The descriptions of all cases with the simplified case names in this section are depicted in Table 5.9. Consequently, cases 25-1, 25-2, 50-1, and 50-2 have 20.8, 10.4, 41.6, and 20.8 BCF of original gas in place of source gas reservoirs connected to the dumping well, respectively. It is worth to note that the number in cases 25-1 and 50-2 is the same.

Table 5.9: Descriptions of all cases in Section 5.3.1.3

Cases	Starting time of dumpflood	Perforation sequence of dumping well	Original source gas in place (BCF)	Thickness of source reservoirs
25-1	Beginning	Simultaneously perforate four source gas reservoirs	20.8	25 ft
25-2	Beginning	Perforate only two lower source gas reservoirs	10.4	
50-1	Beginning	Simultaneously perforate four source gas reservoirs	41.6	50 ft
50-2	Beginning	Perforate only two lower source gas reservoirs	20.8	

Figure 5.44 shows that cumulative cross-flowing gas strongly depends on the available source gas in place. With the same source gas in place in cases 25-1 and 50-2, these two cases have insignificant difference in cumulative cross-flowing gas. While case 25-2 have lower cumulative cross-flowing gas because of less amount of the original source gas in place, and the opposite manner appears in case 50-1.

As the dumped gas can maintain the reservoir pressure, cumulative gas production is strongly influenced by the dumped gas. The original source gas in place connected to the dumping well in cases 25-1 and 50-2 is the same, the cumulative cross-flowing gas and gas production profiles of both cases have insignificant difference as shown in Figure 5.44 and Figure 5.45. Due to more perforated source gas in place, cases 50-1 can recover more gas by a higher amount of cross-flowing gas. This behavior also appears in case 25-2 in which less source gas in place is perforated, resulting in less recovered gas.

For condensate recovery, only small differences appear in the result among these cases as depicted in Figure 5.46. From Table 5.10, condensate recovery slightly varies in the range of 57.8% – 59.1%. These slight variations of condensate recovery proportionally depends on perforated original gas source in place. Although the HC gas production widely scatters around 10.97 – 16.084 BCF, the HC gas recoveries are not much different because higher gas production needs to be subtracted by higher dumped gas. This results in slightly different recovery among all cases.

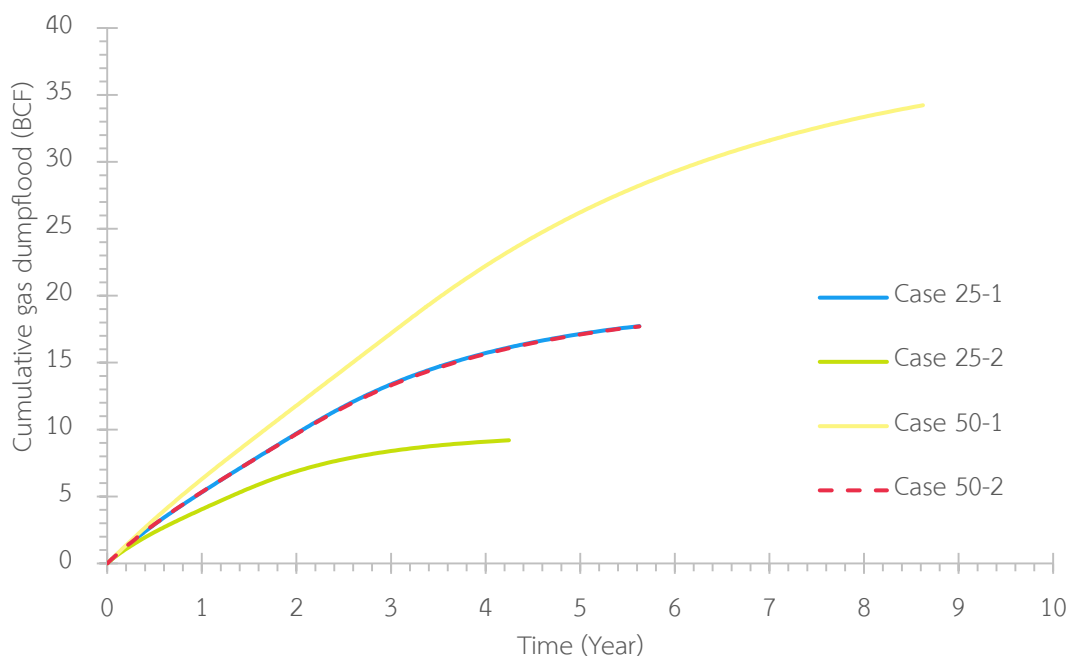


Figure 5.44: Cumulative gas production versus time for different thickness of gas source reservoirs and numbers of perforated source reservoirs with high CGR composition of original reservoir fluid

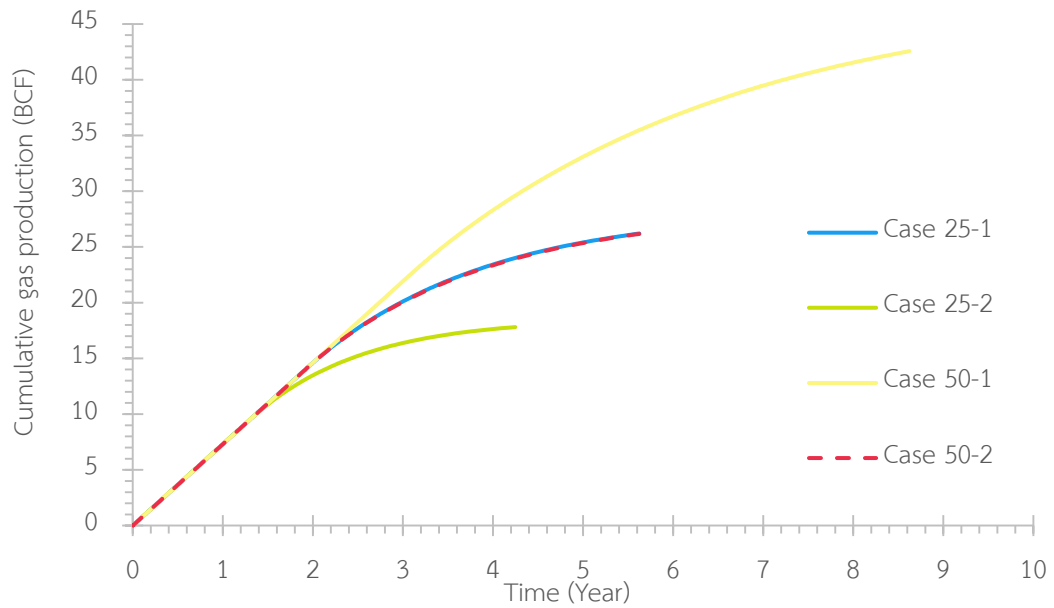


Figure 5.45: Cumulative gas production versus time for different thickness of gas source reservoirs and numbers of perforated source reservoirs with high CGR composition of original reservoir fluid

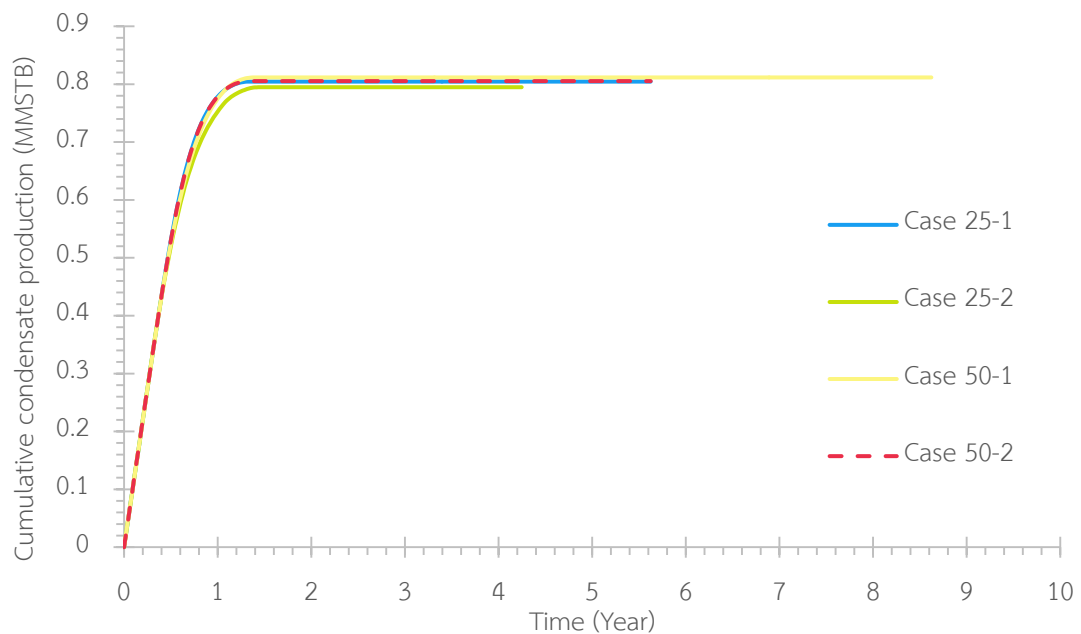


Figure 5.46: Cumulative condensate production versus time for different thickness of gas source reservoirs and numbers of perforated source reservoirs with high CGR composition of original reservoir fluid

Table 5.10: Summarized results of different thickness of gas source reservoirs and numbers of perforated source reservoirs with high CGR composition of original reservoir fluid

Cases	25-1	25-2	50-1	50-2
Cumulative condensate production (MMSTB)	0.805	0.795	0.812	0.805
Original condensate in place (MMSTB)	1.374	1.374	1.374	1.374
Condensate recovery factor (%)	58.5%	57.8%	59.1%	58.6%
Cumulative gas production (BCF)	26.204	17.811	42.557	26.169
Original gas in place (BCF)	9.149	9.149	9.149	9.149
Gas recovery factor (%)	92.6%	94.2%	91.1%	92.5%
Cumulative HC gas production (BCF) *	12.743	10.972	16.084	12.736
HC gas recovery factor (%) **	100.5%	99.8%	101.0%	100.5%
Cumulative gas production (MMBOE)	3.349	2.986	3.976	3.347
Cumulative total BOE production (MMBOE)	4.153	3.780	4.788	4.152
Original BOE in place (MMBOE)	4.496	4.496	4.496	4.496
Total BOE recovery factor (%)	78.6%	76.9%	80.0%	78.6%

Note: * HC gas is produced gas deducted by nitrogen and carbon dioxide content

** Percentage of HC gas production gas production compared to original gas in place

5.3.2 Composition Yielding Low CGR of Original Reservoir Fluid

5.3.2.1 25-ft Thickness of Source Gas Reservoirs

Cases with the same time of starting dumpflood at the beginning and different perforation sequences including cases 1-1, 2-1, 3-1, and 4-1 are first discussed in this section in order to emphasize the effect of perforation sequence. Carbon dioxide breakthrough causes the decline of condensate production rate for all cases as demonstrated in Figure 5.47. This leads to slightly higher condensate production rates after the breakthrough in cases 3-1 and 4-1 comparing to cases 1-1 and 2-1. This is because cases 3-1 and 4-1 perforate only two source gas reservoirs which is a half of that in cases 1-1 and 2-1, resulting in a smaller amount of dumped gas as depicted in Figure 5.48. As there is less amount of carbon dioxide mixing with the original reservoir fluid in cases 3-1 and 4-1, the phase envelope of the mixed fluid is larger than the one for cases 1-1 and 2-1, meaning that there is a higher amount of condensate or richer hydrocarbon fluid composition. Due to less drying effect, cases 3-1 and 4-1 can recover more condensate comparing to the others by yielding slightly higher condensate production rates during the decline period as demonstrated in Figure 5.49.

The higher ability to maintain the reservoir pressure by a larger amount of cross-flowing gas in cases 1-1 and 2-1 can prolong gas production at the plateau rate better than the other two cases as depicted in Figure 5.50. This ability also extends the production lives with higher gas production, inducing a significantly larger amount of cumulative gas production.

Since there is the same number of perforated source gas reservoirs between cases 1-1 and 2-1, there is no significant difference in the production profiles between those two cases though their perforation sequences are dissimilar. In the same respect for the cases with two perforated source reservoirs (cases 3-1 and 4-1), although there is the difference in average pressure of gas source reservoirs for 200.5 psi between these two cases, their gas and condensate production profiles are similar.

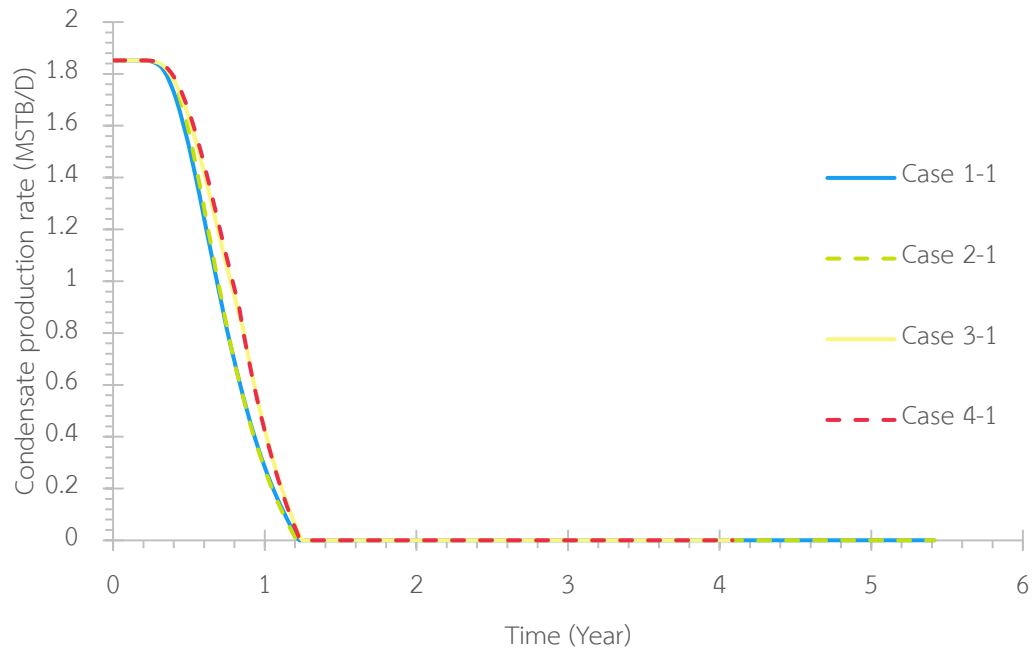


Figure 5.47: Condensate production profiles for different perforation sequences of gas dumpflood scenarios starting at the beginning with low CGR composition of original reservoir fluid and 25-ft thickness of the source gas reservoirs

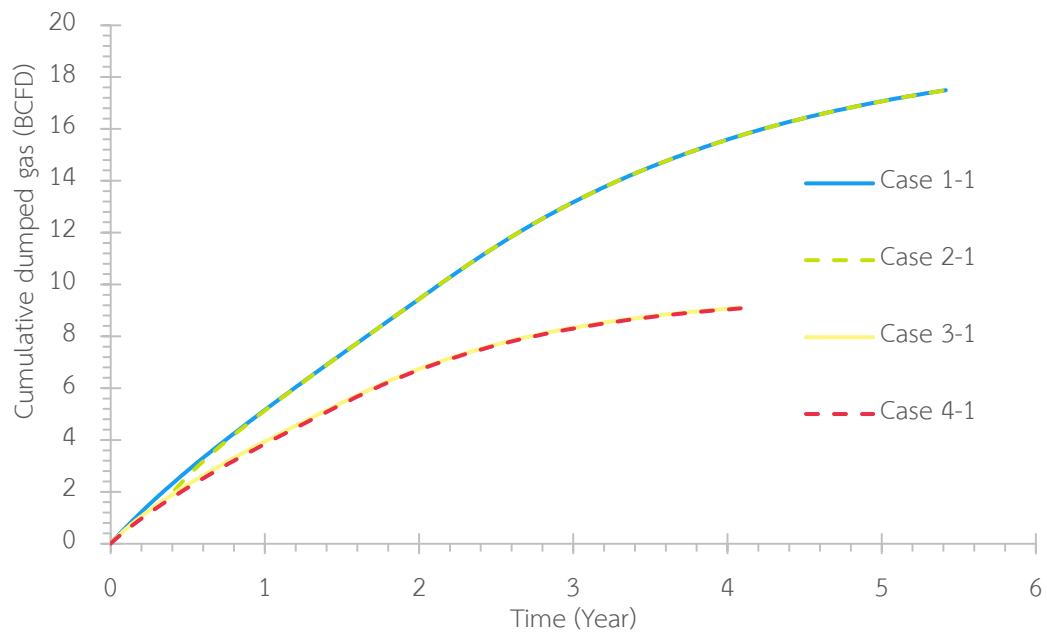


Figure 5.48: Cumulative dumped gas for different perforation sequences of gas dumpflood scenarios starting at the beginning with low CGR composition of original reservoir fluid and 25-ft thickness of the source gas reservoirs

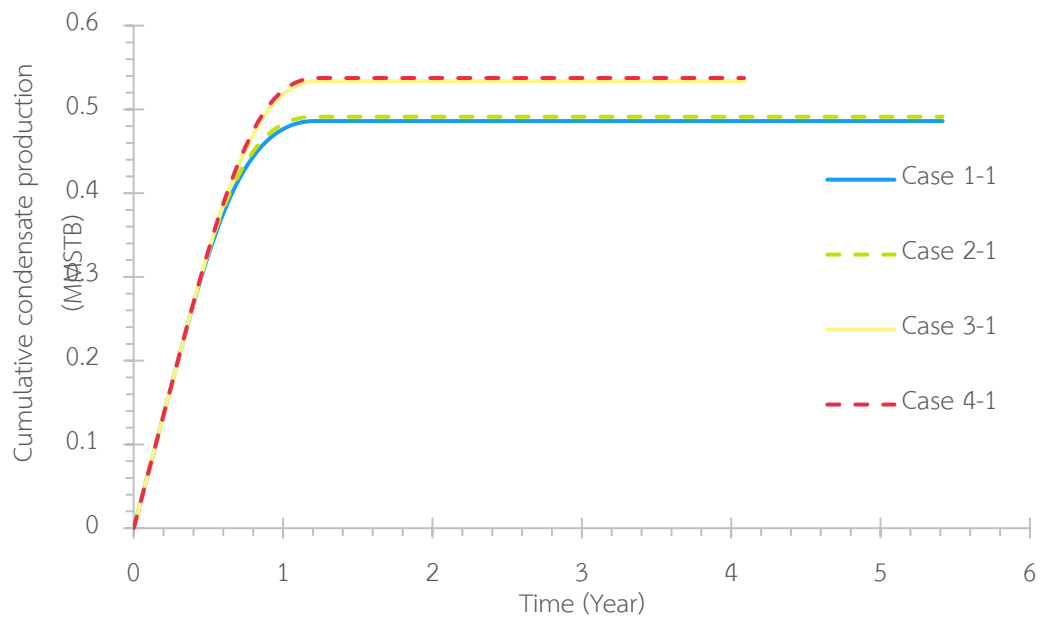


Figure 5.49: Cumulative condensate production for different perforation sequences of gas dumpflood scenarios starting at the beginning with low CGR composition of original reservoir fluid and 25-ft thickness of the source gas reservoirs

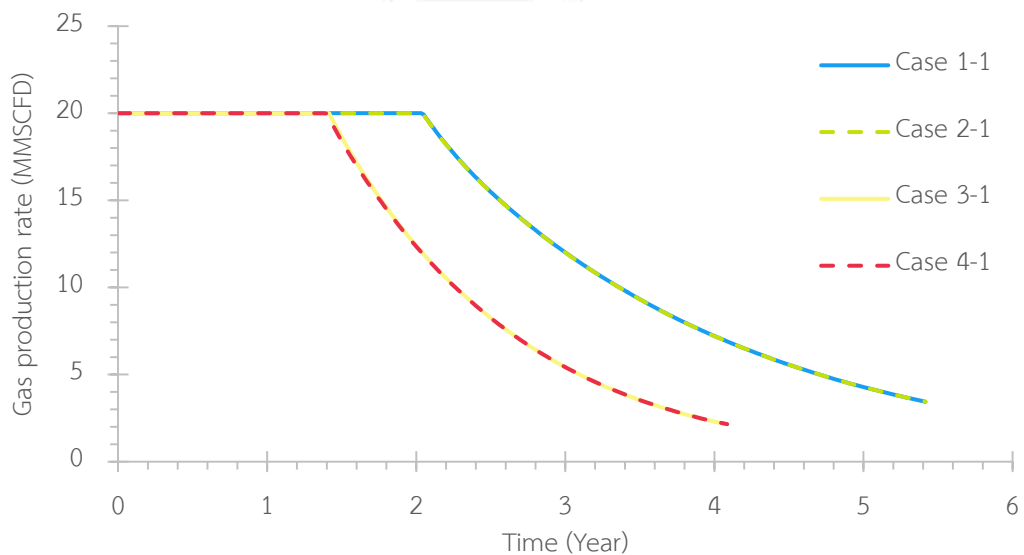


Figure 5.50: Gas production profiles for different perforation sequences of gas dumpflood scenarios starting at the beginning with low CGR composition of original reservoir fluid and 25-ft thickness of the source gas reservoirs

From Table 5.11, cumulative HC gas production mainly depends on the amount of dumped gas. Nevertheless, after subtraction of amount of cross-flowing gas, all cases

result in quite similar HC gas recovery in the range of 99.1% to 99.8%. With the same reason, gas and total BOE recovery factors vary in a small range of 91.6% to 93.3% and 85.3% to 85.7%, respectively. The limited amount of carbon dioxide cross-flowing to the target reservoir in cases 3-1 and 4-1 significantly improve condensate recovery by 4.7% to 5.7% comparing to cases 1-1 and 2-1 with less production time for almost a year.

Table 5.11: Summarized results of different perforation sequences of gas dumpflood scenarios starting at the beginning with low CGR composition of original reservoir fluid and 25-ft thickness of the source gas reservoirs

Cases	1-1	2-1	3-1	4-1
Cumulative condensate production (MMSTB)	0.486	0.491	0.534	0.538
Original condensate in place (MMSTB)	0.896	0.896	0.896	0.896
Condensate recovery factor (%)	54.3%	54.9%	59.6%	60.0%
Cumulative gas production (BCF)	26.365	26.357	18.133	18.098
Original gas in place (BCF)	9.673	9.673	9.673	9.673
Gas recovery factor (%)	91.7%	91.6%	93.3%	93.3%
Cumulative HC gas production (BCF) *	13.151	13.146	11.412	11.402
HC gas recovery factor (%) **	99.8%	99.7%	99.1%	99.1%
Cumulative gas production (MMBOE)	3.710	3.706	3.353	3.349
Cumulative total BOE production (MMBOE)	4.197	4.197	3.887	3.887
Original BOE in place (MMBOE)	4.186	4.186	4.186	4.186
Total BOE recovery factor (%)	85.7%	85.7%	85.3%	85.3%

Note: * HC gas is produced gas deducted by nitrogen and carbon dioxide content

** Percentage of HC gas production gas production compared to original gas in place

In order to investigate the effect of starting time of dumpflood operation, two set of the cases with the same perforation sequence are separately discussed. This includes simultaneously perforation of all four source reservoirs and perforating only the two upper reservoirs. Two sets of different perforation sequences were investigated to emphasize the different effect of starting time between high and low amounts of dumped gas cases.

The first set consists of cases 1-1, 1-2, and 1-3 where all four gas source reservoirs are simultaneously perforated at different triggering conditions to represent high gas cross-flowing cases. The second set includes cases 4-1, 4-1, and 4-3 where only the two upper reservoirs are simultaneously perforated at different triggering conditions to represent low gas cross-flowing cases.

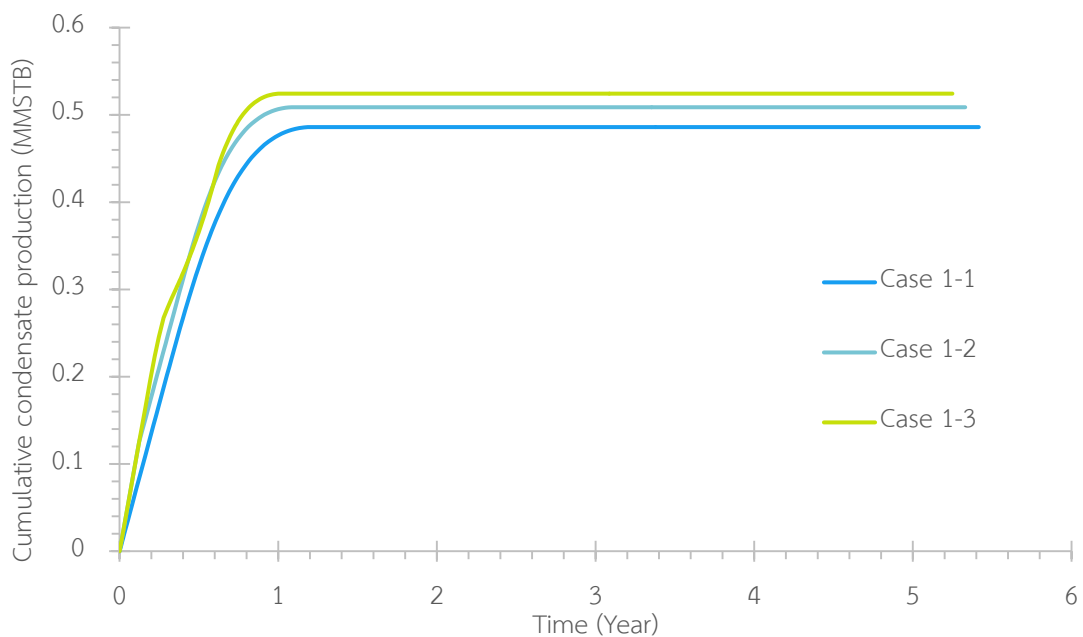


Figure 5.51: Cumulative condensate production for different starting times of dumpflood operation for simultaneous perforation of all source reservoirs with low CGR composition of original reservoir fluid and 25-ft thickness of the source gas reservoirs

Figure 5.51 illustrates the results of cumulative condensate production of cases 1-1 to 1-3. The highest condensate recovery of 58.6% appears in case 1-3 where the latest starting time of dumpflood operation is performed. The trend is straight forward.

The later the dumpflood operation, the higher the condensate recovery as there is a larger amount of condensate recovered prior to gas dumpflood.

On the other hand, there is opposite behavior on the gas recovery, varying in the small range of 91.2% to 91.7% as shown in Table 5.12. Therefore, total BOE recoveries, resulting from both gas and condensate, are almost the same for all cases. This is because the gas and condensate recovery have opposite behavior among cases.

Table 5.12: Summarized results of different starting times of dumpflood operation for simultaneous perforation of all four source reservoirs with low CGR composition of original reservoir fluid and 25-ft thickness of the source gas reservoirs

Cases	1-1	1-2	1-3
Cumulative condensate production (MMSTB)	0.486	0.509	0.524
Original condensate in place (MMSTB)	0.896	0.896	0.896
Condensate recovery factor (%)	54.3%	56.8%	58.6%
Cumulative gas production (BCF)	26.365	26.315	26.297
Original gas in place (BCF)	9.673	9.673	9.673
Gas recovery factor (%)	91.7%	91.4%	91.2%
Cumulative HC gas production (BCF) *	13.151	13.123	13.110
HC gas recovery factor (%) **	99.8%	99.5%	99.4%
Cumulative gas production (MMBOE)	3.710	3.691	3.679
Cumulative total BOE production (MMBOE)	4.197	4.200	4.204
Original BOE in place (MMBOE)	4.186	4.186	4.186
Total BOE recovery factor (%)	85.7%	85.8%	85.9%

Note: * HC gas is produced gas deducted by nitrogen and carbon dioxide content

** Percentage of HC gas production gas production compared to original gas in place

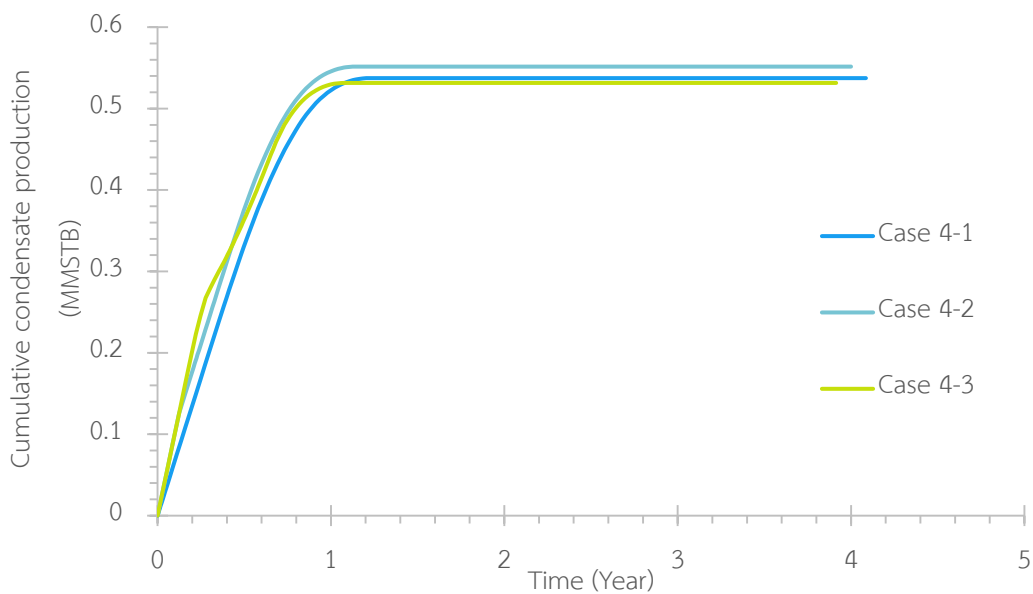


Figure 5.52: Cumulative condensate production for different starting times of dumpflood operation for simultaneous perforation of the two upper source reservoirs with low CGR composition of original reservoir fluid and 25-ft thickness of the source gas reservoirs

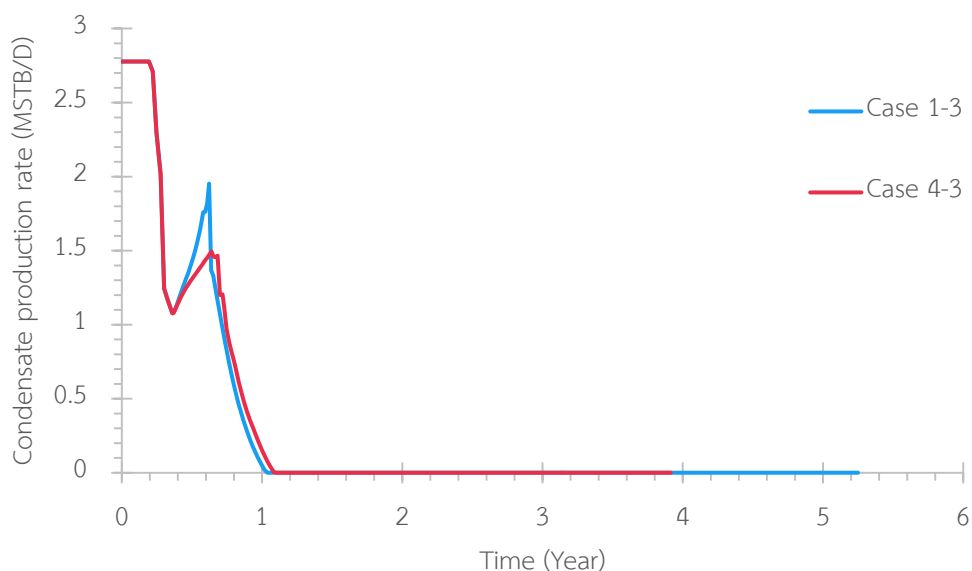


Figure 5.53: Condensate production profiles for cases 1-3 and 4-3 with low CGR composition of original reservoir fluid and 25-ft thickness of the source gas reservoirs

Table 5.13: Summarized results of different starting time of dumpflood operation for simultaneous perforation of the two upper source reservoirs with low CGR composition of original reservoir fluid and 25-ft thickness of the source gas reservoirs

Cases	4-1	4-2	4-3
Cumulative condensate production (MMSTB)	0.538	0.552	0.532
Original condensate in place (MMSTB)	0.896	0.896	0.896
Condensate recovery factor (%)	60.0%	61.6%	59.3%
Cumulative gas production (BCF)	18.098	18.069	18.076
Original gas in place (BCF)	9.673	9.673	9.673
Gas recovery factor (%)	93.3%	93.1%	93.2%
Cumulative HC gas production (BCF) *	11.402	11.386	11.401
HC gas recovery factor (%) **	99.1%	99.0%	99.1%
Cumulative gas production (MMBOE)	3.349	3.338	3.351
Cumulative total BOE production (MMBOE)	3.887	3.889	3.883
Original BOE in place (MMBOE)	4.186	4.186	4.186
Total BOE recovery factor (%)	85.3%	85.4%	85.2%

Note: * HC gas is produced gas deducted by nitrogen and carbon dioxide content

** Percentage of HC gas production gas production compared to original gas in place

For the second set, as seen in Figure 5.52, there are some differences in condensate recovery among cases 4-1 to 4-3 where only the two upper source reservoirs are perforated at different times. From Table 5.13, the highest condensate recovery factor of 61.6% is obtained in case 4-2 where gas dumpflood is performed when the reservoir pressure reaches the dewpoint pressure. Case 4-3 can recover the least condensate. This result is in contrast with the result when four layers are perforated because gas dumpflood in case 4-3 is started after condensate banking

already occurs near the producers. Since only two source gas reservoirs are perforated in case 4-3, there are less source gas available for case 4-3 comparing to case 1-3 to raise the reservoir pressure and increase condensate production rate as illustrated in Figure 5.53. This results in decrement of condensate production in case 4-3 comparing to case 4-2.

The condensate, HC gas, and total BOE recovery for all cases in this section are demonstrated in Figure 5.54. For higher amounts of dumped gas including cases 1-1 to 2-3 where all four source gas reservoirs are perforated, the later time of starting dumpflood operation, the higher condensate production. This behavior is dissimilar when less amount of carbon dioxide is cross-flowing in cases 3-1 to 4-3 where only two source gas reservoirs are perforated. Cases in which dumpflood is started when the target reservoir pressure falls below the dewpoint (cases 3-2 and 4-2) provide the optimum condensate recovery of 61.5% and 61.6%, respectively, which are the highest value among all cases in this section.

In the aspect of HC gas recovery, the results vary with in a small range of 99.0% to 99.8%. Cases 1-1 to 2-3 which have all four source reservoirs perforated result in significantly higher HC gas production than those of cases 3-1 to 4-3 in which only two source reservoirs are perforated due to higher amount of cross flowing gas. However, after deduction of cross-flowing gas, the HC gas recoveries are quite similar among all cases as shown in Figure 5.54. As the majority of production is gas, total BOE recoveries are quite similar among all cases.

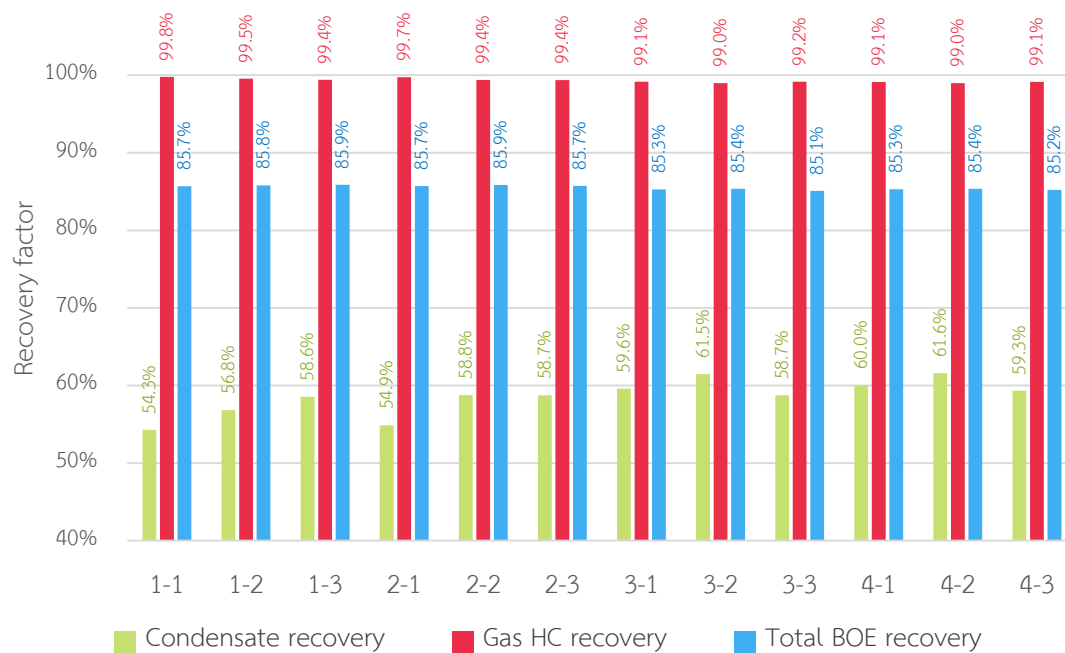
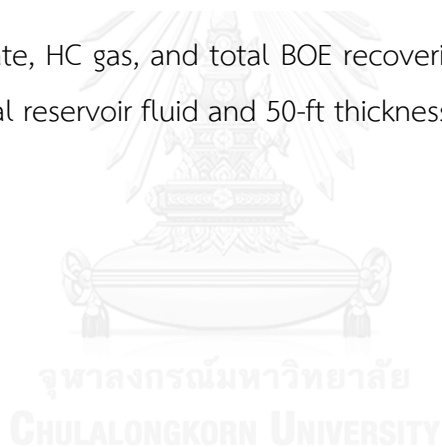


Figure 5.54: Condensate, HC gas, and total BOE recoveries for all cases with low CGR composition of original reservoir fluid and 50-ft thickness of the source gas reservoirs



5.3.2.2 50-ft Thickness of Source Gas Reservoirs

The cumulative gas production versus time of cases 1-1, 2-1, 3-1, and 4-1 are plotted in Figure 5.55 in order to investigate the effect of perforation sequence. The higher cumulative gas production at late time in cases 1-1 and 2-1 are caused by higher amounts of cross-flowing gas which is the main factor for pressure support. This results in longer production time and larger cumulative gas production at abandonment for cases 1-1 and 2-1.

As seen in Figure 5.56, the condensate production can be increased by limiting cross-flowing carbon dioxide. For cases 1-1 and 2-1 comparing to cases 3-1 and 4-1, as the number of perforated gas source layers increases, the condensate production decreases. The phenomenon is caused by larger carbon dioxide contents in the target reservoir when all four source gas reservoirs are perforated, resulting in leaner hydrocarbon content in the produced fluid compositions. There is no significant difference between cases with the same number of perforated gas source reservoirs for both gas and condensate production. This is because these cases provide the same amount of original source gas in place and insignificant different dumped gas rates.

From Table 5.14, a small difference of 1.0% in condensate recovery between cases 1-1 and 2-1 is caused by delaying the other half portion of cross-flowing gas sources, resulting in a slightly lower amount of in dumped gas. In the same manner, the small difference of 0.8% in condensate recovery between cases 3-1 and 4-1 is caused by the pressure difference between these two cases, which results in a slight different amount of dumped gas as well.

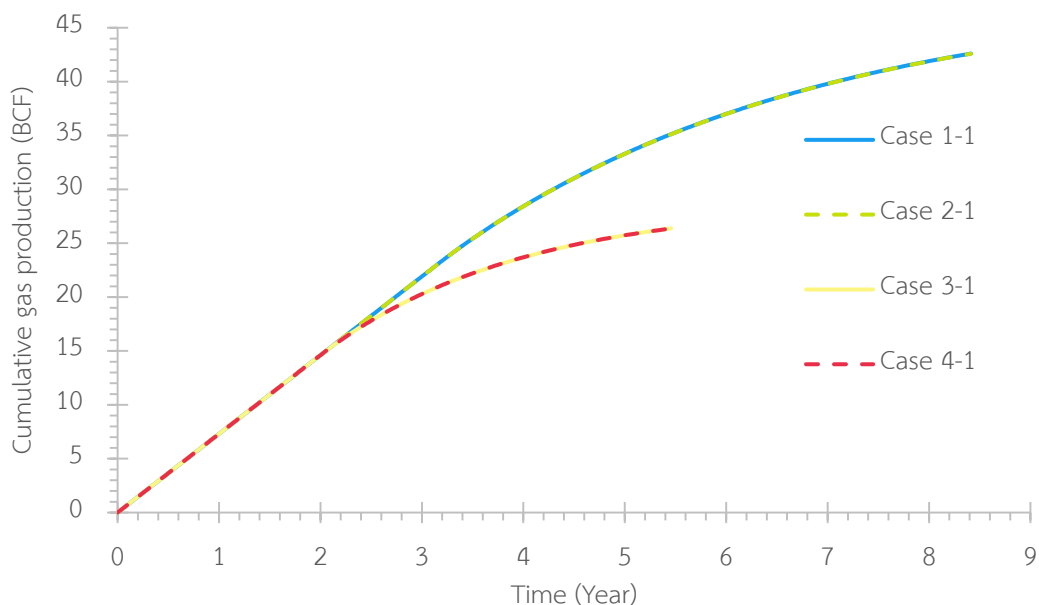


Figure 5.55: Cumulative gas production for different perforation sequences of gas dumpflood scenarios starting at the beginning with low CGR composition of original reservoir fluid and 25-ft thickness of the source gas reservoirs

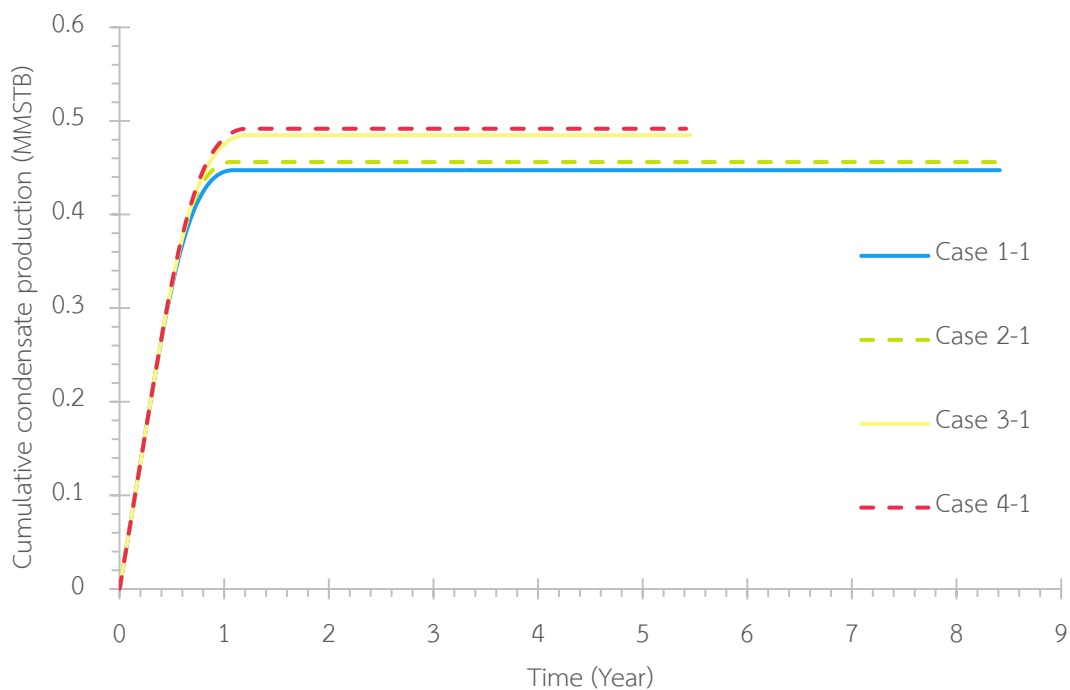


Figure 5.56: Cumulative condensate production for different perforation sequences of gas dumpflood scenarios starting at the beginning with low CGR composition of original reservoir fluid and 25-ft thickness of the source gas reservoirs

Table 5.14: Summarized results of different perforation sequences of gas dumpflood scenarios starting at the beginning with low CGR composition of original reservoir fluid and 50-ft thickness of the source gas reservoirs

Cases	1-1	2-1	3-1	4-1
Cumulative condensate production (MMSTB)	0.447	0.456	0.485	0.492
Original condensate in place (MMSTB)	0.896	0.896	0.896	0.896
Condensate recovery factor (%)	49.9%	50.9%	54.1%	54.9%
Cumulative gas production (BCF)	42.609	42.590	26.375	26.320
Original gas in place (BCF)	9.673	9.673	9.673	9.673
Gas recovery factor (%)	90.4%	90.3%	91.7%	91.6%
Cumulative HC gas production (BCF) *	16.475	16.465	13.155	13.138
HC gas recovery factor (%) **	100.3%	100.2%	99.8%	99.7%
Cumulative gas production (MMBOE)	4.337	4.329	3.712	3.705
Cumulative total BOE production (MMBOE)	4.784	4.785	4.197	4.196
Original BOE in place (MMBOE)	4.186	4.186	4.186	4.186
Total BOE recovery factor (%)	86.1%	86.1%	85.7%	85.7%

Note: * HC gas is produced gas deducted by nitrogen and carbon dioxide content

** Percentage of HC gas production gas production compared to original gas in place

Figure 5.7 demonstrates condensate, HC gas, and total BOE recovery for all cases in this section. All perforation sequence cases have the same effect of starting

time of dumpflood operation that the later time to start dumpflood, the higher condensate recovery and slightly lower HC gas recovery. This is because higher condensate is recovered prior to gas dumpflood for cases of late starting time. However, the main parameter that significantly impacts total BOE recovery is HC gas recovery since it is much larger amount in term of BOE when compared to condensate recovery. Both total BOE and HC gas recoveries vary in a small range for all cases.



Figure 5.57: Condensate, HC gas, and total BOE recoveries for all cases with low CGR composition of original reservoir fluid and 50-ft thickness of the source gas reservoirs

5.3.2.3 Comparison between 25-ft and 50-ft Thickness of Source Gas Reservoirs

In order to investigate the effect of size of the source gas reservoirs, cases with bottom-up perforation and simultaneous perforation of the two upper gas source reservoirs when the average reservoir pressure declines less than the dewpoint pressure are investigated. The details of all cases in this section as well as simplified case names are identified in Table 5.15. Therefore, cases 25-1, 25-2, 50-1, and 50-2 have 20.8, 10.4, 41.6, and 20.8 BCF of original gas source in place connected to the dumping well, respectively. Note that the values of original source gas in place in cases 25-1 and 50-2 are the same.

Table 5.15: Descriptions of all cases in Section 5.3.2.3

Cases	Starting time of dumpflood	Perforation sequence of dumping well	Original source gas in place (BCF)	Thickness of source reservoirs
25-1	$P_R < P_d$	Bottom-up	20.8	25 ft
25-2	$P_R < P_d$	Perforate only two upper source gas reservoirs	10.4	
50-1	$P_R < P_d$	Bottom-up	41.6	50 ft
50-2	$P_R < P_d$	Perforate only two upper source gas reservoirs	20.8	

As depicted in Figure 5.58, cases with higher original gas source in place result in higher cumulative dumped gas. Although there are differences in reservoir thickness and perforation sequences between cases 25-1 and 50-2, the same amount of connected original gas in place of the source reservoirs of these two cases results in insignificant difference in cumulative dumped gas as shown in Figure 5.58. The amount of recovered gas strongly depends on the connected amount of original gas source in place. According to Figure 5.58 and Figure 5.59, the more cumulative dumped gas, the

higher gas production. There is no significant difference of cumulative gas production between cases 25-1 and 50-2 as they both have the same cumulative dumped gas.

On the other hand, for low CGR composition of the target reservoir fluid, condensate recovery is higher when carbon dioxide content is limited as shown in Figure 5.60. Consequently, case 25-2 which has the smallest amount of cumulative cross-flowing gas yields the highest condensate recovery of 61.6% among all cases discussed in this section as tabulated in Table 5.16. The double amount of source gas cross-flowing to the target reservoirs in cases 25-1 and 50-2 induces a reduction in condensate recovery up to 4.4%. Cases with less connected original source gas in place have shorter production times due to less pressure support.

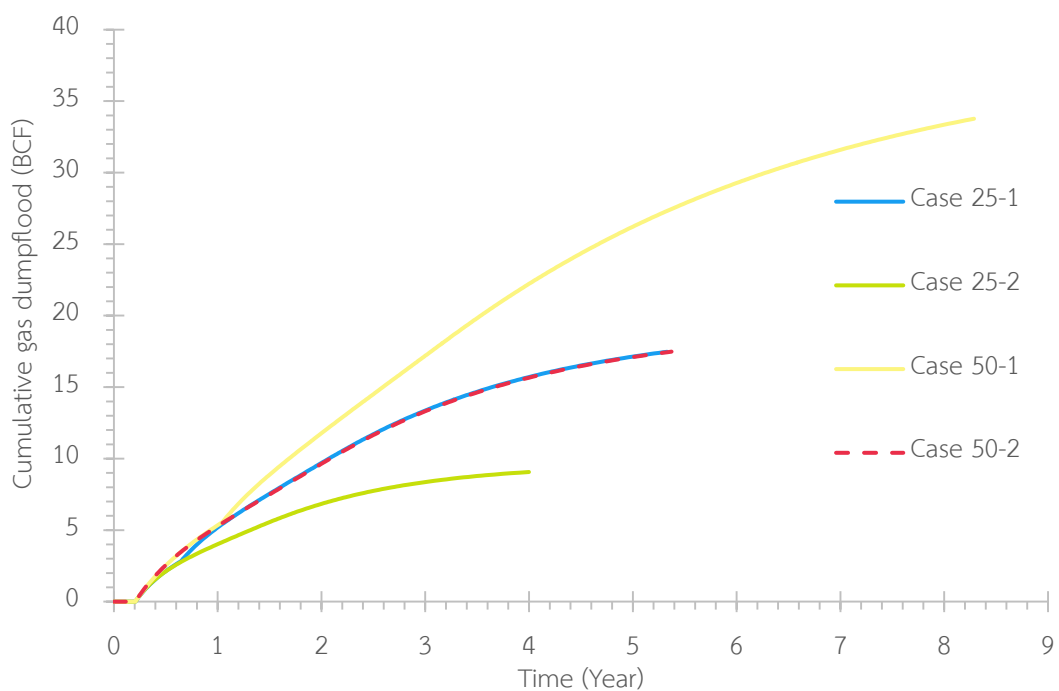


Figure 5.58: Cumulative gas production versus time for different thickness of gas source reservoirs and numbers of perforated source reservoirs with low CGR composition of original reservoir fluid

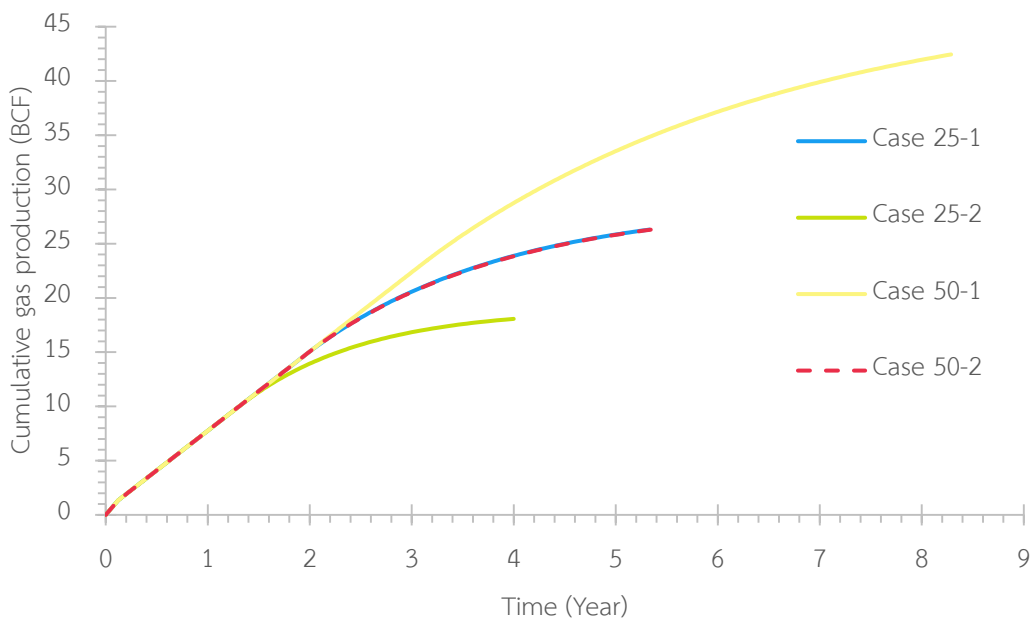


Figure 5.59: Cumulative gas production versus time for different thickness of gas source reservoirs and numbers of perforated source reservoirs with low CGR composition of original reservoir fluid

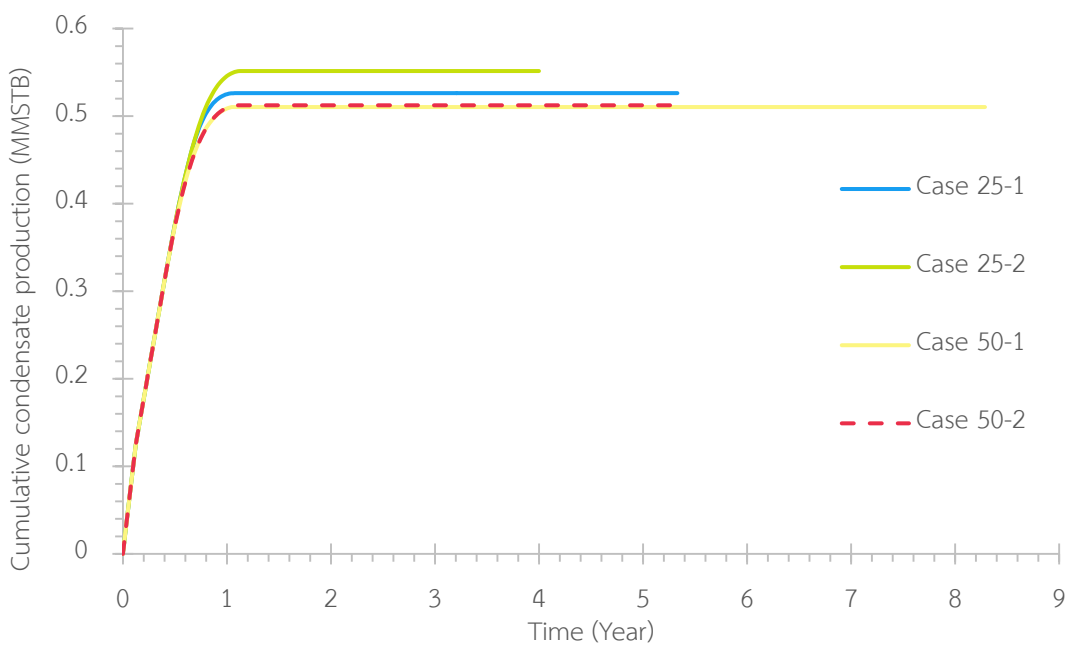


Figure 5.60: Cumulative condensate production versus time for different thickness of gas source reservoirs and numbers of perforated source reservoirs with low CGR composition of original reservoir fluid

Table 5.16: Summarized results of different thickness of gas source reservoirs and numbers of perforated source reservoirs with low CGR composition of original reservoir fluid

Cases	25-1	25-2	50-1	50-2
Cumulative condensate production (MMSTB)	0.526	0.552	0.510	0.512
Original condensate in place (MMSTB)	0.896	0.896	0.896	0.896
Condensate recovery factor (%)	58.8%	61.6%	57.0%	57.2%
Cumulative gas production (BCF)	26.297	18.069	42.443	26.326
Original gas in place (BCF)	9.673	9.673	9.673	9.673
Gas recovery factor (%)	91.2%	93.1%	89.7%	91.5%
Cumulative HC gas production (BCF) *	13.107	11.386	16.393	13.125
HC gas recovery factor (%) **	99.4%	99.0%	99.7%	99.5%
Cumulative gas production (MMBOE)	3.677	3.338	4.280	3.689
Cumulative total BOE production (MMBOE)	4.203	3.889	4.791	4.202
Original BOE in place (MMBOE)	4.186	4.186	4.186	4.186
Total BOE recovery factor (%)	85.9%	85.4%	86.3%	85.8%

Note: * HC gas is produced gas deducted by nitrogen and carbon dioxide content

** Percentage of HC gas production gas production compared to original gas in place

5.4 Comparison among Different Production Scenarios

The optimal cases from each scenario are selected to compare their performances in terms of condensate recovery, HC gas recovery, and production time. The effects of two fluid compositions that yield high and low condensate to gas ratios are individually discussed in Section 5.4.1 and 5.4.2 respectively.

5.4.1 Composition Yielding High CGR of Original Reservoir Fluid

Based on results in Sections 5.1, 5.2.1, and 5.3.1, the optimal case for each scenario for fluid composition yielding high condensate to gas ratios are compared in this section. These cases include:

1. Natural depletion
2. Conventional gas injection with injection rate of 1.0 MMSCFD starting when the average reservoir pressure reaches the dewpoint pressure
3. Gas dumpflood from four layers of 25 ft. source gas reservoirs simultaneously perforated starting from the beginning
4. Gas dumpflood from four layers of 50 ft. source gas reservoirs simultaneously perforated starting from the beginning

Figure 5.61 and Figure 5.62 illustrate the cumulative gas and condensate production profiles, respectively. Natural depletion recover more gas at early time comparing to the other scenarios due to the fact that all three wells are used as production wells while only two wells are produced for the other scenarios. However, because of less pressure support and condensate banking, the field in natural depletion case is abandoned the earliest.

Gas dumpflood and conventional gas injection can maintain the reservoir pressure and prolong the production life of the field. Condensate is produced faster in gas dumpflood scenario comparing to conventional gas injection scenario at early time because of higher gas flowing rate into the target reservoir. Nevertheless, gas dumpflood recovers less condensate at abandonment due to higher carbon dioxide content in the reservoir, resulting in less and less condensate at late time. As seen in

Table 5.17, thicker source gas reservoir of 50 ft thickness results in slightly higher HC gas and condensate recoveries, respectively, when compared with the results from the case with 25 ft thickness source gas reservoirs. However, three more years are required for production.

In summary, optimal cases of gas dumpflood scenario which is 25 ft thickness of source reservoirs can recover 11.4% higher condensate and 9.8% higher HC gas than those of natural depletion scenario. Comparing to conventional gas injection, gas dumpflood scenario can recover 3.5% higher HC gas and 10.4% lower condensate. In term of BOE, gas dumpflood with 25 ft thickness of four layers of source gas reservoir provides 4.7% and 15.7% more total BOE recovery comparing to conventional gas injection and natural depletion scenarios, respectively. This is because of recovery of some dumped gas from the lower four reservoirs.



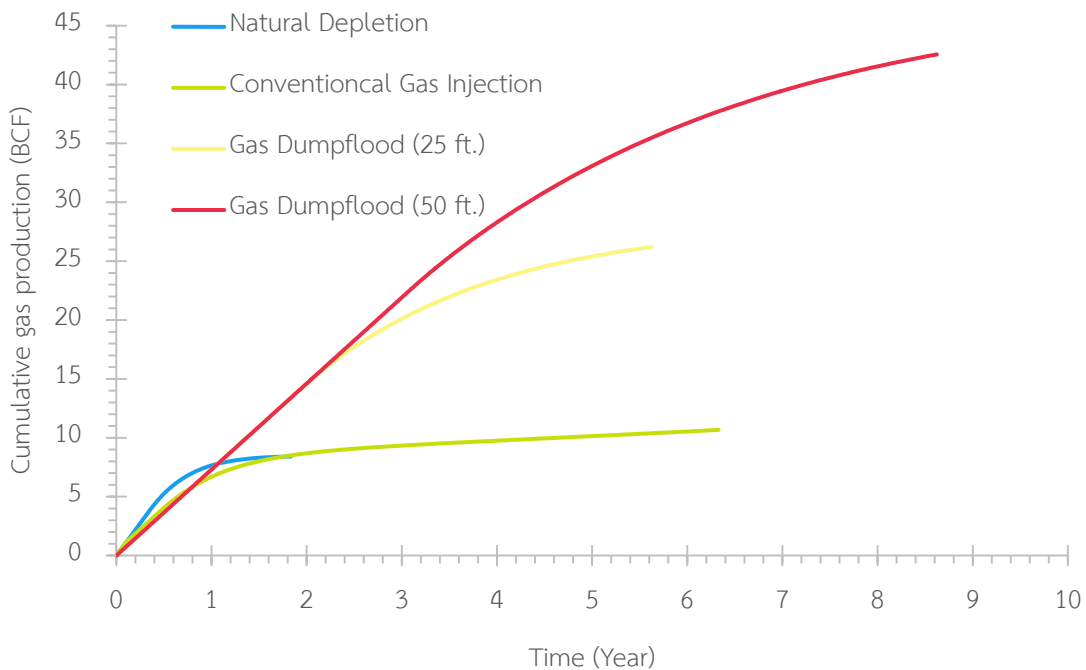


Figure 5.61: Cumulative gas production profiles of the optimal cases for each production scenario

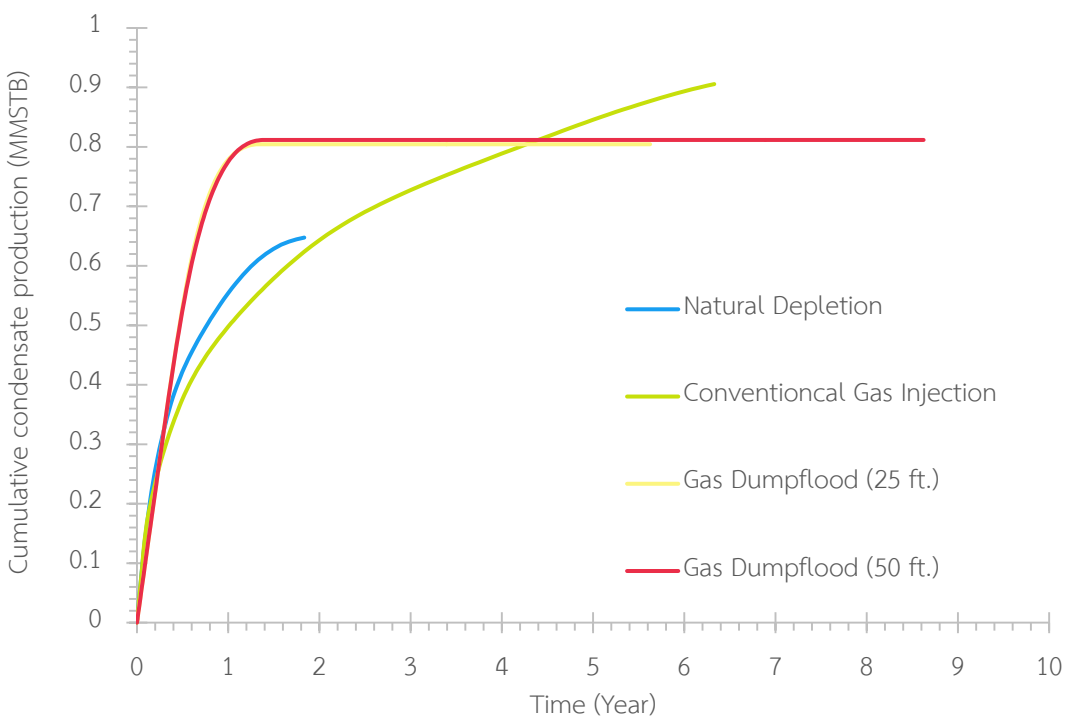


Figure 5.62: Cumulative condensate production profiles of the optimal cases for each production scenario

Table 5.17: Summarized results of the optimal cases for each production scenario in high CGR

Cases	Natural Depletion	Conventional Gas Injection	Dumpflood (25 ft.)	Dumpflood (50 ft.)
Cumulative condensate production (MMSTB)	0.647	0.906	0.805	0.812
Original condensate in place (MMSTB)	1.374	1.374	1.374	1.374
Condensate recovery factor (%)	47.1%	65.9%	58.5%	59.1%
Cumulative gas production (BCF)	8.416	10.667	26.204	42.557
Original gas in place (BCF)	9.149	9.149	9.149	9.149
Gas recovery factor (%)	92.0%	92.1%	92.6%	91.1%
Cumulative HC gas production (BCF) *	8.294	9.321	12.743	16.084
HC gas recovery factor (%) **	90.7%	97.0%	100.5%	101.0%
Cumulative gas production (MMBOE)	2.179	2.496	3.349	3.976
Cumulative total BOE production (MMBOE)	2.826	3.401	4.153	4.788
Original BOE in place (MMBOE)	4.496	4.496	4.496	4.496
Total BOE recovery factor (%)	62.9%	73.9%	78.6%	80.0%

Note: * HC gas is produced gas deducted by nitrogen and carbon dioxide content

** Percentage of HC gas production gas production compared to original gas in place

5.4.2 Composition Yielding Low CGR of Original Reservoir Fluid

Based on results in Sections 5.1, 5.2.2, and 5.3.2, the optimal cases for each scenario for fluid composition yielding low condensate to gas ratios are compared in this section. These cases include:

1. Natural depletion
2. Conventional gas injection with injection rate of 1.0 MMSCFD starting when the average reservoir pressure decline more than 500 psi below the dewpoint pressure
3. Gas dumpflood from two layers of 25 ft. source gas reservoirs simultaneous perforated starting dumpflood when the average reservoir pressure fall below the dewpoint pressure
4. Gas dumpflood from two layers of 50 ft. source gas reservoirs simultaneous perforated starting dumpflood when the average reservoir pressure decline more than 500 psi below the dewpoint pressure

Figure 5.63 and Figure 5.64 demonstrate the cumulative gas and condensate production profiles for the optimal cases of each production scenario. Natural depletion scenario quickly recovers gas at early time, and because of less pressure support and condensate banking, the reservoir in this scenario is abandoned the earliest. Injected gas can maintain the reservoir pressure and prolong the production life. Consequently, more 4.7% of HC gas and 10.7% of condensate are recovered in case of conventional gas injection scenario comparing to natural depletion scenario as shown in Table 5.18.

Although gas dumpflood scenario results in higher HC gas recovery factor as there is a very large amount of cross-flowing gas, the high carbon dioxide content dries out all of the condensate in the reservoir quickly, resulting in drastic reduction of condensate recovery at abandonment comparing to natural depletion scenario. Comparing between 25-ft and 50-ft thickness of source gas reservoirs, 25-ft cases can recover 3.0% higher condensate with less 1.3 years of production due to less amount of excessive carbon dioxide flowing to the target reservoir.

In summary, excessive amount of dumped source gas in gas dumpflood scenario largely induces decrement of 18.1% and 7.4% of condensate recovery comparing to conventional gas injection and natural depletion scenarios, respectively. The controlled gas injection at 1.0 MMSCFD can increase condensate recovery for this composition by 10.7% comparing to natural depletion scenario. In term of BOE, gas dumpflood with 25 ft thickness of four layers of source gas reservoir provides 1.5% and 8.2% more total BOE recovery comparing to conventional gas injection and natural depletion scenarios, respectively. This is because of recovery of some dumped gas from the lower four reservoirs.



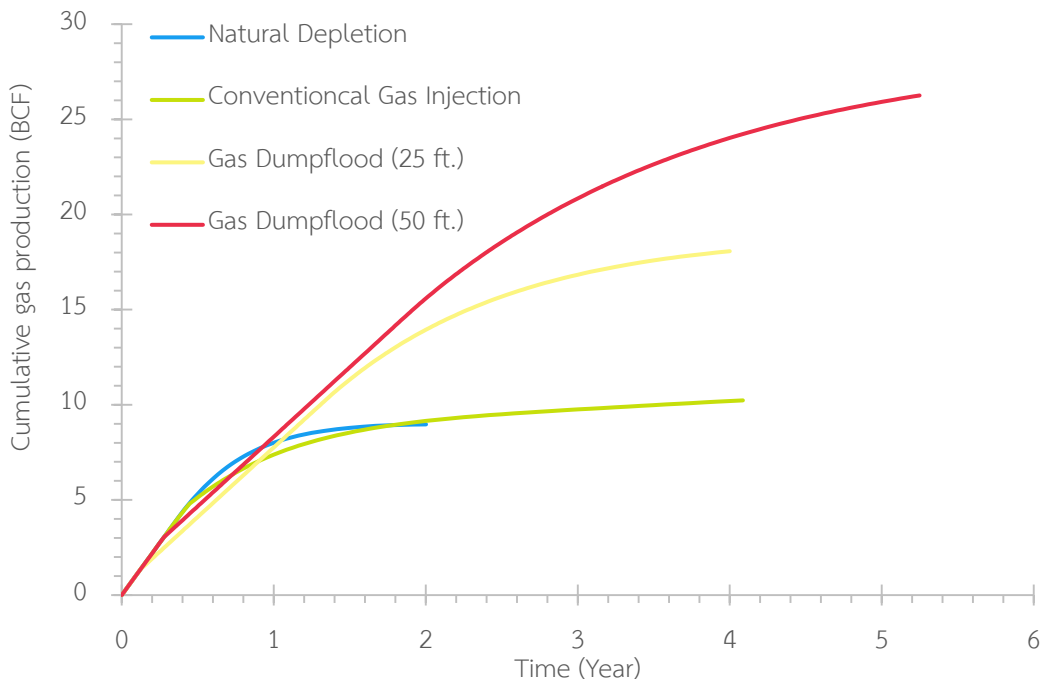


Figure 5.63: Cumulative oil-equivalent gas production profiles of the optimal cases for each production scenario

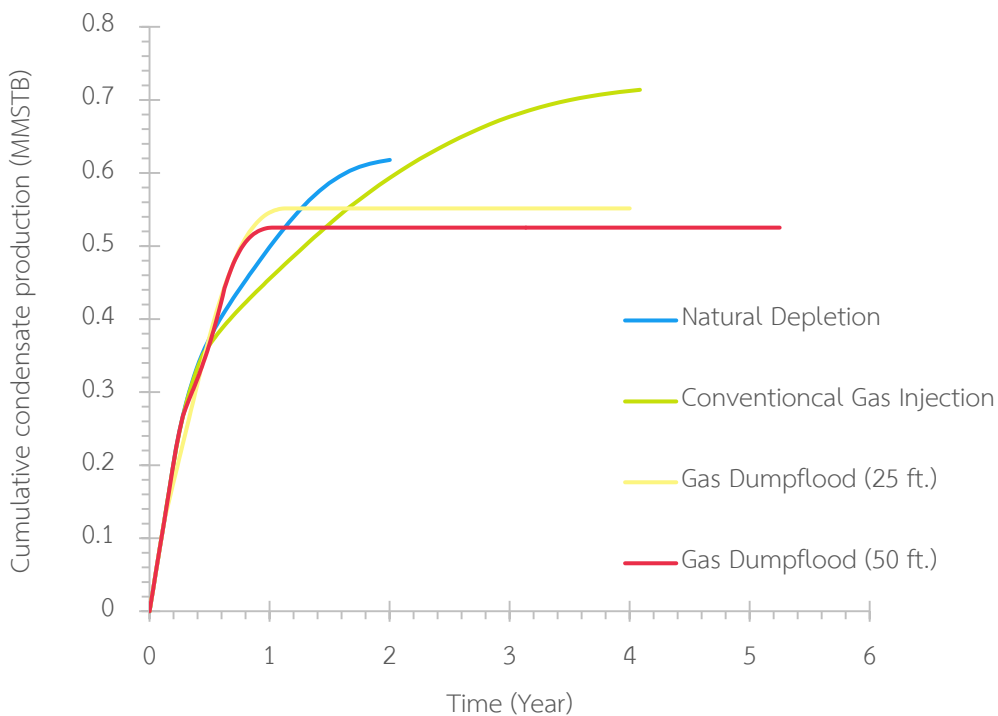


Figure 5.64: Cumulative condensate production profiles of the optimal cases for each production scenario

Table 5.18: Summarized results of the optimal cases for each production scenario in low CGR

Cases	Natural Depletion	Conventional Gas Injection	Gas Dumpflood (25 ft.)	Gas Dumpflood (50 ft.)
Cumulative condensate production (MMSTB)	0.618	0.714	0.552	0.525
Original condensate in place (MMSTB)	0.896	0.896	0.896	0.896
Condensate recovery factor (%)	69.0%	79.7%	61.6%	58.6%
Cumulative gas production (BCF)	8.970	10.233	18.069	26.256
Original gas in place (BCF)	9.673	9.673	9.673	9.673
Gas recovery factor (%)	92.7%	92.4%	93.1%	91.2%
Cumulative HC gas production (BCF) *	8.850	9.563	11.386	13.102
HC gas recovery factor (%) **	91.5%	96.2%	99.0%	99.4%
Cumulative gas production (MMBOE)	2.612	2.846	3.338	3.677
Cumulative total BOE production (MMBOE)	3.230	3.560	3.889	4.202
Original BOE in place (MMBOE)	4.186	4.186	4.186	4.186
Total BOE recovery factor (%)	77.2%	83.9%	85.4%	85.9%

Note: * HC gas is produced gas deducted by nitrogen and carbon dioxide content

** Percentage of HC gas production gas production compared to original gas in place

CHAPTER 6

CONCLUSIONS AND RECOMMENDATIONS

All key findings from the results of the cases in this study are concluded in this chapter. The conclusions can be used to determine the feasibility of gas dumpflood from multiple high carbon dioxide content reservoirs into a condensate reservoir for different conditions. Furthermore, possible improvements are recommended in this chapter as well.

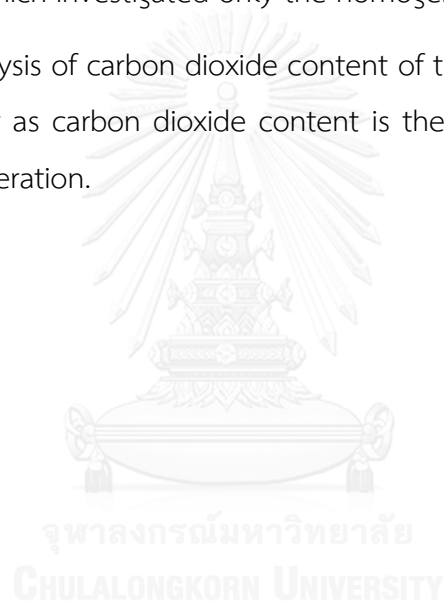
6.1 Conclusions

1. For natural depletion scenario, the case with fluid composition yielding high condensate to gas ratio has less recovery factor for both gas and condensate comparing to those in the low CGR case. This behavior has been observed before in other studies. The explanation for such behavior is because the larger amount of condensate banking occurs in the high CGR case.
2. For conventional gas injection scenario, lower gas injection rate provides higher condensate recovery for both high and low CGR cases.
3. The condensate recovery can be slightly increased by delaying gas injection for both high and low CGR cases. However, in cases of high gas injection rate and high-CGR fluid composition, delaying gas injection can reduce condensate recovery.
4. From the cases with low CGR fluid composition, 8.0 MMSCFD or more gas injection rate can cause reduction of condensate recovery comparing to natural depletion scenario while every injection rate cases can improve some amount of condensate recovery in high CGR cases.
5. For gas dumpflood scenario, the higher connected amount of total gas source in place leads to an increase in the cumulative HC gas. However, after deducting dumped HC gas, the HC gas recovery does not vary much among cases for both high and low CGR cases.

6. Typically, perforation sequence and reservoir thickness of source gas reservoirs do not significantly impact HC gas and condensate recovery as long as there is the same amount of total original source gas in place. The same result is observed for both low and high CGR fluids. This is the observation in this study where amount of original gas source in place is very high. The effect for lower amount of original gas source in place should be investigated further.
7. For the fluid composition yielding high condensate to gas ratio, the sooner the dumpflood, the higher condensate recovery. On the contrary, more condensate can be recovered when starting dumpflood operation at late time in case of low CGR fluid composition.
8. Gas dumpflood can recover condensate of 59.1% which is 17.5% over natural depletion and 6.8% less than conventional gas injection for cases with high-CGR composition. However, reduction of condensate recovery factor of 7.4% comparing to natural depletion is found when gas dumpflood is implemented for low-CGR composition cases.
9. Fluid composition is the key parameter for gas dumpflood operation. For rich gas condensate composition, higher amount of dumped gas containing high carbon dioxide cross flowing into the target reservoir results in more favorable for dumpflood operation. While excessive amount of dumped gas cross flowing into the reservoir having lean condensate composition results in a large reduction of condensate recovery. The amount of dumped gas containing high carbon dioxide should be limited in the case lean condensate composition.

6.2 Recommendations

1. A smaller source gas volume should be studied further as all the cases of gas dumpflood scenario in this study have the source gas volume that quite large comparing to the target reservoir. The smaller source gas reservoir might result in different behavior.
2. Various reservoir heterogeneities should be investigated since heterogeneous rock properties can strongly affect fluid flow and sweep efficiency in the reservoir. The performance of gas dumpflood might be different from the result in this study which investigated only the homogenous one.
3. Sensitivity analysis of carbon dioxide content of the source reservoir should be studied further as carbon dioxide content is the important parameter for gas dumpflood operation.



REFERENCES

- [1] Fan, L., Harris, W.B., and Jamaluddin, A., Understanding Gas-Condensate Reservoirs. **Oilfield Review**, 2006.
- [2] Clapp, T.W. and Lower, G.D., Development of the Erawan Gas Field, Gulf of Thailand. **Journal of Petroleum Technology**, 1982. 34(06): p. 1,204 - 1,210.
- [3] Rinadi, M., et al., Successfully Improve Oil Recovery Using In-Situ Gas Lift and Gas Dump Flood at North Arthit Field, Gulf of Thailand. 2014, Society of Petroleum Engineers.
- [4] Kridsanon, N. **Enhanced Condensate Recovery Using CO2 Dump Flood**. Master's Thesis, Department of Mining and Petroleum Engineering, Chulalongkorn University, 2010.
- [5] Shi, C., Horne, R.N., and Li, K., Optimizing the Productivity of Gas/Condensate Wells. 2006, Society of Petroleum Engineers.
- [6] Al-Hasami, A., Ren, S., and Tohidi, B., CO2 Injection for Enhanced Gas Recovery and Geo-Storage: Reservoir Simulation and Economics. 2005, Society of Petroleum Engineers.
- [7] Jalil, M.A.A., Masoudi, R., Darman, N.B., and Othman, M., Study of the CO2 Injection, Storage, and Sequestration in Depleted M4 Carbonate Gas Condensate Reservoir, Malaysia. 2012, Carbon Management Technology Conference.
- [8] Kalra, S. and Wu, X., CO2 Injection for Enhanced Gas Recovery. 2014, Society of Petroleum Engineers.
- [9] Clark, R.A., Jr. and Ludolph, B., Voidage Replacement Ratio Calculations in Retrograde Condensate to Volatile Oil Reservoirs Undergoing EOR Processes. 2003, Society of Petroleum Engineers.
- [10] Thitaram, P. **Effect of Reservoir Fluid Composition on Carbon Dioxide**. Master's Thesis, Department of Mining and Petroleum Engineering, Chulalongkorn University, 2009.

- [11] William M. McCain, J., *The Properties of Petroleum Fluids*. 1990: PennWell Publishing Company.
- [12] Fang, Y., Li, B., Hu, Y., Sun, Z., and Zhu, Y., *Condensate Gas Phase Behavior and Development*. 1998, Society of Petroleum Engineers.
- [13] Roussennac, B. **Gas Condensate Well Test Analysis**. Master's Thesis, The Department of Petroleum Engineering, Stanford University, 2001.
- [14] Forrest F. Craig, J., *The Reservoir Aspect of Waterflooding*. 1971: The American Institute of Mining, Metallurgical, and Petroleum Engineers, Inc.
- [15] Ramharack, R.M., Aminian, K., and Ameri, S., *Impact of Carbon Dioxide Sequestration in Gas/Condensate Reservoirs*. 2010, Society of Petroleum Engineers.
- [16] Rangponsumrit, M. **Well and Reservoir Management for Mercury Contaminated Waste Disposal**. Master's Thesis, Department of Mining and Petroleum Engineering, Chulalongkorn University, 2004.
- [17] *Nonconventional Source Fuel Credit*. 1998, Internal Revenue Service.
- [18] Association, G.P.S., *Engineering Data Book FPS Version Twelfth Edition*. 2004: Gas Processors Suppliers Association.
- [19] Weisman, J., Two-phase Flow Patterns. in **Handbook of Fluids in Motion**, pp. 409 - 425. Ann Arbor Science, 1983
- [20] *Eclipse Technical Description Version 2014.1*. 2014: Schlumberger.
- [21] Peng, D.-Y. and Robinson, D.B., *A New Two-Constant Equation of State*. 1976, *Industrial and Engineering Chemistry Fundamentals*
- [22] Molina, N.N., *A Systematic Approach To The Relative Permeability Problem In Reservoir Simulation*. 1980, Society of Petroleum Engineers.
- [23] Lee, A.L., Gonzalez, M.H., and Eakin, B.E., *The Viscosity of Natural Gases*. 1966.
- [24] *Prosper User Manual, Version 10*. 2007: Petroleum Experts Limited.



APPENDIX A

PRODUCTION SCHEDULE

There are three production wells in the simulation models of this research which are PROD1, PROD2, and PROD3. Besides, there is a well named DUMP which is physically the same well as PROD2. This well is used in the model for dumping and injecting purpose in case of gas dumpflood and conventional gas injection scenarios. The well was set separately from PROD2 in order to simplify the result exportation from ECLIPSE. The detailed input data for each keyword are summarized in the following sections.

A.1 Well Specification (keyword: WELSPECS)

Three production wells are specified and located in this keyword. Well DUMP which is designated as injector in conventional gas injection scenario and dumper in gas dumpflood scenario are specified at the same location as PROD2 because physically they are the same well. They are specified separately in order to split the cumulative production and the cumulative dumped gas result in the report.

Table A.1: Data for well specification (keyword: WELSPECS)

Parameters	Well PROD1	Well PROD2	Well PROD3	Well DUMP
I Location	8	23	38	23
J Location	8	8	8	8
Preferred phase	Gas	Gas	Gas	Gas

A.2 Well Completion Specification Data (keyword: COMPDAT)

The wellbore diameter of 6-1/8 in. was specified for all wells in this keyword. For production well, layers of the gas condensate are completed full to base as shown in Table A.2. For dumping well, all layers that connected to both gas condensate and gas source reservoirs are completed full to base in the basecase of dumpflood scenario.

Table A.2: Data for well completion specification of production well (keyword: COMPDAT)

Parameters	Well PROD1	Well PROD2	Well PROD3
Wellbore diameter (ft.)	0.5104	0.5104	0.5104
K-Layer of perforated zone	1-10	1-10	1-10

Table A.3: Data for well completion specification of dumping well (keyword: COMPDAT)

Parameters	Reservoir (Well DUMP) *				
	Target Reservoir	Source Reservoir 1	Source Reservoir 2	Source Reservoir 3	Source Reservoir 4
Wellbore ID (ft.)	0.5104	0.5104	0.5104	0.5104	0.5104
K-Layer of perforated zone	1-10	12-16	18-22	24-28	30-34

Note: * Completion specification of dumping well was defined during dumpflood operation

A.3 Segmented Well Definition (keyword: WELSEGS)

Since the dumping well is connected to multiple reservoirs, multi-segment well option needs to be assigned.

Table A.4: Data for segmented well definition (keyword: WELSEGS)

Parameters	Segments (Well DUMP)									
	1	2	3	4	5	6	7	8	9	10
Length	6000	50	1000	25	200	25	200	25	200	25
Depth	6000	50	1000	25	200	25	200	25	200	25
Tubing ID (ft.)						0.2034				
Roughness (ft.)						0.00015				

A.4 Segmented Well Completion (keyword: COMPSEGS)

Table A.5: Data for segmented well completion (keyword: COMPSEGS)

Parameters	Segment (Well DUMP)				
	2	4	6	8	10
Start grid (i,j,k)	23,8,1	23,8,12	23,8,18	23,8,24	23,8,30
End grid (l,j,k)	23,8,10	23,8,16	23,8,22	23,8,28	23,8,34
Start length (ft.)	0	1050	1275	1500	1725
End length (ft.)	100	1075	1300	1525	1750

A.5 Segmented Vertical Flow Performance Table (keyword: WSEGTABL)

Table A.6: Data for segmented vertical flow performance table (keyword: WSEGTABL)

Parameters	Well DUMP (Well DUMP)			
First segment	3	5	7	9
Last segment	3	5	7	9
VFP table	3	4	5	6
Components of the pressure drop	FH *	FH *	FH *	FH *
Handling negative flow	FIX **	FIX **	FIX **	FIX **
Scaling the interpolated pressure drop	LEN ***	LEN ***	LEN ***	LEN ***

Note: * FH stands for "Friction and hydrostatic losses."

** FIX stands for "Fixing the lookup value of the flow rate at the first flow point in the table."

*** LEN stands for "The interpolated pressure drop is scaled in proportion to the length of the segment relative to the table's datum length."

A.6 Production Well Control (keyword: WCONPROD)

Table A.7: Data for production well control of PROD1 and PROD3 (keyword: WCONPROD)

Parameters	Well PROD1	Well PROD3
Open/Shut flag	OPEN	OPEN
Control	Gas rate	Gas rate
Gas rate (MSCF/D)	10000	10000
BHP target * (psia)	14.7	14.7
THP target (psia)	200	200
VFP table number	1	1

Note: * These numbers need to be entered in ECLIPSE 300 to override the default value of 1470 psia. Since THP target and VFP table are specified, ECLIPSE 300 will use the THP target as constraint rather than BHP target.

Table A.8: Data for production well control of PROD2 and DUMP (keyword: WCONPROD)

Parameters	Well PROD2		Well DUMP	
	Before dumpflood	During dumpflood	Before dumpflood	During dumpflood
Open/Shut flag	OPEN	SHUT	SHUT	STOP
Control	Gas rate	-	-	-
Gas rate (MSCF/D)	10000	-	-	-
BHP target * (psia)	14.7	-	-	-
THP target (psia)	200	-	-	-
VFP table number	1	-	-	2

Note: * These numbers need to be entered in ECLIPSE 300 to override the default value of 1470 psia. Since THP target and VFP table are specified, ECLIPSE 300 will use the THP target as constraint rather than BHP target.

A.7 Vertical Flow Performance (keyword: VFPPROD)

PROSPER software was used to model vertical lift performance of the two production wells and one dumpflood well. A VFP table identifies performance for one particular segment of the tubing as defined in segmented vertical flow performance table (keyword: WSEGTABL) and production well control (keyword: WCONPROD). VFP table 1 indicates performance of well PROD1, PROD2, and DUMP1 (before starting dumpflood). While VFP tables 2 - 5 indicate performance for different segments of well DUMP1 (during dumpflood operation). The input data are summarized in Table A.9 - Table A.11.

Table A.9: Data for VLP modeling by PROSPER software

Parameter	VFP table number					
	1	2	3	4	5	6
Well	PROD1 PROD2 PROD3					DUMP
Segment	-	1	3	5	7	9
Fluid	Dry and wet gas					
Method	Black Oil					
Flow type	Tubing Flow					
Well type	Producer					
Gas specific gravity	0.8			0.7		
Condensate gravity (API)	50			-		

Parameter	VFP table number					
	1	2	3	4	5	6
CGR	-			0		
WGR	-			0		
Water salinity (ppm)			5,000			
CO ₂ mole percent	1.06			20		
N ₂ mole percent			0			
Gas viscosity correlations			Lee et al [23]			
Dip angle			0 degree			
Tubing ID (in.)			2.441			
First node depth (ft.)	0	0	6050	7075	7300	7525
Last node depth (ft.)	6000	6000	7050	7275	7500	7725
Correlations			Petroleum Experts 2 [24]			

Table A.10: Temperature gradient for VLP modeling by Prosper

True vertical depth (ft.)	Temperature (°F)
0	80
6000	264.7
7750	321.3
Overall heat transfer coefficient: 3 BTU/h/ft ² /°F	

Table A.11: Variables for VLP modeling by Prosper

Variable	Values
	VFP table 1
	0.05, 0.1, 0.5, 1, 1.5, 2, 2.5, 3, 3.5, 4, 4.5, 5, 6, 7, 8, 9, 10, 15, 20, 25
Gas rate (MMSCFD)	VFP table 2, 3, 4, 5, and 6
	0.1, 0.5, 1, 2, 3, 4, 5, 7.5, 10, 15, 20, 25, 30, 35, 40, 50, 60, 70, 80, 100
First node pressure (psig)	100, 300, 500, 750, 1000, 1200, 1500, 2000, 2500, 3000
CGR (STB/MMSCF) *	0, 25, 50, 75, 100, 150, 200, 250, 300, 400

Note: * CGR was used for VFP table 1 only

APPENDIX B ECONOMIC LIMIT

B.1 Field Abandonment Condition

The production gas rate of 0.5 MMSCF/D which is general guideline economic limit natural gas production in the Gulf of Thailand was used as economic limit in this study. However, the produced fluids in the simulation model include carbon dioxide and condensate as well. In order to maximize net gain energy, the recoveries were calculated as barrel of oil equivalent and the economic, hence, should be converted into barrel of oil equivalent as well.

The United States Geological Survey (USGS) defines 6,000 SCF of natural gas are equivalent to 1.0 BOE. Consequence, the natural gas economic limit rate of 0.5 MMSCFD is equivalent to 83.33 BOE/D as the calculation expressed below:

$$\begin{aligned} \text{Equivalent Economic Limit} &= (0.5 \times 10^6 \text{ SCF} / D) \left(\frac{1 \text{ BOE}}{6,000 \text{ SCF}} \right) \\ &= 83.33 \text{ BOE} / D \end{aligned}$$

B.2 Conventional Gas Injection Limit

For conventional gas injection scenario, the gas is injected as long as the compressor power consumption costs compensate with produced condensate. The approximate compressor power is illustrated as Equation (B.1) in order to find economic produced condensate rates for gas injection from Table B.1.

$$P = 0.23 q_g \left[\left(\frac{P_2}{P_1} \right)^{0.2} - 1 \right] \quad (\text{B.1})$$

where

P = compression power (HP)

q_g = gas compression or injection rate (MSCF/D)

p_1 = compressor suction pressure (psia) = 300 psia

p_2 = compressor discharge pressure (psia) = 2500 psia

unit conversion

1 HP = 0.746 kW

1 kWh = 0.09977 USD (EGAT Power average cost in 2015)

1 STB = 49.47 USD (average oil price in 2015)

Table B.1: The economic condensate rates for gas injection of different injection rates

Injection rate (MMSCFD)	Power (HP)	Power (kW)	Power cost (USD/D)	Economic condensate rate (STB/D)
20.0	2429.5	1812.4	4307.6	87.1
16.0	1943.6	1449.9	3446.1	69.7
12.0	1457.7	1087.4	2584.6	52.2
8.0	971.8	724.9	1723.1	34.8
4.0	485.9	362.5	861.5	17.4
1.0	121.5	90.6	215.4	4.4

VITA

Wisaroot Lertthaweedeche was born on July 14th, 1990 in Bangkok, Thailand. He received Bachelor of Science in Chemical Engineering from Chulalongkorn University in 2012. After that, he worked as a research assistant in PTT Global Chemical Public Company Limited which is the largest integrated petrochemical and refining company in Thailand for 2 years. Then, he got a full scholarship from Chevron Thailand Exploration and Production Limited in order to pursue the Master's Degree in Petroleum Engineering at Chulalongkorn University and has been a graduate student since 2014.

